AN INNOVATIVE ELECTROPORATION PROTOCOL TO STUDY CANDIDATE GENES IN THE DEVELOPING KIDNEY

By

TRISTAN MACKAY ALIE

Department of Human Genetics

Faculty of Medicine

McGill University

Montreal, Quebec, Canada

A thesis submitted to the Faculty of Graduate and Postdoctoral Studies in partial fulfillment of the requirements of the degree of Master's of Science.

May, 2006

Your file Votre référence
ISBN: 978-0-494-24597-2
Our file Notre référence
ISBN: 978-0-494-24597-2

À ma famille,

To my family,

-T

TABLE OF CONTENTS

LIST OF FIGURES AND TABLES

LIST OF ABBREVIATIONS

ΔV_m	Transmembrane Potential
ALK	Activin Like Kinase
BCIP/NBT	Bromochloroindolyl Phosphate/Nitro Blue Tetrazolium
BMP	Bone Morphogenetic Protein
CAKUT	Congenital Anomalies of the Kidney and Urinary Tract
COS	Cosine
DIG	Digoxigenin
DMEM	Dulbecco's Modified Eagle's Media
DNA	Deoxyribonucleic Acid
E	Embryonic Day
E_{ext}	Applied Electric Field
eGFP	Enhanced Green Fluorescent Protein
ES	Embryonic Stem cells
EYA-1	Eyes Absent gene
f	Coefficient relating the impact of a cell on the distribution of an electric field
FBS	Fetal Bovine Serum
FGF	Fibroblast Growth Factor
FOXC	Forkhead Box C
GDNF	Glial Derived Neurotrophic Factor
GFP	Green Fluorescent Protein
GFRα-1	GDNF Family Receptor Alpha – 1
HOXB7	Homeo-Box 7 Gene
HV/SP	High Voltage/Short Pulse electroporation protocol
kb	Kilo Base
LIF	Leukemia Inhibitory Factory
LV/LP	Low Voltage/Long Pulse electroporation protocol
MDCK	Madine-Darby Canine Kidney cell line

MET	Mesenchyme-to-Epithelial Transition
mIMCD-3	Murine Inner Medullary Collecting Duct-3 cell line
mK3	Mouse Kidney cell line 3
MM	Metanephric Mesenchyme
ODN	Oligonucleotide
P	Postnatal
PAX	Paired Box Gene
PBS	Phosphate Buffered Saline
PFA	Paraformaldehyde
P/S	Penicillin and streptomycin
r	Radius
RAR	Retinoic Acid Receptor
RET	Rearranged during Transfection gene
RNA	Ribonucleic acid
RT-PCR	Reverse Transcription Polymerase Chain Reaction
RUB1	Rat Ureteric Bud 1 Cell Line
SALL	Sal-Like 1
SIX	Sine Occulis Homeobox Gene
T	Pulse Time
TGF	Transforming Growth Factor
UB	Ureteric Bud
UVA	Ultra-Violet A rays
VEGFA	Vascular Endothelial Growth Factor A gene
Wnt	Wingless Type
WT-1	Wilm's Tumour 1 gene

ABSTRACT

The kidney filters blood through nephrons, to recycle water and solutes in order to maintain homeostasis in the body. A reduction in nephron formation during fetal development renders the affected individual susceptible to hypertension and end stage renal disease. Nephrogenesis relies on the iterative branching of the ureteric bud epithelium, which triggers the metanephric mesenchyme to condense and form nephrons at its tips.

A critical question during kidney development is to identify the genes that are responsible for nephron formation. The culture of mouse embryonic kidneys has been an important *in vitro* model to examine the effects of candidate genes during nephrogenesis. By culturing embryonic kidneys in the presence of growth factors, blocking antibodies to specific proteins, or by blocking transcription using RNA interference, gene function can be ascertained. Microinjection and electroporation has also been used to overexpress DNA constructs in mouse embryonic kidneys. We have reviewed the method of microinjection and determined the optimal conditions for introducing DNA into embryonic kidneys. We examined high voltage/short pulse parameters and compared them to previously reported low voltage/long pulse settings. The use of a high voltage with a short pulse led to 100 fold more transgene expression and a longer duration of expression, when compared to a low voltage/long pulse protocol. Furthermore, we can target either the ureteric bud or the mesenchyme of the developing kidney, by selectively microinjecting the transgene in the organ.

We have examined the expression pattern of Alk6 and members of the claudin gene family during kidney development. Their expression pattern along with their function has not been fully characterized in the embryonic kidney. In the future we plan to employ our novel electroporation protocol to study the function of these candidate genes in the developing kidney.

RÉSUMÉ

Les reins maintiennent l'homéostase dans le corps en filtrant le sang pour maintenir un équilibre d'eau et de solutés dans le corps. Le recyclage de ces éléments s'effectuent dans les nephrons qui peuplent les reins. Un déficit en nombre de nephrons prédisposent les individus concernés à l'hypertension et à la défaillance rénale. La néphrogènèse nécessite la croissance et le bifurquation des cellules épithéliales du bourgeon uretérique et la transition mésenchyme-épithéliale des cellules mésenchymes.

L'identification des gènes nécessaires pour établir une nombre suffisant de nephrons demeure un thème prédominant dans l'étude de l'organogenèse rénale. La culture de reins d'embryons de souris est une approche utile qui permet l'étude des gènes-candidats dans le développement des reins. Plusieurs études ont démontré le rôle de gènes-candidats pour la croissance du bourgeon uretérique épithélial ou bien lors de la transition mésenchyme-épithéliale, en faisant croître des reins embryoniques de souris avec anticorps, facteurs de croissance et acides nucléiques affectant l'expression génique. Nous avons déterminé une approche plus optimale pour introduire de façon efficace des vecteurs nucléiques dans les reins embryoniques de souris. Cette nouvelle approche consiste d' un voltage élevé accompagné d'une courte durée de pulsation, ce qui permet à une expression génique 100 fois supérieure et d'une durée d'expression double comparativement aux études passées qui utilisaient un voltage bas et une longue durée de pulsation. De plus, nous pouvons intégrer notre transgène tant dans les cellules du bourgeon uretérique que les cellules mésenchymes.

De plus, nous avons débuté une ébauche de l'étude génique des gènes Alk6 et de la famille claudin durant la néphrogénèse. L'expression génique et le rôle de ces gènes sont méconnus durant le développement rénal. Nous désirons utiliser nos nouveaux paramètres d'électroporation afin d'introduire des vecteurs nucléiques qui affecteront l'expression et donc la fonction de nos nouveaux gènes-candidats.

CONTRIBUTIONS OF COLLABORATORS

The author wrote this thesis according to the guidelines stated on the website of the Faculty of Graduate and Post-Doctoral Studies, McGill University (http://www.mcgill.ca/gps/programs/thesis/guidelines/).

The candidate was responsible to plan and conduct all experiments, along with the analysis of the data. Mr. Pavle Vrljicak conducted preliminary electroporation assays during his Master's of Science research project under Dr. Indra Gupta's supervision. Mr. Vrljicak conducted gene expression studies between E12 mouse embryonic kidney mesenchyme and ureteric bud using SAGE technique in Dr. Pamela Hoodless's laboratory at the British Columbia Cancer Research Center. Dr. Hoodless and Mr. Vrljicak provided the candidate with the gene expression data and assistance in the analysis. Mr. Dave Myburgh assisted the candidate to perform microinjection and electroporation experiments. As well, Mr. Myburgh assisted in imaging kidney cultures, measuring kidney surface area and preparation of probes for *in situ* hybridization. Dr. Aimee Ryan, McGill University, provided valuable insight for the electroporation experiments. Further Dr. Ryan prepared preliminary immunohistochemistry data for the claudin gene family project. Dr. Indra Gupta supervised the work carried out in her laboratory, provided assistance in the statistical analysis of the data and corrections of this manuscript.

ACKNOWLEDGEMENTS

« Fais du bien autour de toi, fais toi d'la vie une amie. »

- Ruffneck

Three years ago, I met Dr. Indra Gupta at the Montreal Children's Hospital; from this engaging encounter and her belief in my potential, my adventure in academic research took off. I am obliged to Indra for taking me under her wing, her careful guidance during my scientific training and assisting me to reach my personal goals, such as applying successfully to medical school. Most importantly, Indra, I thank you for always having full conviction in my abilities and skills to resolve scientific disappointments and turning them into success . . . "I know you'll figure it out", you'd say. "Really?", I'd question myself. And I would make it through. Thanks.

I was fortunate to go to work and share my days not with colleagues, but rather with friends; which is not something that everyone can say about their work place. First, I would like to thank my immediate lab members, Mr. Dave Myburgh and Ms. Inga Murawski. Our days in the lab, punctuated by jokes, laughter, teasing and positive vibe. Inga was a great lab partner to work with: studious, bright and dedicated; I wish you success and happiness in your academic endeavour as a PhD student, and your life with your soul mate. My work is truly the end result of Dave's unwavering assistance and support. I cannot imagine having been able to do all of this work, learn about the intricate world of computers and software imaging without your insight, calm, resilience and willingness to help. *Meneer, dankie.*

Obviously, the lab environment is not complete without our fellow members in Dr. Paul Goodyer's lab, which I thank for reagents, equipment and valuable viewpoint. Dr. Diana Iglesias, 'che, with flair and fun " con quien podi praticar mi español". The now Dr. Alison Dziarmaga, who led by setting a great example of what a graduate student ought to be. Pierre-Alain Hueber, with whom I would daydream with about riding on fresh snow and travel adventures. Jackie Quinlan your resilience and kind spirit for which I will remember you by, will take you around the world on great adventures! Elena Pascuet, we shared the U of O as a training debut, the National Capital Region as a home and our recent animated strolls on Sherbrooke after work. And finally, Lee Lee Chu, thank you for your patience, laughs and expertise. To past and new PG lab member,

Tiffany Cohen, Anne-Marie Pattenaude and Dr. Zhao Zhang, I value our paths having crossed.

My work at the Children's was the end result of much collaboration. First I extend my thanks to Dr. Aimee Ryan and her lab, predominantly to Annie Simard, Dr. Erminia DiPietro and Nikki Parkinson, who shared insights in staining techniques, materials and equipment needed for our experiments, including the use of the microinjector and electroporator. I thank my supervisory committee Dr. Cynthia G. Goodyer and Dr. Jean-Jacques Lebrun for their insight. A commendable student centered staff, Dr. David Rosenblatt (Chair), Ms. Laura Benner, Ms. Kandace Springer and Ms. Fran Langton, organizes the Human Genetics department. As well, I thank the animal center staff, Stéphanie Grenon and Jodie Middleton for their help in ordering and taking care of our precious animals, without which this study wouldn't exist. Finally, many thanks to Dr. Pamela Hoodless and Pavle Vrljicak for sharing with us the SAGE data.

Finally, my journey in *la belle ville de Montréal* was a time of glee, merriment and discovery. To my fantastic friends, your love of living and your distinctive passions have truly shaped me in better ways. Carolyn, Greg, Cleo, Lori, Karine, Darren, Tammy, Samuel, Laura, Graham, Grae, Steve, Amy and others . . . you taught me so much . . . I couldn't have been able to make it without you . . . I will always treasure our jaunts together to our much loved hang-outs: The Dip, Bella Vista, Chez Jose, Korova, Sablo, U & Me, little India, 3987 . . . *et j'en passe.*

Merci tous du fond du coeur.

I. INTRODUCTION

1. Mammalian kidney development

A. Pronephric and mesonephric kidney development

Kidney development in mammals requires the formation of three serial kidneys: the pronephros, the mesonephros and the metanephros. The pronephric and mesonephric kidneys form in mice at embryonic day (E) 8 and 9.5 that corresponds to day 22 and 24 in humans [1]. In amphibians and fish, the embryonic kidney is the pronephros while the adult kidney is the mesonephric kidney. In contrast, amongst vertebrates, all amniotes, which includes reptiles, birds and mammals, develop a metanephric kidney as their adult kidney [1]. In spite of the fact that the pronephric and mesonephric kidneys are transitory structures in amniotes, they have been important models to understand general themes during kidney development such as mesenchymal-to-epithelial transition and tubule formation [2-4].

The pro-, meso-, and metanephric kidneys originate from two primordial tissues that develop from the intermediate mesoderm: the nephric duct and nephrogenic cord [2]. The nephrogenic cord refers to the mesenchyme that extends along the length of the embryo that gives rise to the three serial kidneys. The pronephros develops from the nephrogenic cord that is located between the somites and the lateral plate mesoderm at the level of the forelimbs [3]. The nephric or Wolffian duct is generated when cells within the intermediate mesoderm undergo epithelialization. The nephric duct extends caudally along the length of the embryo to the cloaca; cranially, it induces the adjacent mesenchyme to form the mesonephric tubules, and caudally, at the level of the hindlimbs, it gives rise to an outgrowth known as the ureteric bud that induces the formation of the metanephric kidney. Nephrons, which are the functional units of the metanephric kidney, arise when the undifferentiated mesenchymal cells of the nephrogenic cord are induced by the adjacent ureteric bud to undergo mesenchymal-to-epithelial transition (Figure1) [1, 5].

Figure 1. Development of the pronephric, mesonephric and metanephric kidney.

A) The nephrogenic duct and nephrogenic cord arise from the intermediate mesoderm. At E8.0 in the mouse, the pronephric tubules are formed.

B) The nephric duct extends caudally towards the cloaca. Along the nephric duct, the mesonephric tubules are formed from the inductive processes between the nephric cord and nephric duct. These tubules form the mesonephric kidney.

C) By E10.5, the ureteric bud extends from the nephric duct, also known as the Wolffian Duct, and invades the metanephric mesenchyme. The ureteric bud will branch and grow whereas the mesenchyme will epithelialize at the ureteric bud tips to form nephrons.

Modified from [6] – See agreement form in Appendix B

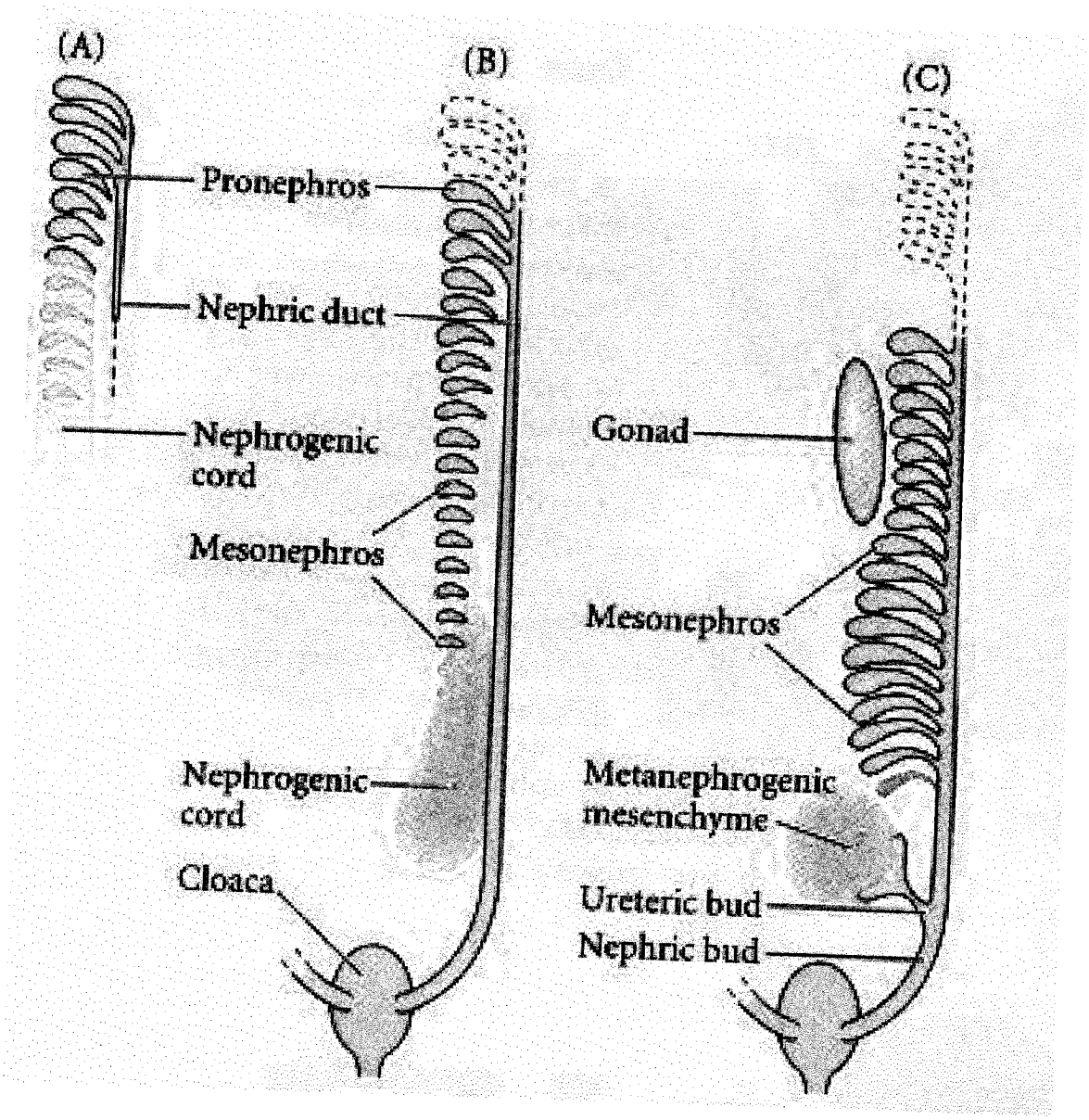
(A)
(B)
(C)
Pronephros
Nephric duct
Nephrogenic cord
Mesonephros
Nephrogenic cord
Cloaca
Gonad
Mesonephros
Metanephrogenic mesenchyme
Ureteric bud
Nephric bud

B. Metanephric kidney development

The nephric duct gives rise to an outgrowth, the epithelial ureteric bud (UB) that interacts with the adjacent mesenchyme, the metanephric mesenchyme (MM), such that together these two tissues form the metanephric kidney [1, 7]. At embryonic day (E) 10.5 in the mouse, the ureteric bud (UB) first appears in response to signals released by the MM. As the UB invades the surrounding mesenchyme, it branches and forms a T-like structure at E11.0 [8]. The UB continues to grow and branch in an iterative process known as branching morphogenesis that continues up until the first two weeks postnatally. At each new UB tip, the adjacent metanephric mesenchymal cells are induced to undergo condensation (Figure 2). The condensation of the MM cells is the first step in the process by which these cells become epithelialized, also known as mesenchymal-to-epithelial transition (MET). During MET, mesenchymal cells form discrete structures known as the renal vesicle, the comma-shaped body, and the S-shaped body [1, 7]. The final steps of MET occur when endothelial cells invade the epithelial cleft of the S-shaped body and form the glomerulus. The S-shaped body will give rise to the future glomerulus, the proximal tubule, the loop of Henle and the distal tubule. As well during this time, the S-shaped body will fuse with the UB which contributes to the collecting duct network of the mature kidney (Figure 3) [7].

The initial molecular trigger that induces the formation of the metanephric kidney is still poorly understood. It is not known if it is the MM that initiates the formation of the UB from the nephric duct, or if the nephric duct itself initiates formation of the UB, which then induces the formation of the MM [7]. However, in spite of the uncertainty of the identity of the initial molecular trigger, it is evident that there is a long list of growth factors, receptors, and transcription factors that are all implicated in the proper growth and patterning of the UB and the MM [3, 9].

Figure 2. The developing metanephric kidney.

A) The development of the metanephric kidney originates from the interaction of the ureteric bud, here in bright green, and the metanephric mesenchyme, darker green. The image is a cryosection taken at 10 μm thickness from an E13 *HoxB7/GFP* embryo (20x magnification).

B) Annotated schematic representation of Figure 2A. The outer edge of the kidney, the cortex, consists of the tips of the ureteric bud along with a population of uninduced mesenchymal cells. The glomeruli of the mature nephron are located in the cortex. The medulla of the kidney consists of the stalks of the ureteric bud that give rise to the collecting ducts.

Figure 2A.

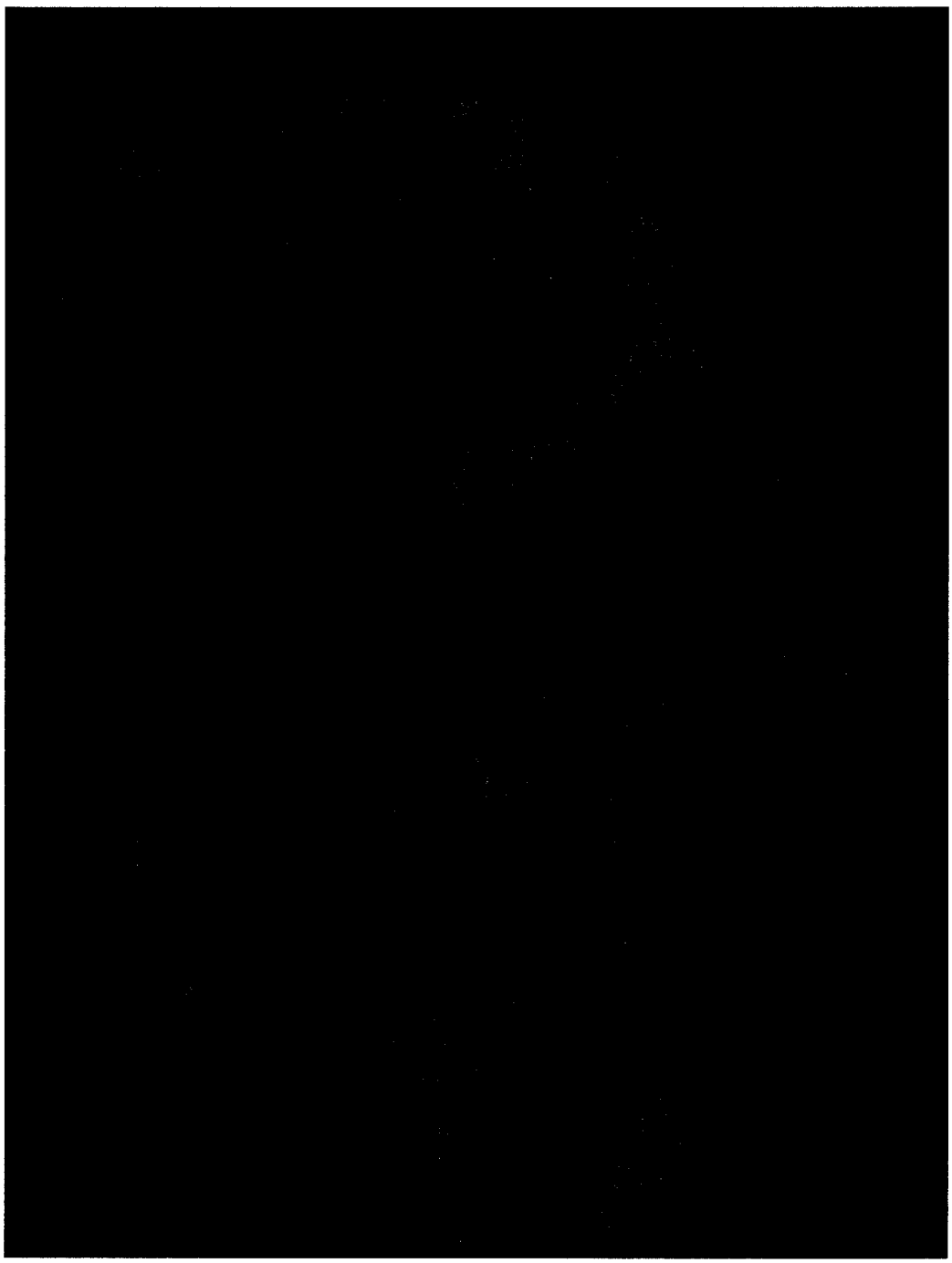

Figure 2B.

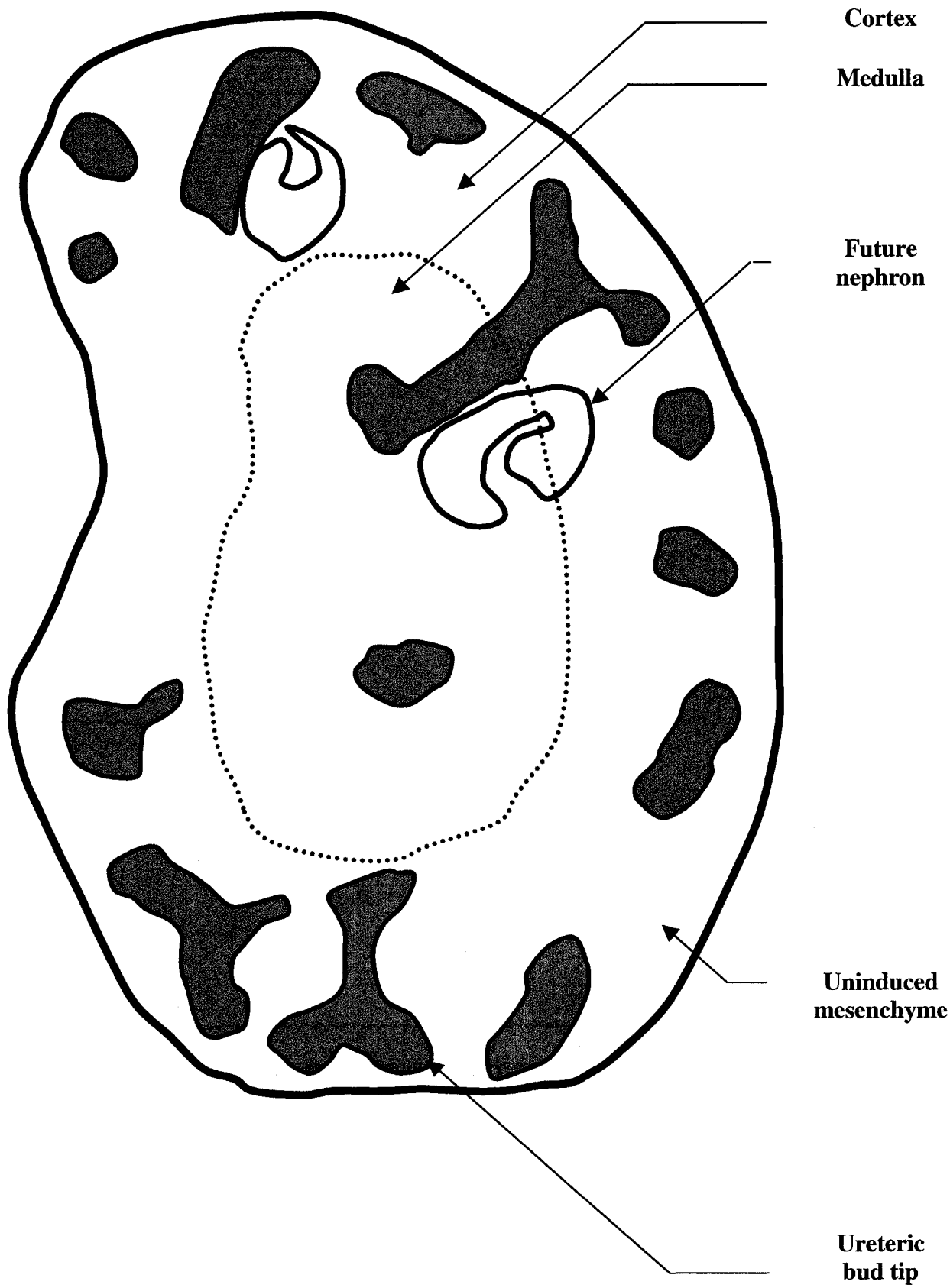
Cortex
Medulla
Future nephron
Uninduced mesenchyme
Ureteric bud tip

Figure 3. Mesenchymal to epithelial transition in the metanephric kidney.

Once induced by the ureteric bud, the metanephric mesenchyme undergoes structural and functional changes. The mesenchyme will first (A) condense at the tips of the ureteric bud, then (B) form a renal vesicle, (C) a comma-shaped body, and (D) an S-shaped body. (E) Endothelial cells will invade the distal cleft of the S-shaped body, which (F) will allow for the function of the future nephron.

From [1] – See agreement form in Appendix B

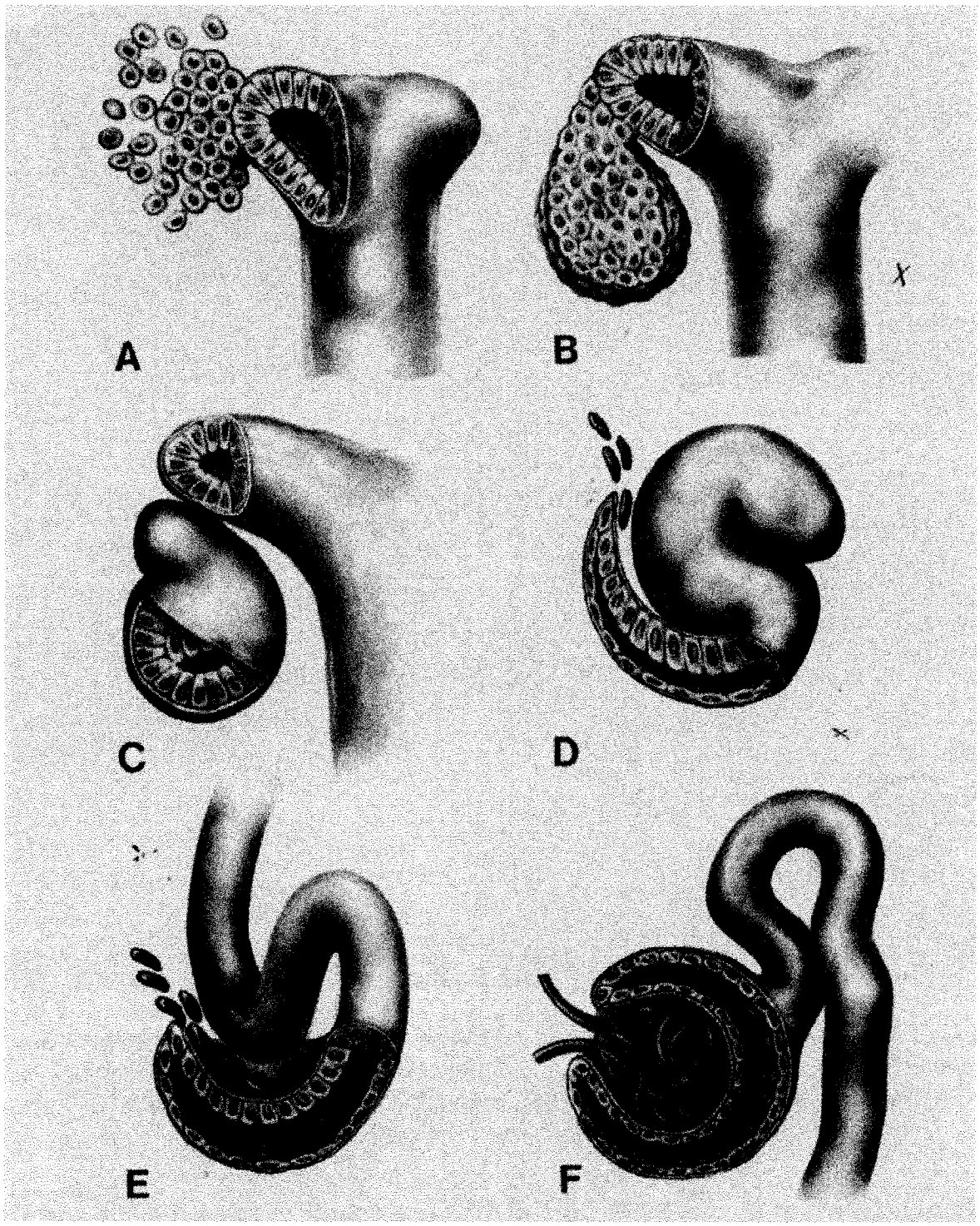
A
B
C
D
E
F

2. *The process of ureteric bud induction, extension and renal branching morphogenesis*

A. The Gdnf/Ret/Gfrα1 pathway promotes ureteric bud induction from the nephric duct

Many growth factors and transcription factors have been identified to be critical for ureteric bud induction. One of the main ligands that regulates the location and the initiation of ureteric budding is glial-derived neurotrophic factor (GDNF) that is secreted by the MM and then binds to its receptor, Ret and its co-receptor, Gdnf family receptor (Gfr) α1, situated on the surface of the future UB [5, 10]. Gdnf/Gfrα1/Ret signaling is critical for kidney development: if any of these genes are inactivated in the mouse, either no kidney forms or a malformed kidney arises due to a failure of the UB to invade the MM and undergo branching morphogenesis [11-14]. Furthermore, Pichel *et al.* cultured nephric ducts from either wildtype and *Gdnf* $^{-/-}$ mice in the presence of GDNF-soaked beads [15]. Remarkably, nephric duct explants from *Gdnf* $^{-/-}$ animals formed multiple buds in the presence of GDNF, similarly to what was seen in wildtype nephric ducts. This result shows that the duct and the UB respond to GDNF signaling from the MM in a dose-dependent manner. Therefore, both the formation and the subsequent branching of the UB are dependent on GDNF signaling from the MM to the nephric duct and the UB.

The role of GDNF during branching morphogenesis has been further characterized by Qiao *et al.* [16]. They cultured UBs under a variety of conditions where GDNF was either present in isolation, neutralized by the presence of a blocking antibody, or combined with other growth factors. For the UB to undergo branching morphogenesis, GDNF in combination with other growth factors was required. When GDNF was present alone or neutralized using an antibody, the UB failed to survive. Taken together, these results indicate that the Gdnf/Gfrα1/Ret cascade is necessary but not sufficient for UB development.

A number of other growth factor/receptor molecules and transcription factors are expressed by the MM and act upstream of *Gdnf* to affect its function [17]. Pax2 is a transcription factor that is critical for kidney development [18, 19]. It is expressed throughout the mesonephric duct, the UB and the adjacent MM at E10.5, and can bind to upstream regulatory elements within the *Gdnf* promoter and transactivate reporter genes, suggesting that it regulates *Gdnf* expression [20]. Pax2 appears to function within a

cascade of transcription factors including Eya1, Six1, Sall1, and Hox11 that all positively regulate expression of *Gdnf* in the metanephric mesenchyme [3, 21-23]. In contrast, other transcription factors such as Foxc1 and Foxc2 appear to negatively regulate *Gdnf* expression [24]. Growth factors that negatively regulate the expression of *Gdnf* include bone morphogenetic protein (Bmp)-4 [20] and Slit2 [25]. Most recently, Sprouty-1 has been shown to negatively regulate the expression of Ret [26].

In contrast, much less is known about the molecules that function downstream of the Gdnf/Gfrα1/Ret pathway. One target, is a member of the *Wnt* gene family, a group of secreted glycoproteins first identified in *Drosophila* [10]. *Wnt11* is expressed at the tips, but not the stalk of the developing UB and is believed to be required for UB branching [27]. Furthermore, when embryonic kidney explants are grown in the presence of an antibody to Ret, *Wnt11* mRNA is downregulated at the UB tips [28]. This suggests that the expression of *Wnt11* at the tips of the UB is modulated by Gdnf/Gfrα1/Ret signaling. Sulfated proteoglycans have been shown to modulate UB branching in embryonic kidney explants, and it has been postulated that they sequester high concentrations of growth factors like GDNF at the UB tips where they can exert their effects on branching morphogenesis [10, 29].

Figure 4. Branching and maturation of the ureteric bud.

The ureteric bud of the metanephros gives rise to the future collecting ducts and ureter (arrowhead) of the functional kidney. The trunks (arrow) of the ureteric bud will extend and allow for the tips (asterisk) to branch and induce the surrounding mesenchyme. The ureter (arrowhead) of the metanephric kidney extends and inserts into the future bladder. A whole mount image of an E12 mouse kidney labeled with an antibody to cytokeratin is shown (20x magnification).

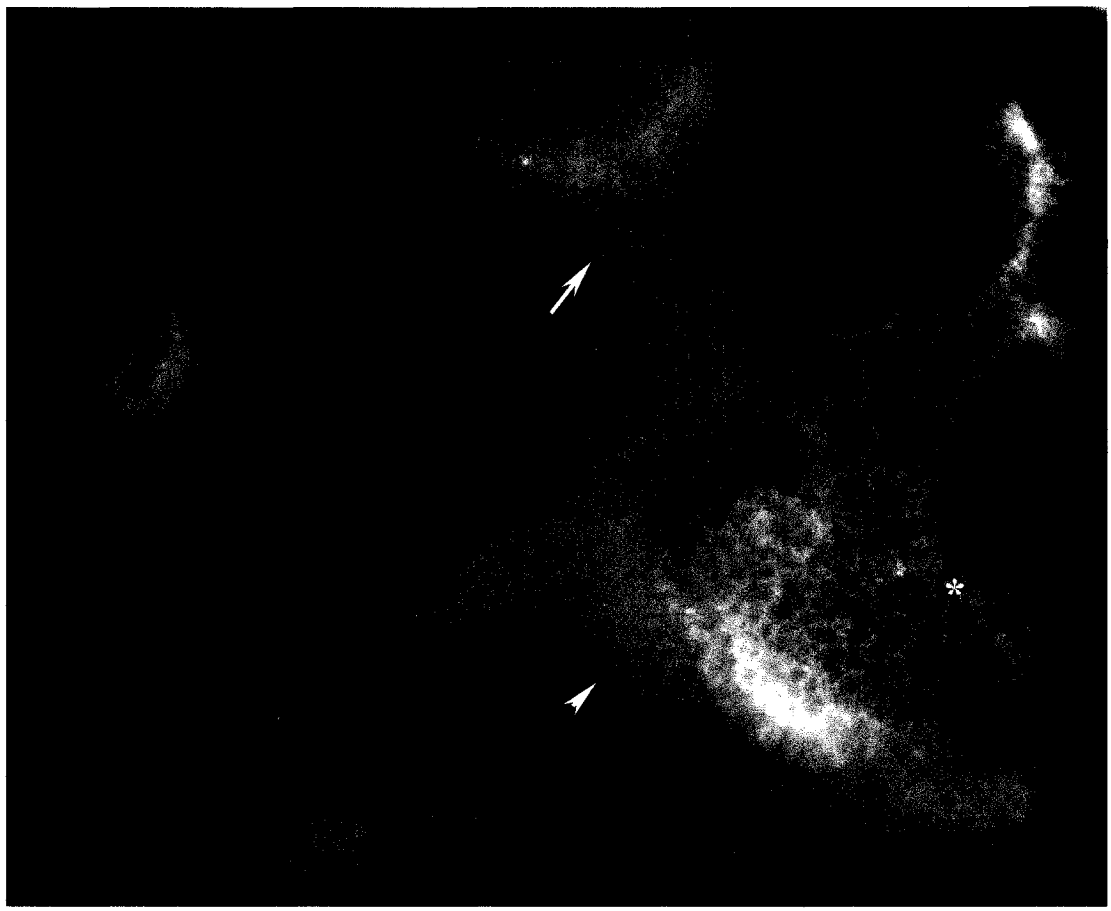

B. The TGF-β superfamily regulates ureteric bud branching and maturation

Members of the transforming growth factor-β (TGF-β) superfamily have also been shown to play a role in the growth and branching of the UB. Mesenchymal cells surrounding the nephric duct and the stalk of the ureteric bud express *Bone morphogenetic protein (Bmp)-4* [30]. Elongation of the UB has been shown to be sensitive to the presence of BMP-4. When embryonic kidney explants were grown in conditions that decreased the presence of sulfated proteoglycans (needed for UB branching) the addition of BMP-4 beads was shown to permit elongation of the UB stalks [30]. Interestingly, *BMP4* $^{+/-}$ mice show multiple defects in the development of the UB, such as hypo/dysplastic kidneys, hydroureters, and double collecting systems [30]. These congenital anomalies of the kidney and urinary tract (CAKUT) stem from two other effects of BMP4. BMP-4 inhibits the formation of supernumerary UBs from the nephric duct: in the *BMP4*$^{+/-}$ mouse, urinary tract duplications arise from ectopic UBs that develop and survive. In addition, BMP-4 is required for UB branching, and this process is reduced in the *BMP4*$^{+/-}$ mice leading to the hypo/dysplastic kidney defect [31].

The transforming growth factor-β (TGF-β)-1 ligand also affects renal branching morphogenesis. Bush *et al.* (2004) noticed that there was a significant reduction in the number of UB tips formed by kidneys cultured in the presence of TGF-β1 compared to those grown without TGF-β1. Furthermore, there was a reduction in both the width and length of the UB stalks. The observed defect in branching morphogenesis was significant: it resulted in a smaller kidney with a decrease in nephron number [32, 33]. Other TGF-β superfamily members also affect the development of the UB and have been recently reviewed [9, 34].

C. Transcription factors involved in the developing ureteric bud

Pax2, a transcription factor that is a member of the "paired-box" homeotic genes, is expressed by both the nephrogenic cord, which will give rise to the metanephric mesenchyme, and the nephric duct, which will give rise to the UB [35]. Targeted inactivation of Pax2 in the mouse leads to a striking phenotype where there is lack of formation of the kidneys, the urinary tracts and the genital tracts [36]. Analysis of

embryos at E11 demonstrated that the nephric duct did not extend caudally to the cloaca, but had degenerated and therefore no UB developed. This suggests that Pax2 is important for the growth of the nephric duct and UB formation.

Other transcription factors needed for UB development include Lim1. *Lim1* is expressed by the intermediate mesoderm, where it is thought to be necessary for its differentiation [37]. The metanephric kidney shows strong *Lim1* expression in the developing UB [38]. Kobayashi *et al.* (2005) conditionally knocked-out Lim1 from the UB lineage, using the *HoxB7* promoter. The kidneys of these mice were smaller secondary to a decrease in UB branching leading to the formation of fewer nephrons [38].

For the UB to develop, it must emerge from a specific location in the nephric duct, undergo elongation, and then branch repeatedly to induce nephron formation by the MM. From some of the examples outlined previously, it is evident that signaling pathways and transcription factors are important regulators of UB development, which ultimately determines the organization of the kidney and the final number of nephrons that form. Defects in the site of UB initiation or in UB branching can predispose individuals to conditions such as vesico-ureteric reflux, hypertension, and renal failure [8, 39].

D. Vitamin A is needed for ureteric bud and kidney development

As described previously, many signaling cascades, including the Gdnf/Gdnfrα1/Ret pathway, and transcription factors play a crucial role in allowing the ureteric bud to 1) extend from the Wolffian duct; 2) branch and form the future collecting ducts; and 3) form the future ureter. Studies have shown that *in utero*, kidney development and the molecular cues involved in the process are sensitive to micronutrients present in the fetal environment. The evidence for the role of vitamin A and its active biological form, retinoic acid, comes from rodent studies where animals have been deprived of vitamin A or members of the pathway have been knocked-out [40]. Lelièvre-Pégorier *et al.* (1998) monitored the effect of maternal vitamin A intake on the development of the fetal rat kidney. They showed that a decrease in the maternal intake of vitamin A, led to a reduction in the number of glomeruli in the fetal kidney [41].

A better molecular understanding of the relationship between retinoic acid and kidney development, can be obtained by examining studies on the retinoic acid nuclear receptors (RARs). RARs are transcriptional transducers of the vitamin A signaling pathway that can be divided into three families (α, β and γ), which have multiple isoforms [42]. Inactivation of certain RARs in the mouse has been shown to cause kidney and urogenital malformations. The Rarα$^{-/-}$β2$^{-/-}$ mouse model, where all Rarα isoforms were knocked-out, is an important model to understand the kidney malformation. In wildtype kidneys, *Rarα* and *Rarβ2* are expressed by the stromal cell compartment of the developing kidney. When these genes were knocked-out, the stromal cells were able to survive, as seen by the expression of the stromal cell marker *BF-2*. However, there was an increase in uninduced mesenchymal cells and a decrease in the number of ureteric bud tips. As well, Rarα$^{-/-}$β2$^{-/-}$ kidneys showed an absence in *c-Ret* at the ureteric bud tips and a reduction of *Wnt11* within the ureteric bud [43]. Taken together, these results suggests that maternal vitamin A is critical for fetal kidney development, through the interaction of its active form, retinoic acid, with the RARs expressed in the stromal cells in the developing kidney. This allows for signaling from the stroma to the ureteric bud, possibly via the metanephric mesenchyme, which in turn allows for proper ureteric bud branching and maturation, through the Gdnf/Gdnfrα1/Ret pathway [43].

The link between retinoic acid and Ret expression has been shown to affect the maturation of the urinary tract [44-46]. Defects that compromise the careful balance between vitamin A and *Ret* may lead to urinary tract defects such as vesico-ureteric reflux [8].

3. *Mesenchymal to epithelial transition and the final nephron*

A. From stem cells to the nephron

Remarkably, the cells of the metanephric mesenchyme are able to give rise to at least 14 to 26 different epithelial cell types during the process of nephrogenesis [47, 48]. Herzlinger *et al.* (1992) was the first to tag uninduced mesenchymal cells and demonstrate that they gave rise to both glomerular and tubular cells. These results

suggested for the first time that the MM were pluripotent stem cells, which could form all of the nephron except for the collecting duct [49].

Oliver *et al.* (2002) also examined the ability of MM cells to form other cell types in the developing kidney using an immortalized mesenchymal cell line and primary mesenchymal cells [50]. This work showed that MM cells can differentiate into epithelial cells as well as endothelial cells, myofibroblasts, and smooth muscle cells when cultured in the appropriate conditions. The demonstration that MM cells were able to express endothelial markers such as vascular endothelial growth factor (VEGFR)-2 and Tie-2 was particularly significant. Previously, it was believed that endothelial cells migrated into the kidney from an exogenous source, but weren't formed locally within the kidney [48]. Understanding the steps by which an undifferentiated mesenchymal cell can form these various cell types continues to be an important area of research since it has the potential to lead to new strategies to repopulate sick or damaged kidneys with healthy pluripotent stem cells.

B. Markers of the stages of mesenchymal to epithelial transition

Many researchers have attempted to identify specific molecular markers that correlate with the discrete morphological stages observed during MET. When mesenchymal cells first condense at the tips of the ureteric bud, they express *Pax2*. *Pax2* continues to be expressed in the renal vesicle, comma-shaped and S-shaped bodies, as well as the developing ureteric bud, and then is turned-off in the mature nephron [51]. While expression of Pax2 in the MM is important for inducing the future UB, it also plays a role in the differentiation of the MM itself. From tissue recombination experiments, it has been demonstrated that MMs harvested from *Pax2* $^{-/-}$ embryos were unable to undergo MET even when recombined with wildtype heterologous inducers like UB or spinal cord [20]. Furthermore, kidneys from *Pax2* $^{-/-}$ mice showed a marked reduction in the number of mesenchymal cells that aggregated around the UB tips and underwent MET [19]. Dressler *et al.* (1993) created a transgenic mouse line in which *Pax2* was overexpressed using the CMV promoter [52]. In this model, the newborn pups died from renal failure and examination of their kidneys revealed the presence of microcysts and foot process loss and fusion as observed in congenital nephrotic

syndrome. These changes demonstrate that it is important that Pax2 is repressed in the mature nephron; otherwise the mesenchymally derived renal epithelium will undergo abnormal proliferation and lead to cyst formation. Taken together, correct spatial and temporal expression of Pax2 is critical for normal kidney development since the protein regulates the development of both the MM and the UB.

The Wilm's tumour suppressor gene (WT-1) is a transcription factor, which is initially expressed at E9.0 in the nephric duct of the intermediate mesoderm. It is then expressed by the uninduced metanephric mesenchymal cells (E10.5), the comma-shaped bodies, the S-shaped bodies, and the glomerulus [53]. *Wt1*$^{-/-}$ embryo fail to form a metanephric kidney [54]. In this model, Kreidberg *et al.* demonstrated that MM cells within the blastema underwent apoptosis and were then unable to induce the UB to emerge from the nephric duct [54]. Interestingly, MM blastemas from *Wt-1* $^{-/-}$ kidneys grown in the presence of inductive factors for MET, do not condense, nor do they express Pax2 [10], suggesting that WT-1 is needed to activate Pax2 in the developing mesenchyme. Finally, Discenza *et al.* (2003) showed protein-protein interaction in vitro and in vivo between WT-1 and PAX2 [55]. Taken together, these results suggest that Pax2 and WT-1 may form a regulatory circuit: Pax2 initially activates WT-1, and then WT-1 represses Pax2 in the MM as it undergoes MET such that Pax2 is no longer detected in the mature nephron [2].

Another marker of MET can be seen in the expression pattern of *Wnt4*. Wnt4 is a member of the *Wnt* gene family that is initially expressed in the renal vesicle and continues to be detected in S-shaped bodies. Thereafter, it is downregulated in the mature nephron [2]. *Wnt4*$^{-/-}$ mice have small malformed kidneys consisting of undifferentiated mesenchyme [56]. Strikingly, the ureteric bud invades the mesenchyme and branches however the mesenchyme fails to undergo MET. Furthermore, Kispert *et al.* (1998) showed that Wnt4 can cause MM blastemas to undergo MET in the absence of an inducer. NIH3T3 cells stably transfected with a vector encoding Wnt4 and cultured in proximity to MM explants lead to the formation of MET structures in the mesenchyme explants [57]. This body of evidence shows that *Wnt4* is important for activating mesenchymal-to-epithelial transition. Recently, Carroll *et al.* (2005) demonstrated that Wnt9b, a member of the Wnt signaling, regulates Wnt4. Wnt9b$^{-/-}$ kidneys show a

reduction in the expression domain of *Wnt4*, and of other markers of pretubular mesenchyme markers, such as *Pax8* and *Fgf8* [58]. In contrast, $Wnt4^{-/-}$ kidneys maintain *Pax8* and *Fgf8* expression. Therefore this data shows that Wnt9b acts upstream from Wnt4, and that the activation of other mesenchyme markers, such as Pax8 and Fgf8, are Wnt9b dependent and therefore Wnt4 independent.

Pax2, WT-1, and *Wnt4* are a few examples of molecular markers that correlate with some of the stages of MET. Other markers also exist and have been recently reviewed [3]. While the expression patterns of these markers are clearly not limited to individual stages of MET, they do influence the cellular and morphogenetic events that are taking place during these stages. With new advances in tissue-specific inactivation of genes, undoubtedly their roles will be further elucidated in the near future.

C. Growth factors needed for mesenchymal to epithelial transition

Conditioned medium extracted from cultured ureteric bud cells has been an important resource to identify the factors that induce MET. When uninduced mesenchymal cells were exposed to conditioned medium from Rat Ureteric Bud 1 (RUB1) cells, they expressed markers of MET such as *WT-1* and *Wnt4* [59, 60]. Barasch *et al.* (1999) went on to purify conditioned medium from UB cells and identified Leukemia Inhibitory Factor (LIF) as a critical growth factor important for MET [61]. He then cultured MM tissue alone without the UB in the presence of LIF and the survival factor known as Fibroblast Growth Factor (FGF)-2 and showed that *Pax2* and *Wnt4*, markers of MET, were now expressed. Furthermore, the induced MM tissue explants also expressed the epithelial marker E-Cadherin. In a similar set of experiments, Plisov *et al.* (2001) identified TGF-β2 as another "inductive" factor in UB-conditioned medium, which promoted MET in uninduced metanephric mesenchyme explants. Explants that were treated with FGF-2 and either LIF or TGF-β2 underwent MET within 7 to 8 days in culture. However, when these same cultures were treated with a combination of all three growth factors: FGF-2, LIF, and TGF-β2, MET happened within 72 hours [62].

Other members of the TGF-β superfamily have also been shown to be important in the differentiation of MM cells. Kidneys from *Bmp4* $^{+/-}$ embryos have cystic lesions, a reduced nephrogenic zone, and an increase in apoptosis in MM cells. These

abnormalities are either primarily due to a failure in MET with a secondary effect on the UB; or a flaw in the UB branching that affected MET. [31]. The same group of investigators went on to speculate that the cystic renal lesions were also likely related to a defect in mesenchymal cell proliferation since the cysts were seen in tubular structures and glomeruli. Interestingly, *Bmp7*$^{-/-}$ mice have a renal phenotype that is also similar to the *Bmp4*$^{+/-}$ mouse, which includes a reduced nephrogenic zone and an increase in mesenchymal cell apoptosis. Both BMP-7 and BMP-4 permit MM cells to survive but neither is sufficient by itself to permit MET to occur [63].

The metanephric mesenchymal cell population is pluripotent during kidney development. It appears that MM cells have several fates: they can be induced to epithelialize when exposed to an inductive signal from the UB, they can become stromal cells, they can become endothelial cells, or they can undergo programmed cell death. Furthermore, it is highly likely that the local concentration of growth factors and transcription factors determines the fate of any given MM cell and ensures that MM cell differentiation is regulated to maintain nephron formation. In summary, the formation of the metanephric kidney is a complex process that requires precise temporal and spatial regulation of both UB branching and MET to ensure that sufficient nephrons form and that they are able attach to collecting ducts. More work still needs to be done to determine the role of signaling cascades and transcription factors in kidney development.

In the next section, I will discuss the use of genetically engineered rodents and cultured mouse embryonic kidneys which are both important models to understand the role of signaling cascades and transcription factors in the developing kidney.

4. *Methods to evaluate gene function in the developing kidney*

A. In vivo approaches to study candidate genes

In 1985, when Smithies *et al.* reported the ability to insert a sequence of DNA in the human β-globin locus using homologous recombination, a genetic revolution was underway. By introducing DNA sequences into mammalian genomes, there was a now a potential means to replace abnormal or absent genes and treat disease at a genetic level [64]. The mechanism of modifying a gene through homologous recombination relies on

the ability of a vector, encoding a homologous sequence to the host's sequence, to recombine within a host's homologous chromosomal sequence. The main components of a targeting vector include the plasmid backbone, the genomic DNA sequence that is homologous to the chromosomal site to be targeted and the selection marker(s) that usually consists of DNA that encodes for antibiotic resistance. Once the vector has been incorporated into embryonic stem cells (ES) via electroporation, antibiotic resistance identifies cells that have successfully incorporated the vector [65]. These ES cells are then injected into blastocysts from which animals containing the targeted allele can be derived [65].

Over the past 20 years of genetic engineering in the mouse, homologous recombination-based targeting strategies have been the method of choice to permit stable site-specific modifications to the genome. While this method has been extremely powerful to understand the function of genes in the mouse, there are some limitations. Firstly, the potential for recombination to occur in random locations in the genome is a frequent event, occurring at a rate as high as 1/100 of treated cells [66]. Furthermore, recombination may occur in multiple regions of the genome and lead to mutagenic effects by inhibiting or activating host genes at the site of integration [65]. Secondly, Smithies *et al.* (1985) reported that the rate of successfully targeted recombinant cells was very low, approximately 1/1000-1/10000 of treated cells. Recent efforts have focused on increasing the rate of successful recombination by manipulating the DNA repair machinery of the host ES cells once the homologous DNA vector has been transfected. One means to increase gene-targeting efficiency is to introduce a double-stranded DNA break in the locus to be targeted: homologous recombination is the major mechanism by which a cell repairs this type of DNA break. The targeting vector is constructed such that it contains a DNA recognition sequence for a rare cutting restriction enzyme such as I-*Sce*I for example. The first step is a classical homologous recombination step using a replacement vector that encodes homologous sequences to the host's chromosome and a positive selection marker. In the second step, the locus is re-targeted by co-transfection of a second replacement vector with a plasmid-expressing I-*Sce*I. This enhances the rate of successful recombination by as much as 10 to 10 000 fold [66]. Another method to stimulate the cell's DNA repair machinery and increase the rate of homologous

recombination is to use triplex-forming oligonucleotides (TFOs), a chemical agent that damages poly-purine DNA regions in combination with irradiation of cells using UVA rays [66].

Finally, knocking out genes using homologous recombination leads to genetic inactivation in all cell types, tissues and organs of the developing embryo. If a particular gene has an important role in early embryonic development, then when it is inactivated, this may result in embryonic lethality. While this phenotype is informative, it does not permit an understanding of how a particular gene functions at later stages of development. The formation of the metanephric kidney occurs relatively late during embryonic development of the mouse (E10.5-E11; [8, 67]). When genes that are essential for embryonic survival are inactivated, early lethality may arise prior to formation of the kidneys as observed in mice where Smad1 has been inactivated [68]. SMAD1, a transcription factor that is activated during BMP signaling, and expressed in the uninduced mesenchyme, has been shown to be important in the development of the ureteric bud and the metanephric mesenchyme [69, 70] (See *I.1 Mammalian kidney development*). However, $Smad1^{-/-}$ mice die at E9.5; therefore, this model is not useful for understanding the role of this transcription factor during kidney development [71]. Taken together, there is a definite need for alternative approaches where genes can be conditionally inactivated to avoid embryonic lethality.

An alternative to homologous recombination is the conditional excision of a gene. Conditional targeting involves the use of site-specific recombinase proteins that recognize and mediate the recombination between short DNA sequences. Two such recombinases are Cre, identified in the P1 bacteriophage and Flp, identified in *S. cerevisae* [72]. Deletion of the DNA polymerase β gene in mice leads to embryonic lethality; therefore in 1994, Gu *et al.* developed a new method where they used the Cre recombinase enzyme to selectively excise the DNA polymerase β gene only in T cells. This innovative approach now permitted them to generate mutant animals that were viable [73]. Cre and Flp recognize a specific 34-nucleotide sequence that consists of two 13 nucleotide palindromic sequences separated by a 8 nucleotide spacer. The Cre and Flp proteins recognize respectively the *loxP* or the *FRT* target site [65] and can excise with great fidelity, nucleic fragments of up to 4 Mb which are located (also referred as

"floxed") between two target sites by cleaving, exchanging and ligating the chromatin [72, 74].

Gene excision can occur in a specific tissue and at a selected time during development if the recombinase is being driven by an appropriate promoter element. In the developing kidney, the *HoxB7* gene is expressed in the ureteric bud and its derivatives. Srinivas *et al.* (1999) fused the open reading frame of the green fluorescent protein (GFP) to the *HoxB7* promoter and observed reporter gene expression in the Wolffian Duct, ureteric bud and the collecting ducts of the mature kidney [75]. Yu *et al.* (2002) and Oxburgh *et al.* (2004) both took advantage of the specific tissue expression of *HoxB7* to conditionally knock-out, respectively, *Sonic Hedgehog* and *Smad4* from the developing ureteric bud by crossing mice with a floxed allele to mice that were carrying a *HoxB7/cre* transgene [70, 76].

The power to selectively knock-out a gene is only as robust as the specificity of the promoter and the efficiency of the recombinase. For example, it has been difficult to identify a promoter element that is exclusively expressed by the metanephric mesenchymal cells of the developing kidney [67]. Oxburgh *et al.* resolved this difficulty by conditionally knocking out Smad4 in the UB using *Hoxb7/Cre* mice, and then comparing this to a similar cross using *Bmp7/Cre* mice where SMAD4 was excised in both the UB and the MM [70]. While excision of SMAD4 in the UB lineage generated no renal defects, when excised from the MM and the UB, an abnormal kidney phenotype was noted. At E16.5, the kidneys showed an increase in the number of stromal cells and a decrease in the mesenchymal cell population. This result suggests that the TGF-β pathway is essential for maintenance of mesenchymal cell number during kidney nephrogenesis [70]. Recent efforts to excise *Fgf8* and *Lim1* in the mesenchyme have used respectively the *Pax3* and the retinoic acid receptor *Rarb2* promoter [38, 77, 78]. Although both *Pax3* and *Rarb2* mainly localize to the metanephric mesenchyme, expression still remains in tubules and collecting ducts of ureteric bud origin [38, 79]. Therefore, gene excision solely in the mesenchyme of the kidney still remains an elusive endeavour, which will only be resolved when a promoter element that is specific for metanephric mesenchymal cells is identified.

B. In vitro approaches to study candidate genes

Embryonic rodent kidneys are easy to grow in culture and have become an important *in vitro* model to examine the effect of candidate genes during kidney development. By adding growth factors, antisense oligonucleotides, blocking antibodies and/or pharmacological agents directly to the culture media, one can ask questions about the roles of specific molecules during kidney development [80]. More recently, methods to manipulate gene function *in vitro* have been developed and rely on the overexpression of wildtype and mutant proteins either through viral infection or by electroporation of vectors bearing the gene of interest. In regards to these latter methods, genetic manipulation can occur either through gene-addition by which the vector exists as an extrachromosomal episome, or through gene-targeting where specific genetic changes are introduced by homologous vector sequences [65, 81].

The study of candidate genes using cultured mouse embryonic kidneys has focused on loss-of-function experiments. Anti-sense oligonucleotides (ODNs) have been used to impede on the translation of gene transcript. This method has been used to block the expression of neurotrophin receptors (Durbeej *et al.*, 1993), c-ros and c-ret protooncogenes (Liu *et al.*, 1996), the Cux-1 homeobox gene (Quaggin *et al.*, 1997) and Pax2 (Rothenpeiler and Dressler, 1993) in kidney explants. In these studies, ODNs that target critical regions of the transcript, such as the start codon for example were added directly added to the media (Durbeej *et al.*, 1993; Rothenpeiler and Dressler, 1993; Liu *et al.*, 1996; Quaggin *et al.*, 1997). By inhibiting *PAX2* translation, for example, there was a defect in the number of mesenchymal structures that underwent epithelialization (Rothenpeiler and Dressler, 1993). Certain aspects of this experimental technique are not optimal. The sequence of anti-sense ODNs must be unique for the gene of interest to avoid nonspecific effects due to the inactivation of other genes (Rothenpeiler and Dressler, 1999). As well, since the kidney is exposed to the ODN present in the media, there is no way to preferentially direct ODN uptake in either the ureteric bud or the metanephric mesenchyme. It has been reported that it is much more difficult to block gene expression in the ureteric bud compared to the metanephric mesenchyme (Liu *et al.*, 1996).

The use of virus-mediated gene delivery has been an effective means to misexpress transgenes and to manipulate gene expression in the chick. Here, the method of choice appears to be the use of the replication-competent retrovirus system. While this method offers a high level of efficiency, there are several disadvantages: the length of the transgene can be no larger than about 2.4kb, there is a time lag between viral infection and the onset of transgene expression that may be as long as 12 hours, and infection only occurs in cells that are actively proliferating [81, 82].

The physical insertion of DNA has been reported in various cell types, such as plant cells, endothelial cells and fibroblasts. Physical techniques include microinjecting DNA into cells; submitting cells to an electric field, known as electroporation; and particle bombardment or "shotgun technique", where cells are bombarded with tungsten particles coated with DNA [83]. Microinjection of a DNA plasmid followed by electroporation is one of the most efficient non-viral methods to deliver genes [83]. Electroporation refers to the process whereby an electric field is applied to either cells or a tissue, which leads to the formation of pores and the entry of DNA into the cell's cytoplasm [84] and the nucleus where transcription occurs. There are many advantages to this method: there is no need to propagate a virus using a suitable cell line; large DNA sequences, up to 150kb, can be microinjected and electroporated; both proliferating and non-proliferating cells can be manipulated; and the lag time from injection/electroporation to expression of the gene of interest is markedly reduced [85]. Expression of the gene of interest appears as early as 3 hours after electroporation [82].

5. *Molecular basis of electroporation*

A. Theory of electroporation and electropore formation

Electroporation of cells or tissues refers to the process whereby an electric field is applied to a tissue and leads to the breakdown of cell membranes [85]. This then permits a wide variety of agents to be transferred inside a cell including protein, RNA, or DNA [86]. The electric field is created between two electrodes, one of which is negative, the cathode, and the other positive, the anode. The cell membrane acts as an electrical capacitor, which permits current to pass through ion channels: this weakens the

impermeability of the lipid bilayer and leads to the formation of pores within the membrane, known as electropores [87]. To achieve a high level of DNA transfer, several parameters need to be optimized such as voltage, and the duration of exposure [84, 88].

Gehl (2003) reports that in order for an electrical field to be sufficient to create electropores, it needs to exceed the resting transmembrane potential of the cell at its lipid bilayer [89]. The transmembrane potential induced by electroporation can be mathematically described where:

$$\Delta V_m = f E_{ext} r \cos(\phi)$$

"ΔV_m" is the transmembrane potential, "f" is a coefficient that describes how the cell impacts on the distribution of the electric field, "E_{ext}" is the applied electric field, "r" is the radius of the targeted cell and "ϕ" is the angle by which the cell is oriented with respect to the electric field [89]. Therefore electropores form when an electric field is applied and is greater than the ΔV_m of a cell. The sustained application of the electric field stabilizes the electropores in the membrane and permits DNA molecules to enter the cell's cytoplasm. Finally, when the electric field is stopped, the electropores are annihilated. Membrane impermeability then resumes as the membrane is no longer subjected to an electrical field superior to its transmembrane potential [88].

Tieleman (2004) has presented a model to explain the formation of electropores that permit the passage of macromolecules, meaning molecules whose size is greater than a few kD [90]. In this model, electropores form due to the effect of the electric field on the water molecules located on the cytoplasmic surface of the lipid bilayer. The water molecule, H_2O, acts as an electric dipole, since the electronegative oxygen atom attracts the only electron of both electropositive hydrogen atoms [90]. The negative cathode of the electric field attracts the electropositive hydrogen atoms of the water molecule in its direction. The electric force leads the water molecules to enter the lipid bilayer and therefore disrupt the membrane. A membrane enriched in water will bend, twist and deform, which later allows for weaknesses to form inside the lipid bilayer and form electropores [91]. Because of these disruptions, water molecules enter within the lipid bilayer, and increase the hydrophilicity of the membrane. Once there are a critical number of water molecules within the lipid bilayer, the membrane weakens at certain locations and allows for electropores to form. Through these electropores it is therefore

possible for exchange to occur between the extracellular environment and the cell's cytoplasm (Figure 5) [88].

B. DNA uptake via electropores

Charged macromolecules, such as DNA, have a complex mechanism by which they travel through electropores within the cytoplasm of a cell. When first exposed to cells, DNA tethers to the cell's membrane [86]. Once the electrical field is applied and electropores are formed, the negatively charged DNA molecule is believed to interact with the positively charged hydrogen ion within the water molecule. Therefore, by charge complementarity between the positive water molecule and negative DNA, the macromolecule can make its way through the water-enriched regions of the otherwise impermeable lipid bilayer [87].

Phez *et al.* (2005) showed that the side of the membrane that faces the cathode favours DNA to pass through the membrane. First, on the cathode-facing side of the cell, there will be the greatest change in transmembrane potential leading to the disruption of the water molecules within the bilayer. This will drive the electropositive hydrogen atoms of water molecules to be driven in the direction of the cathode which leads to a greater likelihood of water infiltration in the membrane and electropore formation [87]. Second, the electric force of the negative cathode will have an electrophoretic force on the DNA, causing it to move away from the negative electrode and interact directly with the electropores of the membrane (Potter, 1988). Interestingly, by switching the orientation of the anode and cathode, and therefore the direction of the electric field, at each pulse, 20 % more DNA can be taken up into the cell. The increase in DNA integration allows for macromolecules that were tethered on both sides of the membrane to permeate inside the cytosol [86].

Figure 5. The water molecule and its involvement in the electroporation process.

A) The water molecule consists of two electropositive hydrogen atoms (white spheres – δ^+) and one electronegative oxygen atom (red spheres – δ^-). The electrons of the hydrogen atoms are attracted by the larger oxygen atom, rendering a slight shift of most electrons in the water molecule towards the oxygen atom. The water molecule is therefore an electric dipole, with a dipole moment pointing in the direction of the arrow.

B) Water molecules have a disorganized orientation of their atoms. The hydrophobic tails of the lipid bilayer (black lines) hinder the passage of water and other charged hydrophilic molecules (orange spheres) between the extra-cellular environment and the cell's cytoplasm.

C) When an electric field is applied (black arrow), the slightly positive hydrogen atoms are attracted by the negative charge of the cathode and make their way into the membrane. The water enriched hydrophobic region of the membrane causes disorganization and weaknesses to form at the lipid bilayer.

D) The increase of water molecules in the membrane, due to the presence of the electric field, allows electropores to form and therefore the passage of molecules between the cytoplasm and the extra-cellular environment. The passage of DNA through these electropores (arrow) is increased by the presence of an electrophoretic force which directs the DNA to go from the cathode to the anode.

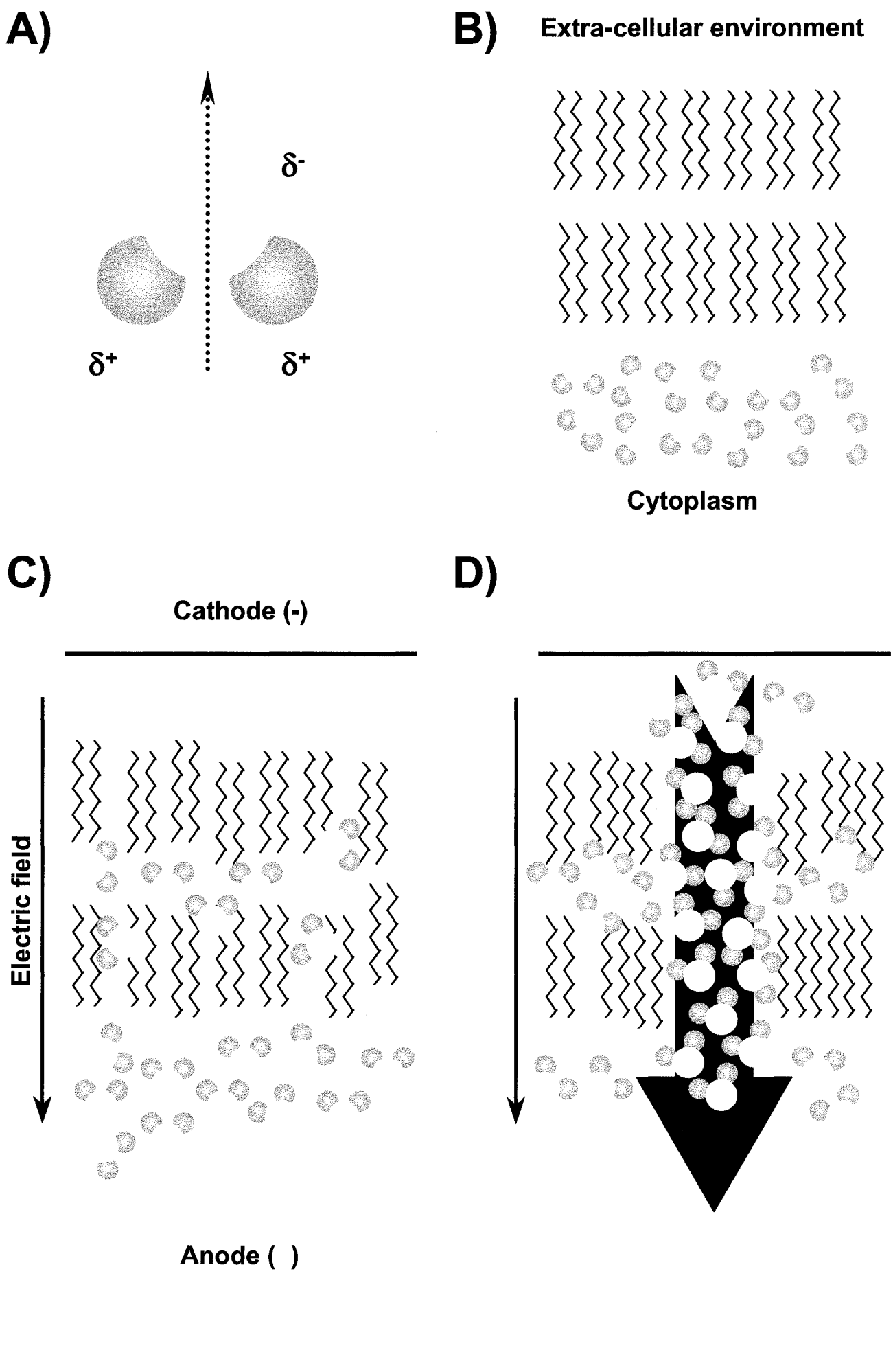
A)
δ-
δ+
δ+
B)
Extra-cellular environment
Cytoplasm
C)
Cathode (-)
Electric field
Anode ( )
D)

C. Effect of the components of an electrical field at a cellular level

Rols and Tessie (1998) have identified the components of an electric field that need to be taken into account when establishing parameters for electroporation. First the electric field strength (E_{ext}) of the pulse determines how much of a cell's surface area will be affected by the electric field. A high electric field strength allows for a larger cell surface area on which electropores can form [88]; and thus increases the opportunity for macromolecules to cross the lipid bilayer and enter the cell's cytoplasm. The duration of the pulse (T) correlates with the diameter of the electropores that are formed at the membrane surface. Such that a longer pulse leads to larger electropores. Macromolecules, such as DNA or β-galactosidase, are only able to penetrate within the cells if the electropores are relatively large. Other critical parameters that need to be considered are the number of pulses to be delivered. An increase in pulse number allows for greater integration of DNA and expression of the transgene [88].

The optimal parameters for establishing a suitable electroporation protocol require an electric field that balances field strength with the duration and the number of pulses [88, 91]. From the literature, electroporation protocols for DNA transfer have been variable: some have used a low voltage combined with a long pulse (LV/LP)[92-95], while others have used a high voltage combined with a short pulse (HV/SP)([96-98]. A LV/LP protocol should lead to a small-targeted surface area, because of the small electric field, however the long pulse time will increase the diameter of the electropores. Furthermore, a longer pulse time will enhance the mobility of DNA across the lipid bilayer by the longer duration of the electrophoretic force [99]. In contrast, a HV/SP protocol should lead to a large targeted surface area on which multiple electropores with smaller radii can form.

In order for a cell to uptake a macromolecule, such as DNA, by electroporation, an electric field greater than the transmembrane potential must be applied. Once this is achieved, water molecules infiltrate into the membrane, causing it to weaken and electropores to form. The DNA molecule enters the cell due its interaction with the water molecules that reside in the electropores. Furthermore, the electrophoretic force applied by the negative cathode onto the negatively charged DNA molecule, allows for greater cellular entry. The electric field strength and the pulse duration are the major

contributing components that determine electroporation efficiency. The applied electric field to the cells must be a balance between pulse length and field strength. If either is excessive, cell lysis and death will occur.

II. RESEARCH PROPOSAL

Many reports that have studied the process of electroporation on cells have focused on using a low voltage/long pulse time (LV/LP)[88]. However, as Canatella *et al.* (2004) demonstrate, electroporating a multicellular is much more complex, than single suspended cells; and therefore a LV/LP protocol may not be adequate [99]. The greatest concern is that the electric field generated with an LV/LP protocol may be too weak to permeate and cause electropores to form on all cells and cell type within a tissue. This is due to the fact that cells within a tissue are heterozygous in size, they may be less accessible because of their location within the tissue and they may vary in terms of their state within the cell cycle. Canatella *et al.* (2004) demonstrate that within a cluster of high-density cells a high voltage/short pulse (HV/SP) protocol permits greater macromolecule incorporation, and thus higher transgene expression.

Recently, microinjection and electroporation has also been used as a method to overexpress DNA constructs encoding wildtype and mutant proteins in embryonic mouse kidney explants [100]. The study examined the regulation of Vegfa by Wt1 in embryonic kidneys by microinjecting and electroporating vectors overexpressing Wt1.

While this was the first to report the use of the electroporation method in embryonic kidneys, there was a limited assessment of its efficacy and its toxicity. Here we report our work where we have examined this method in greater depth to establish the optimal conditions for high-level expression of DNA-encoding vectors and to determine its toxicity. Through these results we have a better understanding of the technique and can use it in an optimal fashion, in order to modulate gene expression and function in the developing kidney.

III. MATERIALS AND METHODS

1. Microinjection and electroporation

A. Animal care, dissection, kidney culture

Time-pregnant CD1 females were ordered from Charles River Laboratories (Inc.). *HoxB7/GFP*$^{+/-}$ heterozygous mice, obtained from Dr. F. Costantini [75] were mated overnight to CD1 females. The presence of a vaginal plug indicated pregnancy, and such embryos were defined as 0.5 days of age. The mice were maintained and sacrificed in accordance with the Canadian Council on Animal Care (CCAC) guidelines (See attached Animal Care Protocol).

Kidneys were dissected under sterile conditions. Dissecting equipment was washed between embryos with 70% ethanol, and embryonic kidneys were stored in filtered phosphate-buffered saline (PBS) prior to microinjection and electroporation. Kidneys were randomized amongst treatments to avoid embryo and litter effects on growth [80].

Kidney cultures were maintained in a humid incubator at 37°C with 5% CO_2. Kidneys were grown in DMEM/F12 (Invitrogen) that was supplemented with 5% fetal bovine serum (FBS) and 1% penicillin/streptomycin on 0.45 μm polyethylene terephthalate membrane (Falcon) in 6-well multiwell plates (Falcon). Kidneys were treated as described [80] and media was changed daily. Up to a maximum of 12 kidneys were placed on a membrane (Falcon) and 2 membranes were used for each 6 well plate to allow the cultured kidneys to be stored in the incubator for as long as possible during the experiment.

B. Microinjection and electroporation

A KOPF 720 needle puller was used to prepare the microinjection needles from glass capillary tubes (Narishige) and the settings for velocity and temperature were set at 13 and 2, respectively. An IM 300 microinjector (Narishige) was used to deliver an average volume of 0.025 μl of eGFP vector (5 μg/μl – Clontech) and FastGreen dye (Fisher) (mixed in a ration of 50:1). A BTX electroporator (ECM 830) delivered a square wave 5-pulse electric field ranging from 25 to 500 volts and 25 μs to 50ms: the delay

between each pulse was set at 500 ms. The kidneys were placed between platinum needle-style L-shaped electrodes (Dr. A. K. Ryan), with a 0.5 mm diameter, that were spaced 4 mm apart. (Figure 6).

When required, spatial targeting of the transgene in the mesenchyme or the ureteric bud was achieved by microinjecting the transgene in the outer cortex or the pelvic area of the kidney, respectively (Figure 7).

C. Antibodies and whole mount staining

An antibody directed to cytokeratin (Zymed), raised in rabbit, was used at a 1/50 concentration in 10% goat serum/PBS. An anti-rabbit secondary antibody, Alexa Fluor 594 (Molecular Probes; kindly provided by Dr. A. K. Ryan), raised in goat, was used at a 1/200 dilution. Embryonic kidneys were fixed in 4% paraformaldehyde (PFA) either overnight at 4°C or for one hour at room temperature. Kidneys were then washed in PBS 3 times for 10-15 minutes, followed by a 1 hour permeabilization step in cold 100 % methanol at -20°C. Note: samples could be stored in methanol at -20°C for many months and still be processed for whole-mount antibody staining. A 5-step rehydration process occurred by passaging the kidneys through 100%, 90%, 70%, 50% ethanol and then 1X PBS, all done at 4°C. This was followed by three washes of 10-15 minutes in 1X PBS. Kidneys were then blocked in 10% goat serum/PBS overnight at 4°C. Over the course of the next day, the samples were washed in 1X PBS 3-5 times for 30-60 minutes for each wash. The kidneys were incubated with the antibody to cytokeratin at the prescribed concentration, overnight at 4°C. This was followed by 3-5 washes with 1X PBS for 30-60 minutes for each wash. Following the washes, kidneys were then incubated with the anti-rabbit secondary antibody, overnight at 4°C. This was followed by another 3-5 washes with 1X PBS for 30-60 minutes for each wash. Samples were mounted with drops of Permount (Fischer) located at each corner of the coverslip.

Figure 6. Electroporation and microinjection set-up.

A) Microinjection, electroporation and microscope set-up used in this study. To the right of the image there is the microinjector that holds the microinjection needle. The electroporator is seen above and behind.

B) The platinum needle-style L-shaped electrodes (0.5 mm radii) were placed 4 mm between each other in order to electroporate embryonic kidneys.

A)

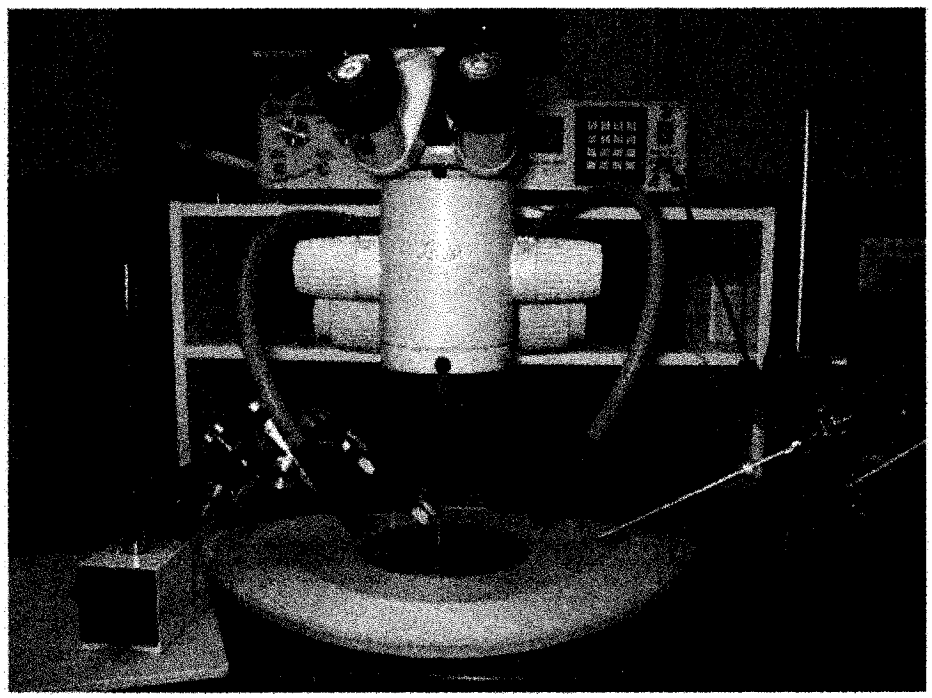

B)

Figure 7. Spatially targeting the mesenchyme or the ureteric bud in the embryonic kidney.

A) Mesenchyme targeting was achieved by positioning the microinjection needle in the other cortex of the kidney.

B) Microinjecting into the pelvis of the mouse embryonic kidneys targeted ureteric bud cells.

A)

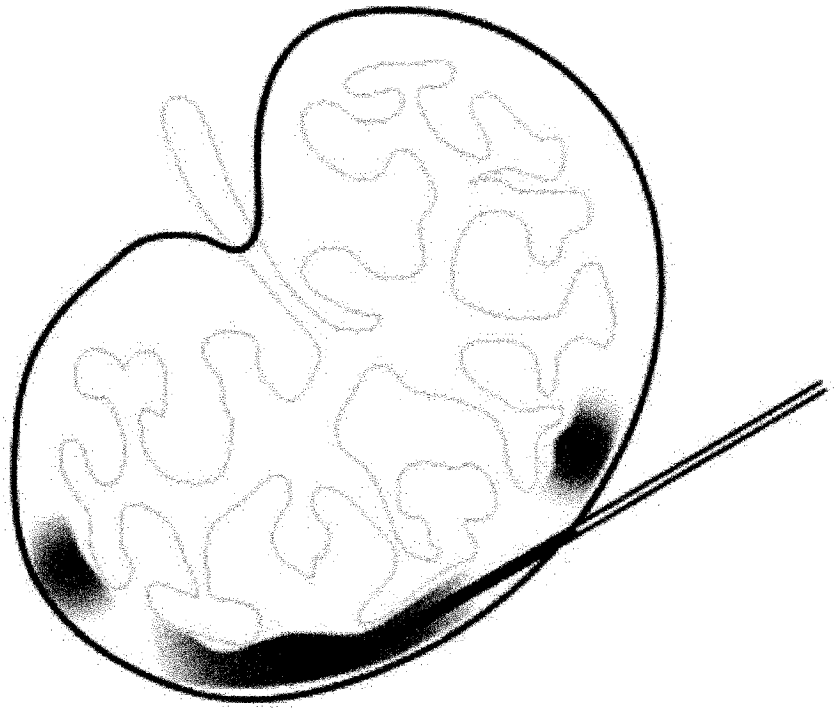

B)

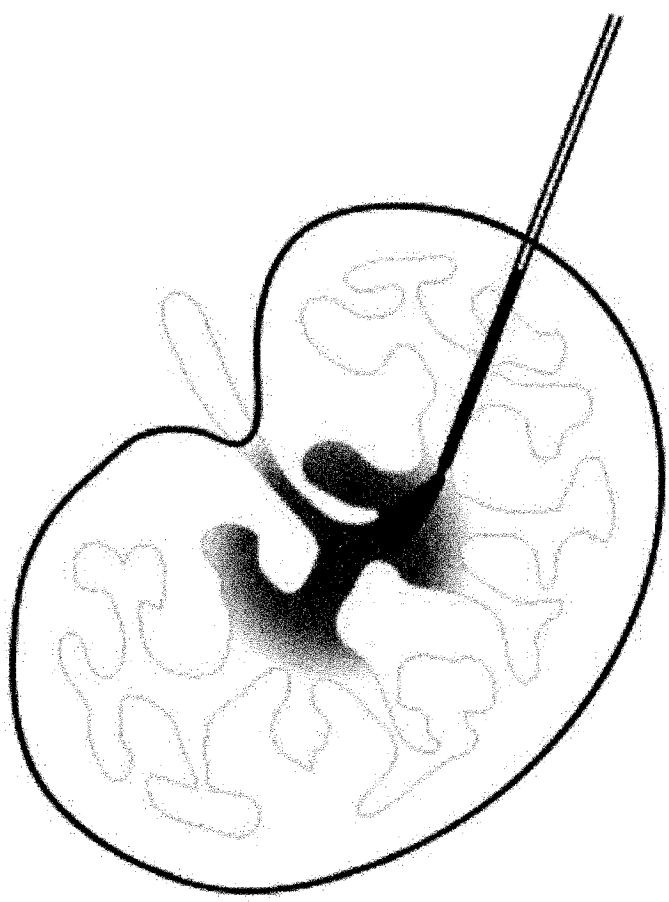

Samples were visualized using a Zeiss confocal microscope (Faculty of Anatomy and Cell Biology, McGill University).

D. Tissue sectioning and hematoxylin and eosin staining

Tissue was fixed using 4% PFA for either one hour at room temperature or overnight at 4°C. The kidneys were then incubated in 5% sucrose/PBS solution for 4-6 hours and then transferred to a 20% sucrose/PBS solution and kept overnight at 4°C. OCT – Tissue Tek (Sakura) was then added to the 20% sucrose solution in 1:1 ratio and the sample was incubated at 4°C overnight. The tissues were then placed in OCT and flash-frozen using cold isopentane. The samples were sectioned using a cryostat (Leica CM3050) at 20 μm thickness. Sections were washed in PBS and rehydrated through a series of alcohol gradients and stained with 0.1% hematoxylin (Sigma) until appropriate staining was achieved. The sections were rinsed in lukewarm tap water for 10 minutes followed by a wash in distilled water for 2 minutes. The sections were incubated in 80% ethanol for 2 minutes and then immersed in 0.5% eosin (Sigma) for 30 seconds. The samples were then dehydrated through a series of alcohol gradients and mounted with Permount (Fisher).

E. Image processing, data acquisition and analysis

Kidney cultures were imaged using a Leica dissecting microscope attached to a Spot CCD camera. Digital images and kidney surface area measurements were processed using Spot Advanced software. Wildtype CD1 kidneys that had been microinjected and electroporated with eGFP vectors were imaged under a set exposure time of 12 seconds and a gain value of 8. ImageJ Software (NIH - rsb.info.nih.gov/ij/) was used to quantify the number of GFP pixels on fluorescent images. Images were split according to red, green and blue colour channels. Quantification of GFP pixels was determined by applying a threshold value that allowed the software to select GFP-expressing pixels. The threshold value for each experiment was determined based on the untreated kidneys. We determined the threshold value for individual untreated kidneys so that ImageJ software would detect a maximum of 20 or fewer pixels. The threshold criteria were

stringent enough to avoid the detection of background. The average threshold value for all of the untreated kidneys was calculated; and applied to analyze GFP pixel count from the electroporated kidneys. Finally we normalized the GFP pixel count from electroporated kidneys by subtracting the mean number of GFP pixels of the untreated kidney from the electroporated kidneys. On average, a threshold value of 185 was used to determine the number of GFP pixels in electroporated kidneys.

The number of ureteric bud tips was manually counted in untreated and electroporated *HoxB7/GFP* kidneys by using ImageJ count tool, "Crosshair".

Statistical calculations, including average, standard error, Student's t-test, were done using Excel Software (Microsoft Inc.).

2. *Future endeavours*

A. Cell culture, BMP2 assay and fluorescent immunocytochemistry

mIMCD-3 cells and mK3 cells (a kind gift from Dr. Steve Potter – [101] were grown in DMEM/F12 (Invitrogen) supplemented with 5% FBS and 1% penicillin/streptomycin. RUB1 cells (a kind gift from Dr. Allan Perantoni – Perantoni *et al.*, 1985) were cultured in DMEM/F12 (Invitrogen) supplemented with 10 ng/ml of transforming growth factor (TGF)-α that was contained in RUB1 media that was also provided by Dr. Allan Perantoni. Cultures were grown in T75 flasks at 37°C and in a 5% CO_2 humidified environment.

To determine if cells were responsive to Bone morphogenetic protein (BMP)2 (R and D, Inc), cell lines were seeded on autoclaved circular coverslips in 6 well-plates and cultured in medium described previously. When cell confluency reached 75-90%, cells were washed once in 1X PBS and incubated in DMEM/F12 for 3 hours. BMP2 was then added to a final concentration of 5 nm and the cells were incubated for an additional hour. Following treatment, the media was removed and the cells were washed using sterile 1X PBS, and then fixed for 10 minutes in 4% PFA. The cells were then washed 5 times for two minutes each time in 1X PBS and then permeabilized by adding 400 μl of 100% methanol for 5 minutes. The cells were then washed 5 times for two minutes each in 1X PBS and then blocking was performed using 1 ml of 10% goat serum/PBS for 1

hour at room temperature. 200 µl of primary antibody to SMAD1, raised in rabbit (UBI), was diluted to a 1/100 dilution in 10% goat serum/PBS, and left overnight at 4°C. The following day, 3 washes of 10 minutes each in 1X PBS were performed and followed by a one-hour incubation at room temperature using a 1/200 dilution of an anti-rabbit secondary antibody, Alexa Fluor 594, (Molecular Probes) diluted in 10% goat serum/PBS. Cell cultures were washed again in 1X PBS and incubated for 5 minutes with 100 µl of 1µg/ml of DAPI (Roche). Following another round of washes the coverslips were mounted with an aqueous mounting agent (Cytoseal 60; Richard Allan Scientific) and visualized under a Zeiss fluorescent microscope. For all experiments negative controls were carried out where the primary antibody step was omitted and only the secondary antibody was added to the cells.

B. RT-PCR

The temporal expression of Claudin gene family members 1, 3, 7 and 11 along with Activin Like Kinase (ALK) receptors was determined in E12 to adult kidneys. Total RNA was extracted from whole embryonic kidneys or a section representing cortical and medullary regions of postnatal kidneys, using the RNeasy kit (Qiagen) as prescribed by the manufacturer. RNA was extracted from mK3 and RUB1 cell lines when they were ~90% confluent. Cells were trypsinized and spun down at 7000 rpm for 5 minutes and then total RNA was extracted using the RNeasy extration kit. DNA present in the RNA pool was removed using the Ambion Inc. DNA-Free kit according to the manufacturer's instructions.

RT-PCR was done using the OneStep RT-PCR kit (Qiagen). Please refer to Table 1 for a list of primers that were used. Control PCR experiments were conducted where the reverse transcriptase step was omitted in order to check that there was no DNA contamination. A 25 µl reaction mix consisted of 100 ng of mRNA. The RT-PCR consisted of a 30-minute reverse-transcription step at 50°C, followed by 15 minutes at 95°C to denature the Reverse Transcriptase enzyme and activate Taq Polymerase. This was followed by 30 cycles of 60 seconds at 94°C, 60 seconds at 60°C and 60 seconds at 72°C. A final step of 10 minutes at 72°C was included in the PCR reaction. Once all the

cycles were complete, the samples were stored at 15°C. They were then run on a 1% agarose/TAE gel for 35 minutes at 90V and visualized using a Gel Doc system (BioRad).

C. Whole mount in situ hybridization and tissue sectioning

Complete or partial coding sequences for the following mammalian genes ALK6, Claudin-3 and Claudin-7, were linearized in the pCRII-Topo vector (Invitrogen) using, respectively, BamH1, Xho1 and Xba1 restriction enzymes. *In vitro* gene transcription was achieved using SP6 enzyme. The probes were labeled with digoxygenin (DIG)-labelled UTP (Roche) according to the manufacturer's specification.

E13-14 CD1 kidneys were dissected and fixed in 4% PFA/PBS overnight at 4°C and then washed the following day in PBST (PBS with 0.1% Tween-20 from Sigma). Kidneys were dehydrated for at least 18 hours in methanol at -20°C before hybridization. In situ hybridization was performed as described previously with some modifications [102]. Briefly, the tissue was bleached with 6% hydrogen peroxide, treated with 10 μg/ml Proteinase K (Invitrogen) for 10 to 30 minutes at room temperature, and then washed in 0.2% glycine prior to re-fixation in 4% PFA/0.2% glutaraldehyde. For 60 minutes, the tissue was prehybridized at 65°C in a solution of 50% formamide, 5X sodium saline citrate (SSC; pH = 5), 50 μg/ml yeast tRNA, 1 % SDS, and 50 μg/ml of heparin. cRNA probe (1 μg/ml) was added for overnight hybridization at 65°C. The tissue was then washed with prewarmed solutions of 50% formamide, 5 X SSC (pH 4.5), and 1% SDS, followed by a solution of 50% formamide and 2X SSC at 65°C. Blocking in 10% sheep serum in TBST (TBS 0.1% Tween) for 1 hour at room temperature was performed and followed by incubation in a 1:2000 dilution of alkaline phosphatase-conjugated anti-digoxygenin antibody (Roche) at 4°C overnight. Samples were developed using NBT/BCIP (Roche) in NTMT (0.1 NaCl; 0.1 M Tris pH 9.5; 50 nM $MgCl_2$; and 0.1% Tween-20).

Samples were visualized as whole-mounts, using a dissecting microscope, and then cryosectioned at 20 μm thickness. Glycerol Gelatin mounting solution (Sigma-Aldrich) was used to coverslip the samples.

Table 1. List of primer sequences used to determine gene expression of ALK and Claudin 1, 3, 7 and 11.

Gene	Name of primer	Sequence (5' → 3')
Claudin – 1	Cldn1cds-fwd	TTTCATCCTGGCTTCTCTGG
	Cldn1cds-rev	CTTCCTTTGCCTCTGTCACAC
Claudin – 3	mCLDN3F	CATATGTCCATGGGCCTGGAGATCACC
	mCLDN3R	TCAGACGTAGTCCTTGCGGTCG
Claudin – 7	mCLDN7F	CCATGGCCAACTCGGGCCTGC
	mCLDN7R	TCACACGTATTCCTTGGAGG
Claudin – 11	mCLDN11F	ACCATGGTAGCCACTTGCC
	mCLDN11R	CTTAGACATGGGCACTCTTGG
ALK – 1	Alk1 – fwd	TTTGATGCTGTCGGTGGCC
	Alk1 – rev	CAGGACTGCTCATCTCGTG
ALK – 2	Alk2 – fwd	GAAGGGCTCATCACCACCA
	Alk2 – rev	CCAGGCCCAAATCTGCTAT
ALK – 3	Alk3 – fwd	TGCTATTGCTCAGGACACTG
	Alk3 – rev	TGCCGAACCATCTGAATCTG
ALK – 4	Alk4 – fwd	GTGGCTTGTCTCTGACTATC
	Alk4 – rev	ATGGACTCCTCCAGAATTGC
ALK – 5	Alk5 – fwd	GGCGAAGGCATTACAGTGTT
	Alk5 – rev	AAACCTGATCCAGACCCTGA
ALK – 6	Alk6 – fwd	TTGAATGCTGCACAGAAAGG
	Alk6 – rev	TCTAAGGTGGTGGATTTCAG
ALK – 7	Alk7 – fwd	CGGAACTAAATGCTCAGGTC
	Alk7 – rev	TGCTCGTGATACTCTGACAC

IV. RESULTS

Embryonic kidney explants that have been harvested from rodents are easy to grow and culture, and therefore, have been used as a model system to elucidate the role of signaling molecules, transcription factors and other molecules during kidney development [80]. Protein expression of specific molecules has been perturbed by exposing cultured kidney explants to pharmaceutical agents, by blocking transcription using anti-sense oligonucleotides, and by overexpressing mutant proteins by infecting explants using viral delivery methods. More recently, microinjection and electroporation has also been used as a method to overexpress DNA constructs encoding mutant proteins in embryonic mouse kidney explants [100]. While this report was the first to report the use of this method in embryonic kidneys, there was a limited assessment of its efficacy and its toxicity. Here we report our work where we have examined this method to establish the optimal conditions for high-level expression of DNA-encoding vectors and to determine its toxicity.

1. Microinjection and electroporation using high voltage and short pulse is more efficient

Electroporation has been used to introduce DNA into cells, tissues, embryos and whole animals. Most electroporation protocols in mammalian tissues have used conditions that were originally described in the chick. These parameters included a low voltage, 25V, a long pulse, 50msec, and anywhere from 1-5 pulses [93, 100]. Vicat et al. (2000) microinjected and electroporated the anterior tibialis muscle of adult mice and demonstrated that the parameters of high voltage, 900V, combined with a short pulse, 100 μsec, led to higher and more sustained transgene expression [97]. The effect of high voltage combined with a short pulse has not been investigated in mouse embryonic kidneys. There has been no report on the effect of either microinjection or electroporation on the growth of cultured embryonic mouse kidneys; nor has there been any optimization to establish the required conditions to obtain sustained expression of a transgene.

At embryonic day (E) 10.5, the ureteric bud invades the metanephric mesenchyme and begins to undergo iterative branching events. At the tips of the branching ureteric bud, the mesenchyme is induced to epithelialize and this is the first step in nephrogenesis. In the mouse, nephrogenesis proceeds from E11 until the first two weeks of postnatal life. Kidneys were dissected from outbred CD1 pups at embryonic day (E) 13. This developmental stage was chosen because nephrogenesis is well underway and these kidneys grow well in culture as opposed to older stages. We microinjected and electroporated a DNA-encoding vector, eGFP, where the pCMV promoter drives expression of the enhanced green fluorescent protein (eGFP) (Clonetech). Kidney explants were microinjected either in the renal pelvis or in the outer cortex and grown in culture for 5 days.

A. Effect of LV/LP and HV/SP electric field on kidney growth rate

We compared the growth rate, GFP expression and efficiency of a low voltage and long pulse protocol (LV/LP) (25 volts = 63 V/cm, 50 msec: protocol A) and two high voltage and short pulse (HV/SP) protocols (175 volts = 440 V/cm, 75 μs: protocol B and 250 volts = 630V/cm, 75 μs: protocol C). The HV/SP protocols were chosen after conducting multiple pilot tests using high voltage combined with short and long pulses. A range of voltages from 100 (400 V/cm) to 500 (1250 V/cm) V were tested while keeping the pulse constant at 100 μs as described previously [97]. Kidneys that were electroporated with a voltage higher than 200 V (500 V/cm) did not grow in culture and appeared to undergo necrosis. We then tested the voltages of 150 (375 V/cm), 175 (440 V/cm) and 200 (500 V/cm) and used variable pulse times of 25, 50, 75, and 100 μs. Overall, kidneys treated with a short pulse time (25 μs) grew better than those treated with a longer pulse time (100 μs). As well, there was higher and more sustained reporter gene expression for kidneys treated with a higher voltage. Therefore, the parameters of 175 V (440 V/cm) and 75 μs were selected as an example of a HV/SP protocol, protocol B, since they permitted adequate growth of the embryonic kidneys while maintaining sustained and high transgene expression. We included another HV/SP protocol, protocol C, using 250V (625 V/cm) and 75 μs as an example of conditions that permitted growth

in culture albeit to a lower extent than that observed for protocol B. Kidneys exposed to protocol C grew similarly to those treated with 175 volts and 250 μs (data not shown – $p>0.05$). We also varied the number of pulses (1, 3 or 5 pulses) and noticed that kidneys that were electroporated with 5 pulses of protocol A, B or C gave the greatest amount of GFP as reported by others [93, 97].

The relative growth, defined as the change in planar surface area over time in culture, was determined for each kidney every 24 hours [80]. By the 5th day in culture, untreated kidneys and those treated with protocol A, B and C, achieved respectively a mean relative growth (+/- SE) of 2.73 +/- 0.16, 3.11 +/- 0.14, 2.00 +/- 0.16 and 1.41 +/- 0.16 fold compared to their starting size (Figure 8A). During the first two days of culture, kidneys treated with protocols A and B grew similarly (protocol A vs. protocol B: $p>0.008$). However, they grew less than untreated kidneys, but more than kidneys treated with protocol C (protocol A or B vs. untreated: $p<0.008$; protocol A or B vs. protocol C: $p<0.008$). Up until the 5th day in culture, untreated kidneys and those treated with protocol A obtained a similar size (untreated vs. protocol A: $p>0.008$) that was significantly greater than protocol B or C treated kidneys (untreated or protocol A vs. protocol B or protocol C: $p<0.008$). Up until and including the 96 hour time point, kidneys exposed to protocol B were bigger than those treated with protocol C (protocol B vs. protocol C: $p<0.008$). After 120 hours in culture, kidneys treated with protocol B and C had a similar relative size (protocol B vs. protocol C $p>0.008$). From the slope of the curves, one can observe that all four treatment groups showed a positive growth rate up to 120 hours. By 96 hours, the growth rate of untreated cultures and those treated with protocol A began to slow down and this trend continued up to 120 hours. In contrast, kidneys treated with protocol B or C slowed down in their growth from 72 hours and onwards. Taken together, the results demonstrate that it is possible to electroporate kidneys using HV/SP parameters and maintain adequate growth in culture.

Figure 8. Kidneys microinjected and electroporated using a high voltage and a short pulse time show satisfactory growth and express exogenous DNA far longer than previously reported parameters.

A) *Growth rate of electroporated kidneys:* Kidneys were microinjected with 5 μg/μL of e-GFP vector and then electroporated with 5 pulses of the following parameters: 25V and 50 ms (protocol A), 175 V and 75 μs (protocol B), or 250 V and 75 μs (protocol C). We calculated the relative growth, defined as the difference in planar surface area (SA) of the kidney normalized to its original SA, $((SA_{Final}-SA_{Initial})/SA_{Initial})$ expressed in mm^2. All images were taken at 3.2x magnification. The data shown represents the mean +/- SE for each group (n=number of kidneys/group). Multiple Student's t-tests were performed and corrected by Bon Ferroni such that significance was set at $p<0.008$. Kidneys that achieved different relative growths are grouped in different box fonts ($p<0.008$). Kidneys treated with protocol B grew similarly to those kidneys treated with protocol A for the first 48 hours of culture ($p>0.008$). From 48 to 120 hours, kidneys treated with protocol B continue to show satisfactory growth although it was less than untreated kidneys or those treated by protocol A.

B) *GFP expression of electroporated kidneys:* The amount of GFP protein expression from the reporter gene was measured by counting the number of GFP pixels, using ImageJ software and a threshold value of 182. All images were taken at 3.2x, with a set exposure time of 12 seconds and a gain value of 8. The data shown was normalized to the mean background signal detected in the untreated kidneys (# of $pixels_{electroporated\ kidneys}$ - # of $pixels_{untreated\ kidneys}$). Within the first 24 hours in culture, protocols B and C expressed ~ 100 fold more eGFP when compared to kidneys treated with protocol A ($p<0.016$). Kidneys treated with protocols B and C showed sustained expression of the GFP transgene up to 5 days in culture, whereas by 72 hours in culture, kidneys exposed to protocol A showed little to no expression of the transgene. At 96 and 120 hours kidneys treated with protocol C showed a large coefficient of variation of 114% and 108% at 96 and 120 hours respectively. This large variability accounts for the statistical similarity in the number of GFP pixels observed between protocols A and C at these time points. The data shown represents the mean +/- S.E. for each group (n = number of kidneys/group). Multiple Student's

t-tests were performed and corrected by Bon Ferroni such that significance was set at p $p<0.016$. Statistical differences between groups are shown as separate small capital letters (a, b c).

C) *The efficiency of electroporation:* Using ImageJ software, the number of pixels of GFP signal was quantified for each kidney treated with either protocol A and B. The efficiency of electroporation was defined as the number of GFP pixels normalized to the number of pixels representing the total planar surface area for each kidney (GFP pixels/total pixels in kidney). All images were taken at 3.2x, with a set exposure time of 12 seconds and a gain value of 8. The data shown represents the mean +/- S.E. of pooled data from multiple experiments of kidneys treated with either protocol after 24 hours in culture (n=number of kidneys/group). Electroporation with protocol B allows for 15% of the kidney surface area to express the transgene. This efficiency ratio indicates that kidneys treated with protocol B shows ~100 fold higher transgene expression compared to kidneys treated by protocol A. A Student's t-Test was used to determine statistical significance (*, $p<0.05$).

Figure 8A.

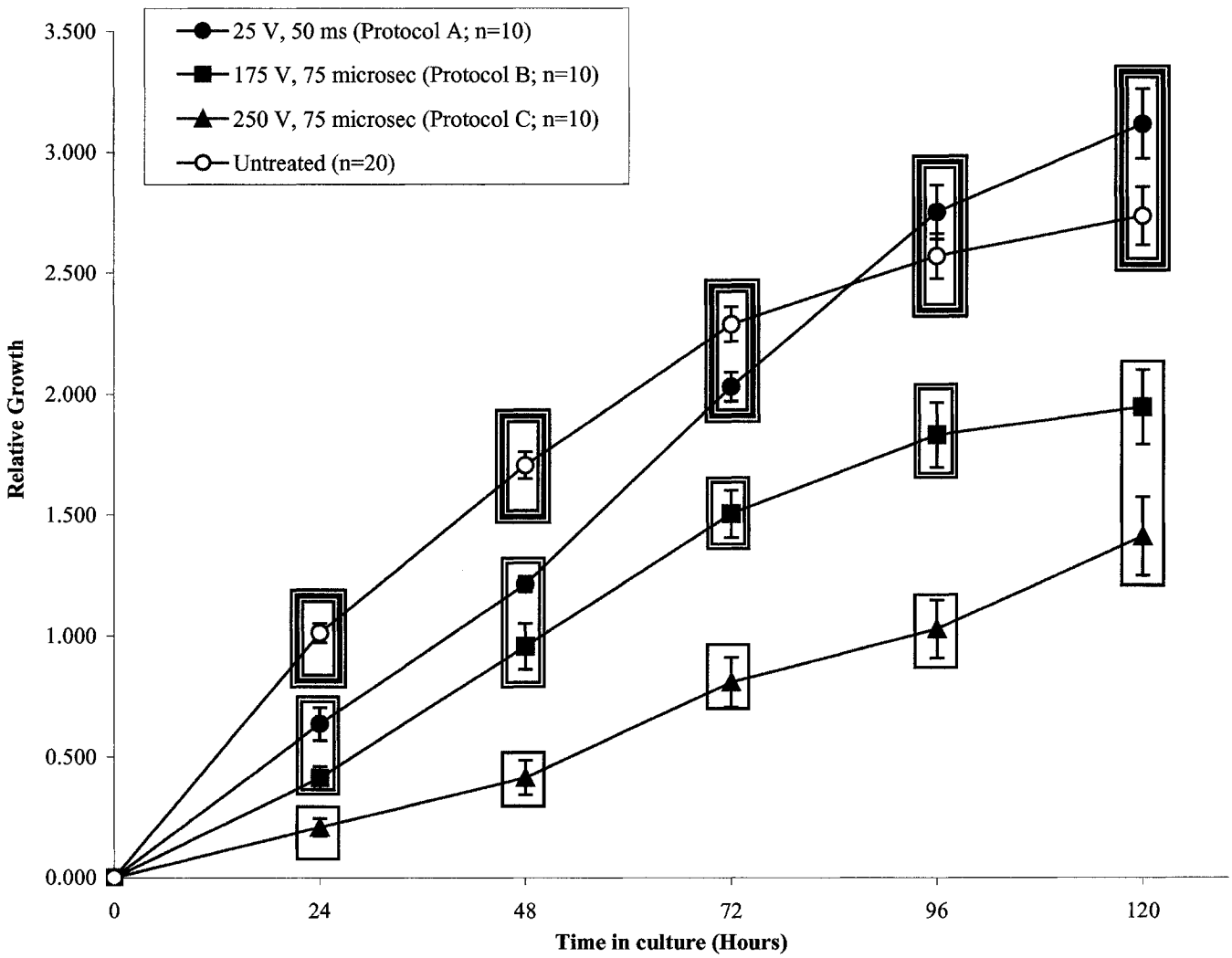
25 V, 50 ms (Protocol A; n=10)
175 V, 75 microsec (Protocol B; n=10)
250 V, 75 microsec (Protocol C; n=10)
Untreated (n=20)
3.500
3.000
2.500
2.000
1.500
1.000
0.500
0.000
Relative Growth
0
24
48
72
96
120
Time in culture (Hours)

Figure 8B.

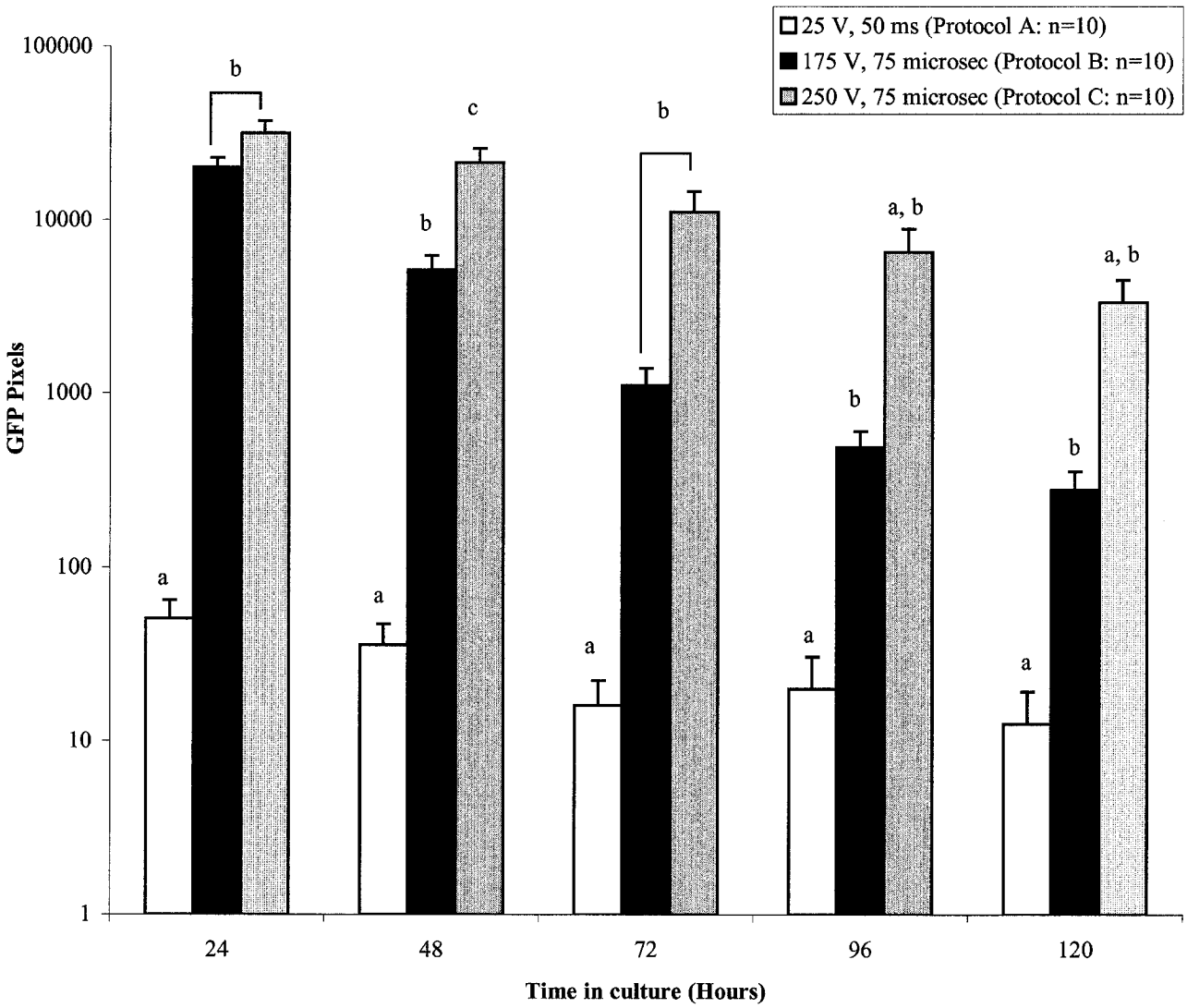
25 V, 50 ms (Protocol A: n=10)
175 V, 75 microsec (Protocol B: n=10)
250 V, 75 microsec (Protocol C: n=10)
GFP Pixels
100000
10000
1000
100
10
1
24
48
72
96
120
Time in culture (Hours)
a
b
a
b
c
a
b
a
b
a, b
a
b
a, b

Figure 8C.

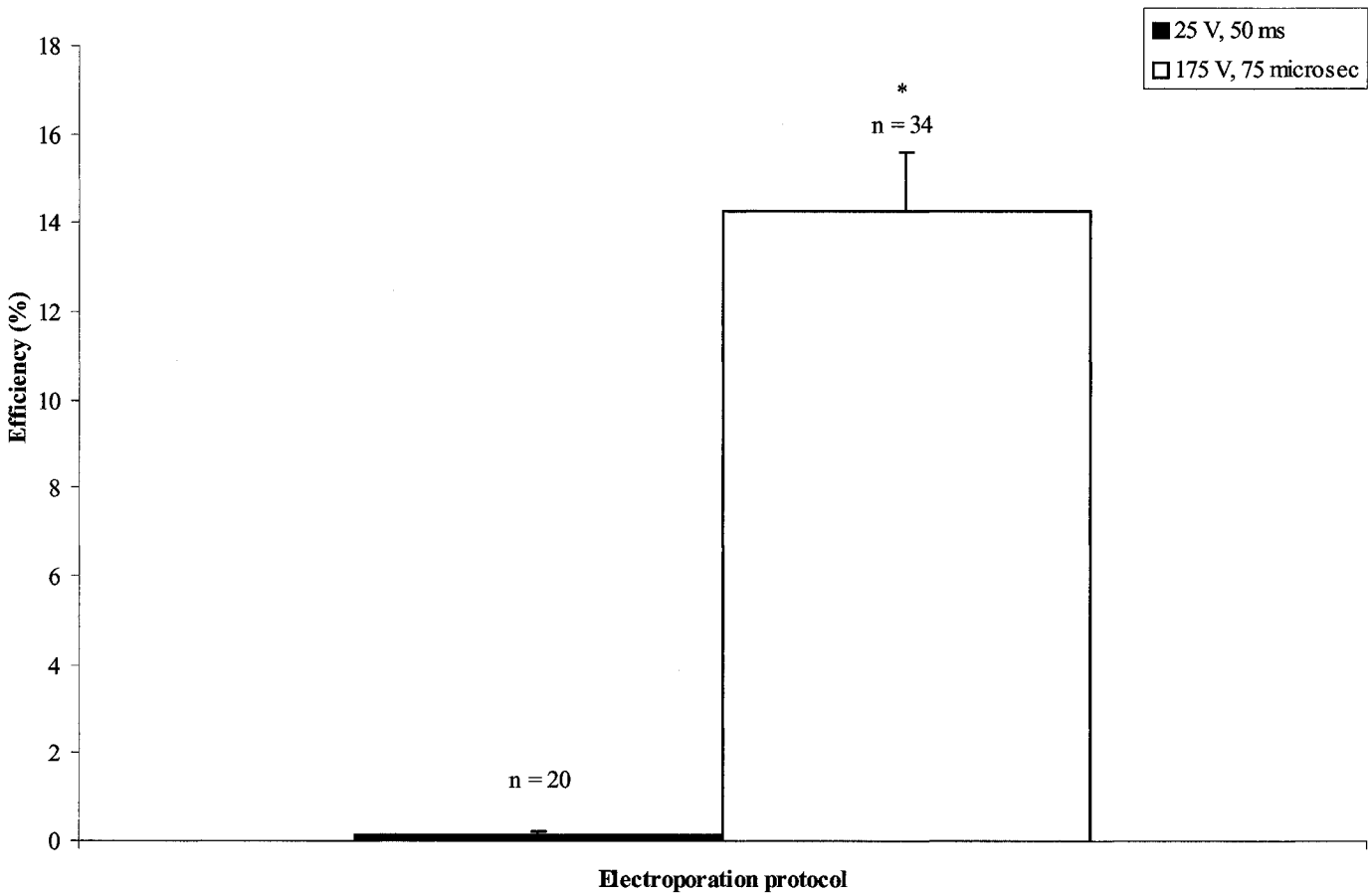
25 V, 50 ms
175 V, 75 microsec
*
n = 34
n = 20
Efficiency (%)
18
16
14
12
10
8
6
4
2
0
Electroporation protocol

Table 2. Green fluorescent protein pixel count in electroporated kidneys treated with LV/LP and HV/SP protocols.

Electroporated kidneys were analyzed using ImageJ software. The data indicated here represents the average number of pixels, +/- S.E, for the data plotted in Figure 8B. The number of replicates for each protocol is of n=10.

	Time in culture (Hours)				
	24	48	72	96	120
Protocol A	82 (+/- 16)	68 (+/- 13)	55 (+/- 9)	56 (+/- 12)	49 (+/- 7)
Protocol B	20041 (+/- 2790)	5164 (+/- 1078)	1147 (+/- 280)	526 (+/- 120)	317 (+/- 77)
Protocol C	31743 (+/- 5503)	21369 (+/- 4461)	11102 (+/- 3435)	6538 (+/- 2362)	3370 (+/- 1158)

B. HV/SP electric fields allow for greater GFP expression

The major reason to optimize the electroporation protocol was to increase the amount and duration of transgene expression. We used an enhanced green fluorescent protein (eGFP) expressing vector to monitor the effect of electroporation on the expression of GFP. We quantified eGFP expression by counting the number of eGFP pixels using ImageJ software (NIH, USA) and reported it as pixel counts. The number of GFP pixels from 24 hours to 120 hours post-electroporation decreased over time for each protocol (Figure 8B). Kidneys treated by protocol B and C had the same number of GFP, 20041 and 31743 pixels respectively, after 24 hours in culture (protocol B vs. C: $p>0.016$), and showed ~100 fold more reporter gene expression than protocol A, which was of 82 pixels (protocol B or C vs. protocol A: $p<0.016$). Kidneys subjected to protocol A had very low levels of GFP by 72 hours, that is of 55 pixels, whereas kidneys treated with protocol B and C continued to demonstrate high GFP expression, which was of 1147 and 11103 pixels (protocol B or C vs. protocol A: $p<0.016$). Kidneys treated by protocol B and C showed a reduction in GFP pixels of ~100 fold and ~10 fold over 5 days in culture. Remarkably, kidneys treated with protocol C showed similar GFP expression to those treated with protocol A at 96 and 120 hours, although there was ~100 fold difference in the mean values (protocol C vs. protocol A: $p>0.016$) (Figure 8B). We noticed a large coefficient of variation in the protocol C treated kidneys, where values of 114% and 108% were obtained at 96 and 120 hours. This large amount of variation was a reflection of the fact that over time in culture, these kidneys began to show some signs of necrosis. Necrotic tissues exhibited an increasing amount of autofluorescence, which limited the precision of the GFP pixel measurement with increasing time in culture. However, the results do show that for all of the time points, there is far greater GFP expression from kidneys treated with a HV/SP protocol, protocol B, compared to a LV/LP, protocol A.

Up until 48 hours of culture, kidneys treated with either protocol A or B grew similarly. Beyond this point, kidneys in protocol B slowed down in their growth rate, although they continued to grow. However, kidneys treated by protocol B showed much higher levels of GFP expression than protocol A and in some cases it persisted for up to 2

weeks. Therefore, for the remainder of our studies, comparisons were limited to two protocols: the LV/LP protocol (protocol A) and the HV/SP protocol (protocol B).

C. Electroporating an embryonic kidney with a HV/SP protocol is more efficient

To examine the efficiency of electoporation, we quantified the number of GFP pixels observed for each kidney and normalized it to the number of pixels that represented the total planar surface of the kidney. Data from multiple experiments using protocol A and B was pooled. For kidneys treated with protocol A, the mean GFP signal (+/-SE) represented 0.15 +/- 0.08% of the kidney planar surface area whereas for kidneys treated with protocol B, it represented 15 +/- 1.32% of kidney planar surface area (Figure 8C: $p<0.05$). This shows that protocol B leads to greater GFP expression in a larger area within the kidney. This level of efficiency appears to be consistent with electroporation protocols that have been optimized in other tissues where the level of reporter gene expression has been shown to vary from 10-50% [84, 92, 103]. By normalizing the number of GFP pixels to the number of pixels that represents the total planar surface area, we are in fact underestimating the level of efficiency. When microinjecting DNA into the embryonic kidney, only part of the organ is exposed to the transgene, therefore, to determine the efficiency of electroporation, it would be better to report the number of GFP pixels as a function of the region that was microinjected. Because GFP expression is not detected until at least 2 hours after injection, we were not able to compare the region of injection to the region of GFP expression.

2. The effect of electroporation on kidney development

In the previous section, we determined whether microinjection and electroporation affected the growth of embryonic kidney explants. In this section, we determined whether there were specific effects on two of the tissues within the developing kidney: the metanephric mesenchyme and the ureteric bud.

A. The GFP protein is not toxic to kidney development

As shown previously, microinjection followed by electroporation affects the growth rate of embryonic kidney explants (Figure 8A). We first determined whether the GFP reporter protein itself had any effect on kidney growth. For this, kidneys were microinjected and electroporated either with dye alone or dye with 5 μg/μl eGFP vector using the parameters of protocol B. The mean relative growth (+/-SE) for the dye alone or dye with eGFP vector by 5 days in culture was 2.19 +/- 0.20 and 2.06 +/- 0.16 (Figure 9). The relative growths for the two groups at all time points are not statistically different from one another ($p>0.008$). Therefore, neither the indicator dye, the DNA, nor the GFP protein itself appears to be deleterious to growth of embryonic kidneys in culture.

B. The electroporation of embryonic kidney prove to show some toxicity on growth

Embryonic kidneys that were either microinjected and electroporated as described previously were compared to kidney culture that were only microinjected with dye containing 5 μg/μl of eGFP. Kidneys that were only microinjected showed a relative growth that was similar to the untreated kidney at all time points ($p>0.008$). This analysis suggests that microinjecting embryonic kidneys does not affect their overall ability to grow in culture (Figure 9). However, the kidney cultures that were microinjected with dye or dye containing DNA and subjected to electroporation achieved a relative growth of 1.18 +/- 0.09 and 0.95 +/- 0.05 at 48 hours, and 1.44 +/- 0.1 and 1.30 +/- 0.07 at 72 hours (dye and electroporation vs. dye, DNA, electroporation: $p>0.008$), which were statistically different from microinjected kidneys that achieved a relative growth of 1.63 +/- 0.10 and 2.05 +/- 0.11 at 48 and 72 hours in culture (dye and electroporation, and dye, DNA and electroporation vs. dye, DNA, microinjection: $p<0.008$). Kidneys that were microinjected with dye and DNA, or those microinjected and electroporated in the presence of dye or dye containing DNA resulted in relative growth of 2.26 +/- 0.11, 1.76 +/- 0.16 and 1.86 +/- 0.11 at 96 hours; and 2.48 +/- 0.12, 2.19 +/- 0.20 and 2.07 +/- 0.14 by 120, which all data was statistically similar ($p>0.008$). This data analysis demonstrates that although the electroporation has some effect on growth, electroporated kidneys manage to recover from the toxic effect of the process.

C. Microinjection and electroporation and renal branching morphogenesis

During kidney development, an outgrowth from the mesonephric duct, the ureteric bud grows and branches to induce the formation of the kidney. At the tip of each ureteric bud, the adjacent metanephric mesenchyme is induced to epithelialize and this is the first step during nephron formation. To establish the effect of electroporation on the growth and branching of the ureteric bud, we took advantage of the *HoxB7/GFP* transgenic mouse. In this mouse model, the *HoxB7* promoter drives GFP expression in the ureteric bud and its derivatives, and thus provides a method to track ureteric bud branching [75].

Kidneys were dissected from *HoxB7/GFP* pups at E13, electroporated using protocol B, and cultured for 120 hours. Kidneys explants were either electroporated using protocol B or not electroporated prior to being grown in culture. In order to quantify the effect of electroporation on renal branching morphogenesis, we counted the number of ureteric bud (UB) tips using ImageJ software. We then calculated the rate of ureteric bud tip formation during the 5 days in culture [(number of UB tips $_{final}$-number of UB tips $_{initial}$)/number of UB tips $_{initial}$]. For both untreated and treated kidneys there was a sustained increase in the rate of ureteric bud tip formation throughout the experiment (Figure 10A). By the end of the experiment, electroporated kidneys and untreated kidneys showed, respectively, a 1.8 +/- 0.15 and 2.60 +/- 0.34 increase in UB tip formation compared to the beginning of the experiment. The rate of ureteric bud tip formation was significantly greater at all time points in the untreated versus the electroporated kidneys ($p<0.05$) which is consistent with the work of Gao *et al.* (2005). However, even kidneys that have been electroporated continue to form new UB tips albeit at a slower rate than their untreated counterparts.

As shown in Figure 10B, there is a difference in the branching pattern of an electroporated kidney compared to an untreated kidney. At 72 hours in culture, it becomes apparent that the main trunks of the electroporated kidneys are thinner and show less branching compared to untreated kidneys. This pattern was consistent up to 120 hours in culture.

D. Effect of electroporation on mesenchymal-to-epithelial transition

Cryosections were examined from kidneys that were electroporated and grown in culture for five days (Figure 10C). Kidney organization looks similar between both treatment groups. The electroporated kidney shows the presence of a medullary region where the ureter enters into the kidney, and a surrounding cortex rich with MET structures. Mesenchymal cells undergo epithelialization in electroporated kidneys as seen by the presence of the renal vesicles and comma-shaped bodies. These observations indicate, that although the ureteric bud shows a decrease in branching, the mesenchymal cells still manage to epithelialize in either electroporated or untreated kidneys.

Figure 9. Electroporation affects kidney growth

Embryonic day 13 kidneys were microinjected and electroporated with 5 pulses of 175V and 75 μs, protocol B, either with indicator dye alone or dye with 5 μg/μl eGFP vector. As well, kidneys were microinjected with dye containing 5 μg/μl eGFP vector, without being electroporated. The relative growth was defined as the difference in planar surface area (SA) of the kidney normalized to its original SA, $((SA_{Final}-SA_{Initial})/SA_{Initial})$ expressed in mm^2. There is no difference in relative growth when comparing kidneys electroporated with dye or dye containing DNA at any of the time points ($p>0.008$). This demonstrates that neither the indicator dye, the DNA, nor the GFP protein itself has a deleterious effect on kidney growth. Kidneys microinjected with dye containing GFP show a relative growth similar to that of untreated kidneys at all time points ($p>0.008$), indicating that needling of the kidneys from the microinjection step does not have any effect on kidney growth. Therefore, the electroporation of kidneys results in some toxicity to the kidney culture. All images were taken at 3.2x magnification. The data represents the mean, +/- S.E., of a sample size of 10 embryonic kidneys per treatment. The Student's t-test was used to determine statistical significance and corrected by Bon Ferroni such that significance was set at $p < 0.008$. Statistically similar treatment groups are grouped in similar box font.

Figure 9.

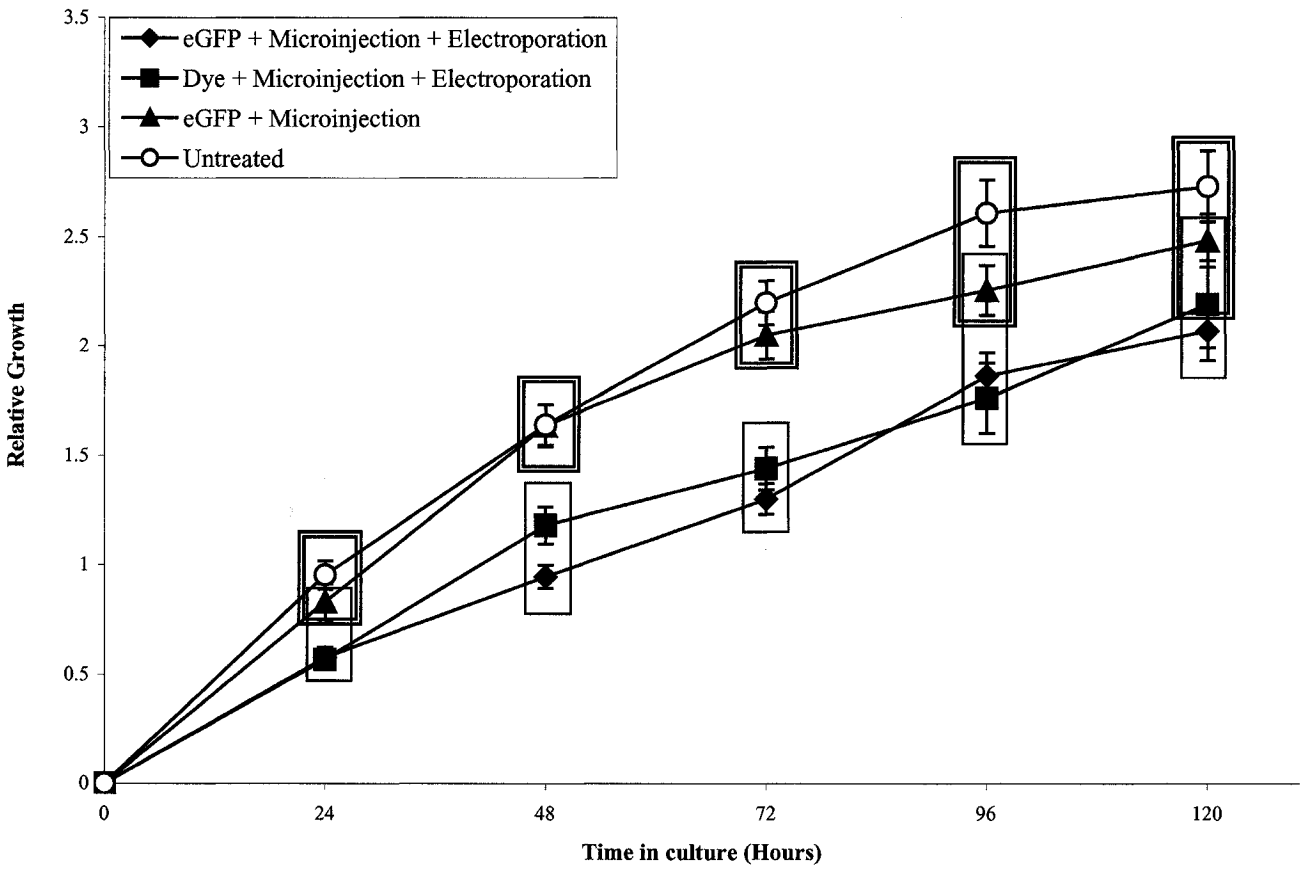
eGFP + Microinjection + Electroporation
Dye + Microinjection + Electroporation
eGFP + Microinjection
Untreated
Relative Growth
3.5
3
2.5
2
1.5
1
0.5
0
0
24
48
72
96
120
Time in culture (Hours)

Figure 10. The effect of electroporation on the developing kidney.

A) E13 kidneys from a HoxB7/GFP mouse on a CD1 background were electroporated using the parameters of protocol B. In this transgenic mouse model, GFP protein is expressed in the UB and its derivatives and can be used to visualize branching morphogenesis. Ureteric bud tips were counted using ImageJ software. The data shown represents the mean in the relative number of ureteric bud (UB) tips (number of UB tips $_{final}$-number of UB tips $_{initial}$)/number of UB tips $_{initial}$) +/- S.E. All images were taken at 3.2x magnification. Electroporated kidneys show a global increase in the rate of ureteric bud tip formation with increasing time in culture. However, the rate of UB tip formation in electroporated kidneys is significantly less at all timepoints compared to the untreated kidneys using the Student's t-test ($p<0.05$).

B) Images depicting renal branching morphogenesis of kidneys grown for five days in culture. Electroporated kidneys show elongated ureteric bud stalks (arrows) with a reduction in the number of lateral branches stemming from the stalk (asterisk).

C) CD1 kidneys were electroporated (175 volts, 75 μs) or left untreated and grown for 5 days. Sections at 20 μm thickness were stained with hematoxylin and eosin. Uninduced mesenchymal cells surround ureteric bud tips in both untreated and electroporated kidneys. Ureteric bud branches (asterisk) and mesenchyme condensing bodies (arrow) are present in both kidney cultures.

Figure 10A.

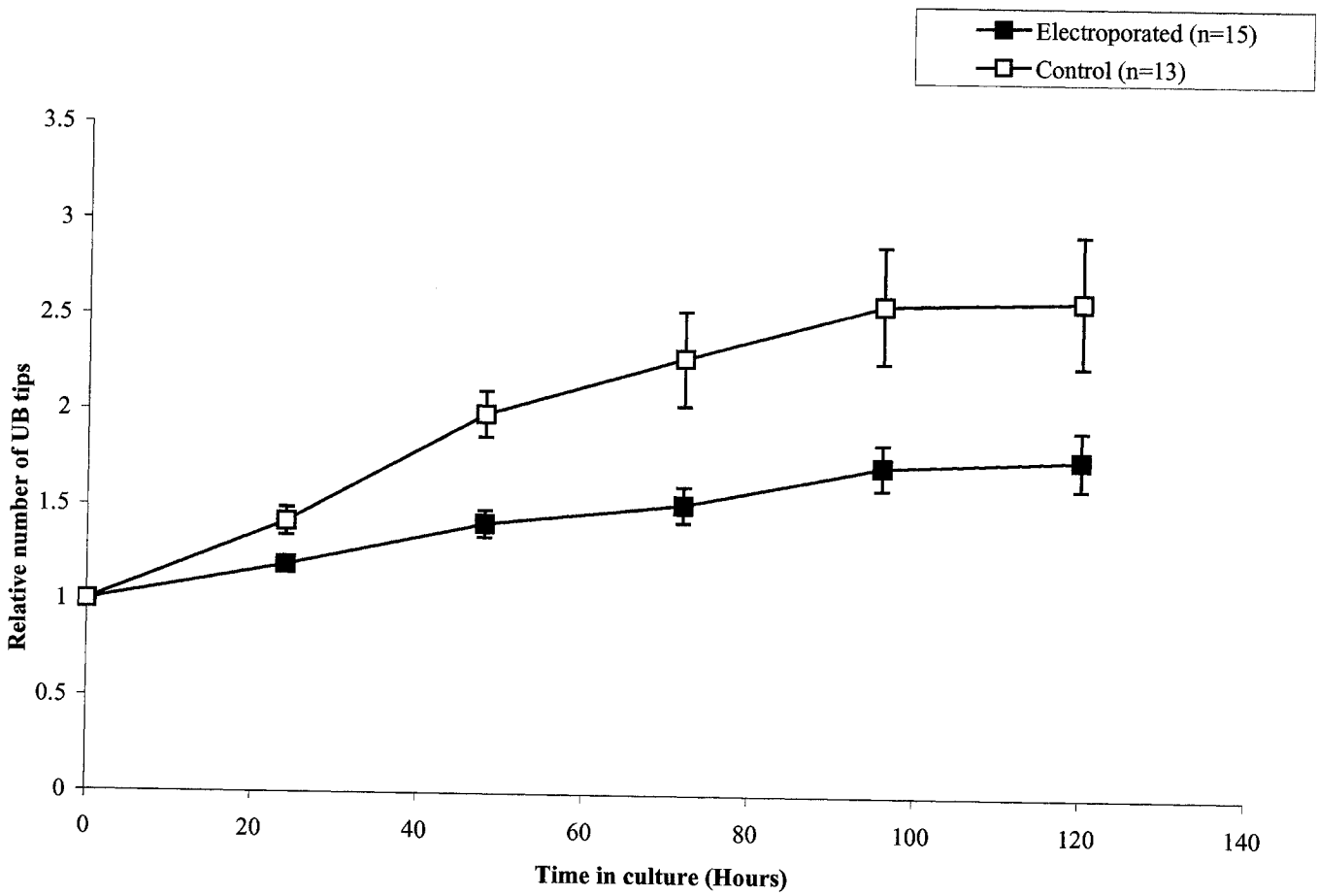
Electroporated (n=15)
Control (n=13)
Relative number of UB tips
3.5
3
2.5
2
1.5
1
0.5
0
0
20
40
60
80
100
120
140
Time in culture (Hours)

Figure 10B.

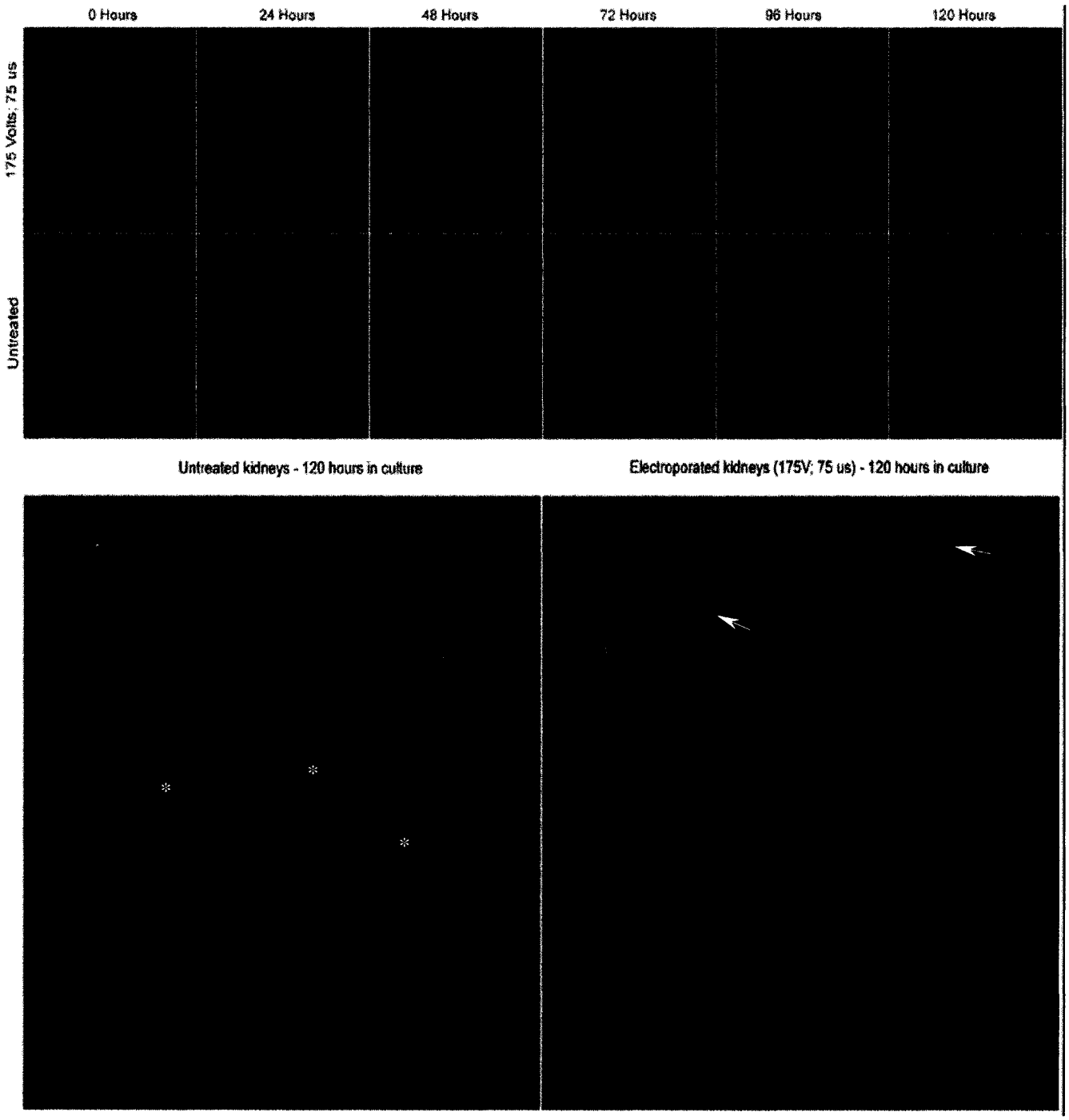
0 Hours
24 Hours
48 Hours
72 Hours
96 Hours
120 Hours
175 Volts; 75 us
Untreated
Untreated kidneys - 120 hours in culture
Electroporated kidneys (175V; 75 us) - 120 hours in culture

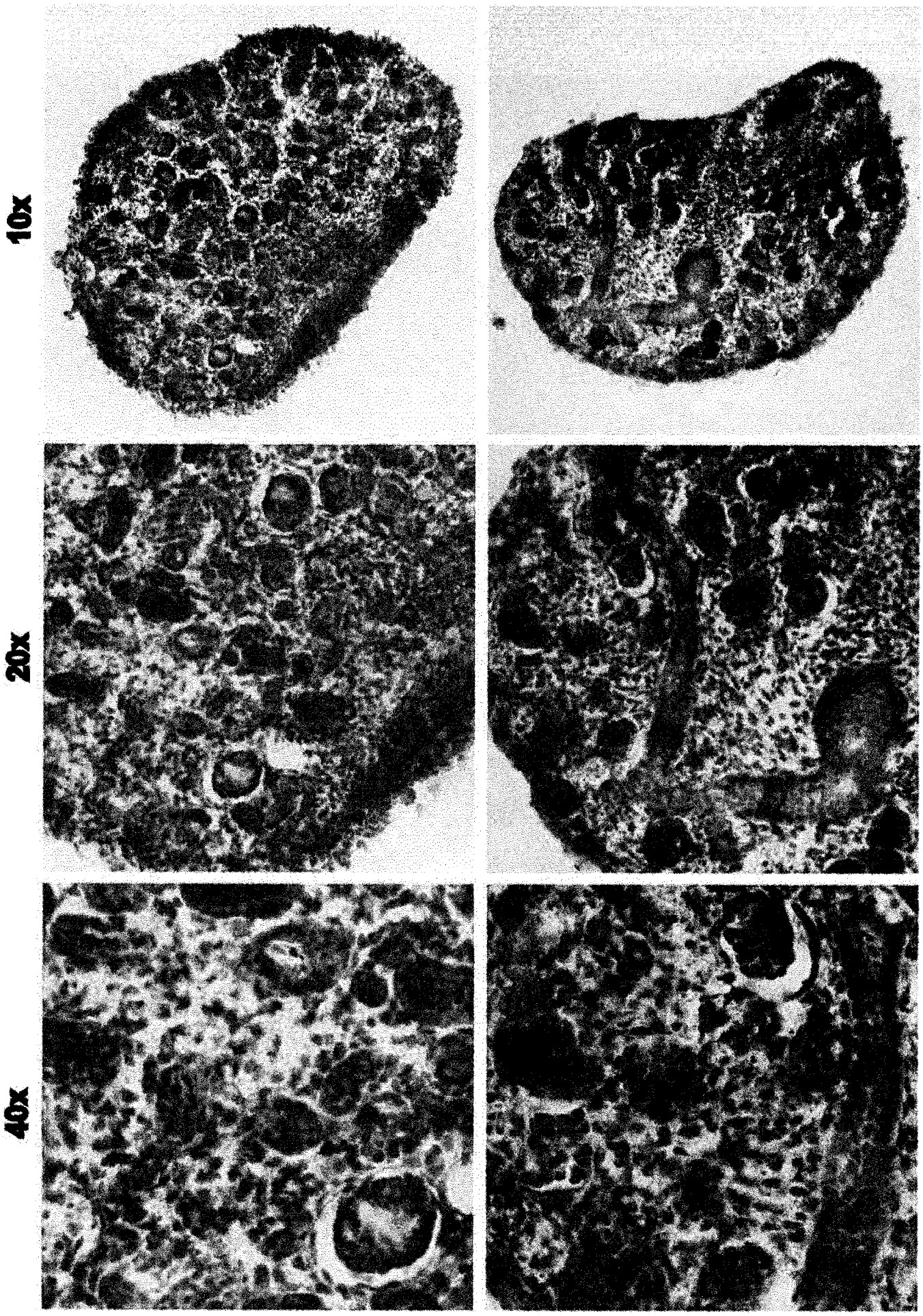
Electroporated kidney
Untreated kidney
10x
20x
40x

3. The effect of kidney age on GFP expression

Vicat *et al.* (2000) showed that multiple parameters including the age of the tissue had an effect on the efficiency of a high voltage and short pulse protocol. This was partly attributed to the increase in complexity and growth of the anterior tibialis muscle in 6 month-old compared to 8 week-old mice. Based on this, we evaluated the effect of different developmental stages on electroporation efficiency. The early developing kidney, at E12, consists of a few ureteric bud tip branches surrounded by loose mesenchyme. A more mature developing kidney, at E14, consists of multiple ureteric bud tips, and adjacent to the tips, mesenchymal cells are in the process of undergoing mesenchymal to epithelial transition, which is required for nephron formation. We determined whether there was a difference in GFP expression for kidneys that were microinjected and electroporated at E12, E13, and E14 using the parameters of protocol B.

As shown, the GFP expression pattern varied at different developmental stages (Figure 11A). E12 and E13 kidneys show diffuse eGFP expression. In contrast, E14 kidneys show a more focal expression of eGFP. Although the data suggests that E12 kidneys have greater GFP expression that E14 kidneys, this did not reach statistical significance (Figure 11B). As expected, the relative growth varies for each age group with E12 kidneys showing the best growth and E14 kidneys the worst growth ($p<0.016$)(Figure 11C).

4. The temporal expression of the transgene

We determined when the GFP reporter gene first became expressed after microinjection and electroporation of cultured kidneys. Kidneys treated with either protocol A or B express the transgene as early as 2 hours post-electroporation (Figure 12A). For kidneys treated with protocol A, the transgene expression decreases significantly at 24 hours compared to kidneys treated with protocol B that continue to maintain a high level of transgene expression (Protocol A: 1845 pixels +/- 734; Protocol B: 15175 pixels +/- 2735, $P<0.05$) (Figure 12A and B).

Figure 11. Age of murine embryonic kidneys does not affect GFP expression.

Kidney explants were dissected from pups taken from timed-pregnant CD1 mice, microinjected and electroporated using protocol B and cultured for 5 days.

A) From top to bottom are shown representative images of E12, 13 and 14 embryonic kidneys cultured at indicated time points. For each embryonic stage at each time point, a light image, a fluorescent image, and an overlay of the two are shown. In E12 and E13 kidneys, GFP expression is broadly expressed throughout the kidney, whereas in E14 kidneys it is more focally expressed. All images are taken at 3.2x magnification. The exposure time for fluorescent images is 12 seconds and the gain fixed at 8.

B) eGFP transgene expression was assessed by measuring the number of GFP pixels detected from images taken using fluorescent microscopy. The GFP pixel count was determined using ImageJ software and a threshold value of 110. Although the data suggests that E12 kidneys have higher GFP expression than E13 or E14 kidneys, this did not reach statistical significance after Bon Ferroni correction. There was no statistical difference in GFP expression for any of the embryonic stages at any of the timepoints. For all groups the data represents the mean +/- SE for each developmental stage (n=number of kidneys per group). Multiple Student's t-tests were performed and corrected by Bon Ferroni such that significance was set at $p < 0.016$.

C) Growth was determined using the relative growth size defined as $(SA_{Final}-SA_{Initial})/SA_{Initial})$ expressed in mm^2. Treatment groups which show statistical similarity are grouped together in boxes. As others have shown, E12 kidneys show the best growth in culture although E13 kidneys also show adequate growth. E14 kidneys tend to grow at a much slower rate. Multiple Student's t-tests were performed and corrected by Bon Ferroni such that significance was set at $p<0.016$.

Figure 11A.

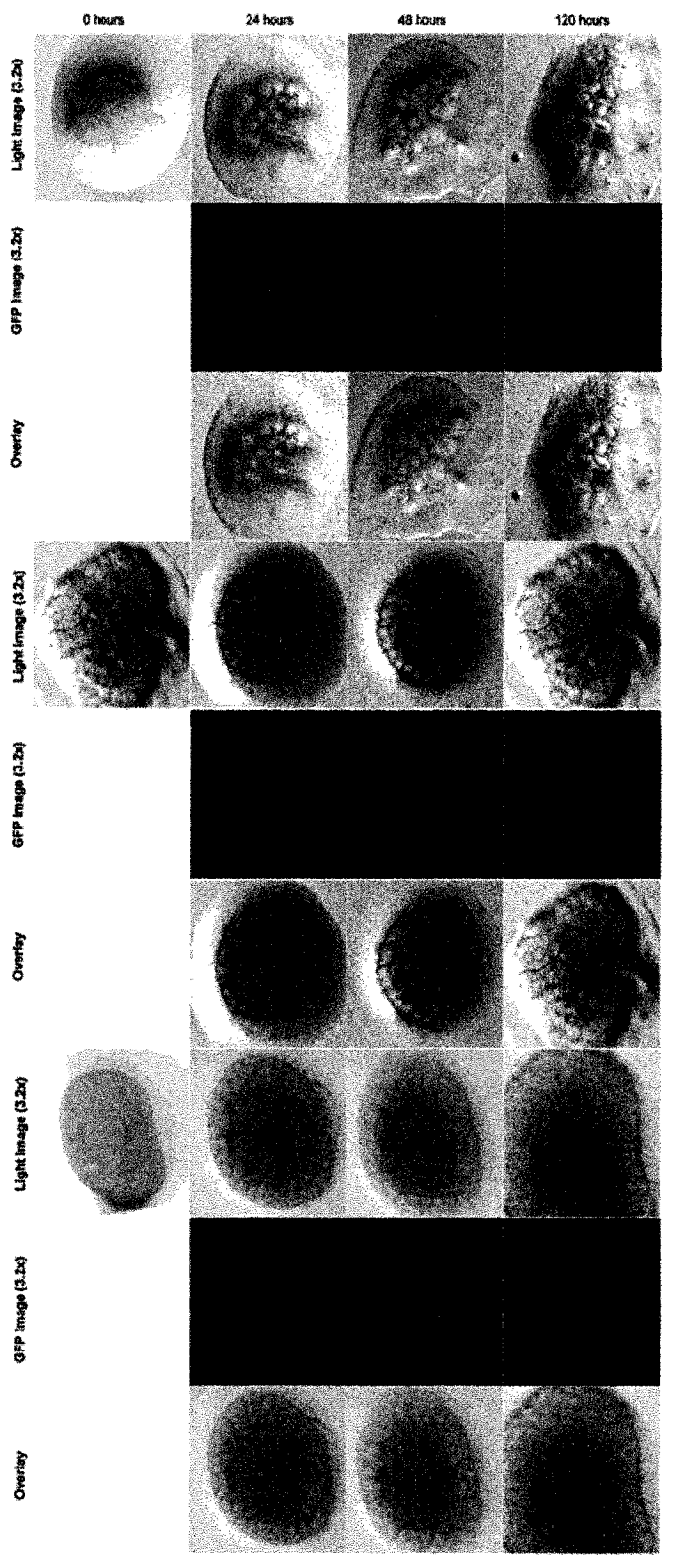
0 hours
24 hours
48 hours
120 hours
Light Image (3.2x)
GFP Image (3.2x)
Overlay
Light Image (3.2x)
GFP Image (3.2x)
Overlay
Light Image (3.2x)
GFP Image (3.2x)
Overlay

Figure 11B.

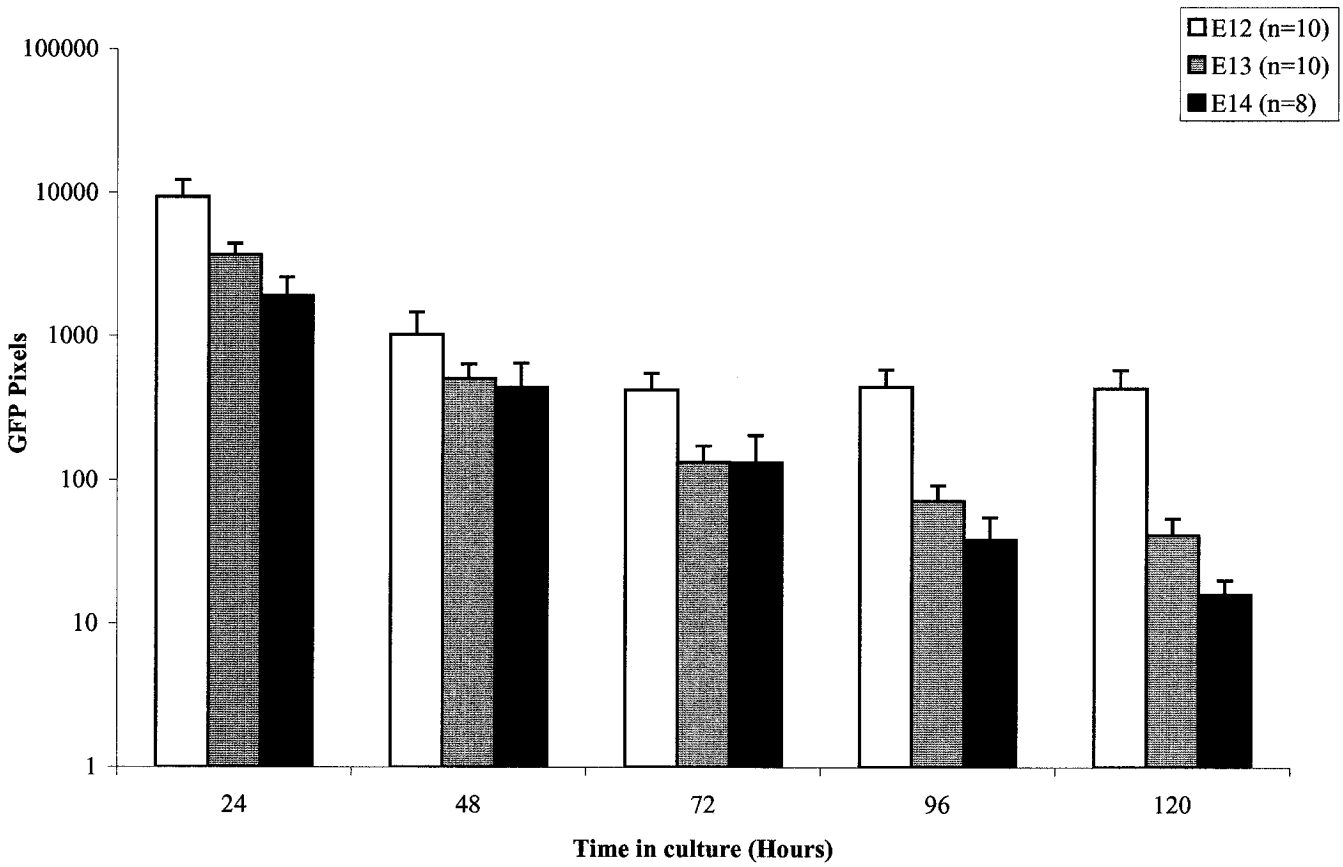
E12 (n=10)
E13 (n=10)
E14 (n=8)
100000
10000
1000
100
10
1
GFP Pixels
24
48
72
96
120
Time in culture (Hours)

Figure 11C.

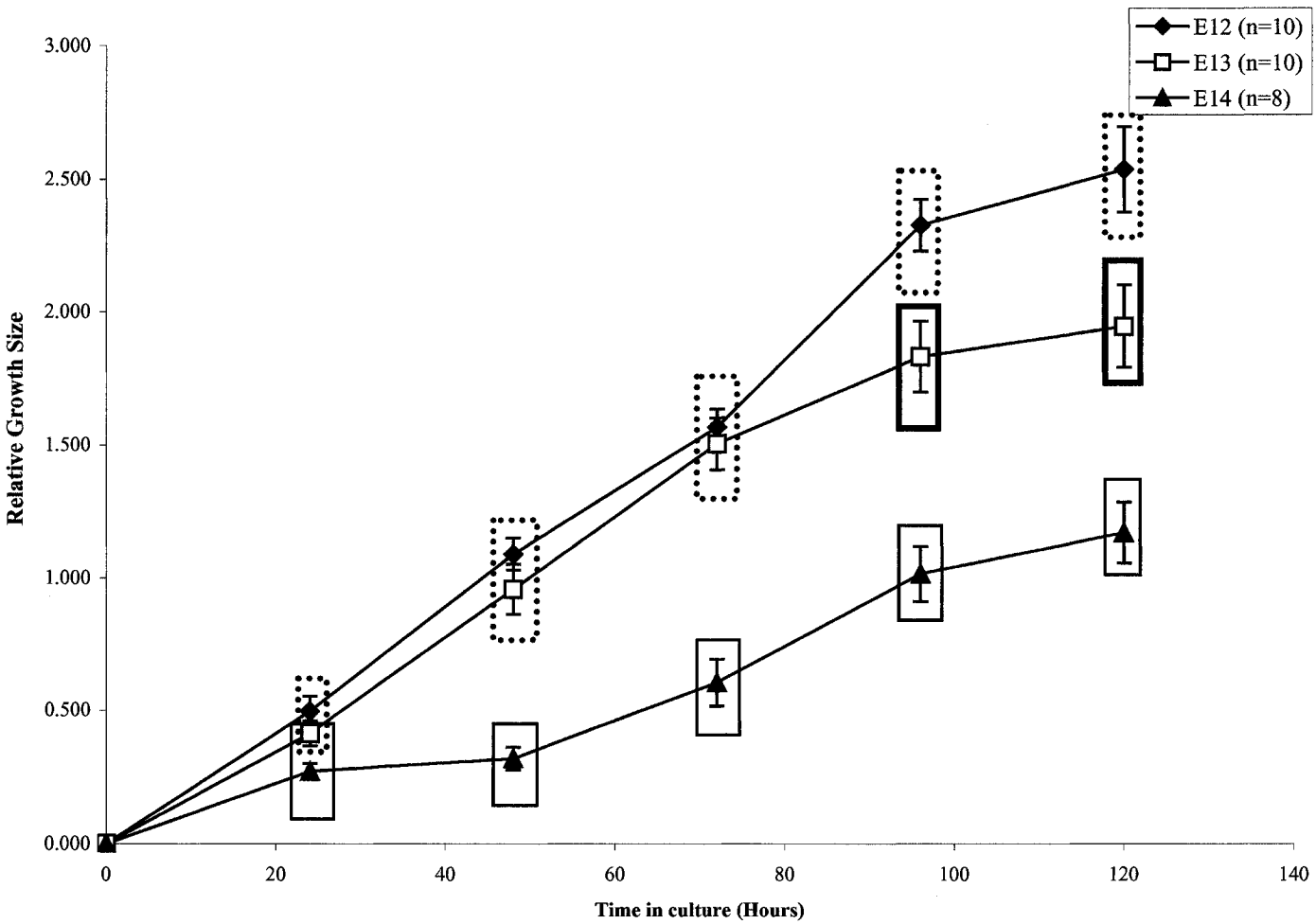
E12 (n=10)
E13 (n=10)
E14 (n=8)
3.000
2.500
2.000
1.500
1.000
0.500
0.000
Relative Growth Size
0
20
40
60
80
100
120
140
Time in culture (Hours)

Figure 12. Reporter gene expression begins two hours post-electroporation and peaks at 12 hours.

E13 kidneys were electroporated with protocol A or B and grown for 5 days in culture.

A) GFP expression shows a similar pattern of expression using both protocols, although there is ~10-fold more GFP expression detected in kidneys exposed to protocol B. With the exception of the 2 hour timepoint, a significantly greater amount of GFP signal is detected at all time points for kidneys treated with protocol B compared to protocol A ($p<0.05$, Student's t-test). The data shown represents the mean for each group +/- S.E. (n=10 kidneys per group).

B) Fluorescent images of kidneys treated with protocol A or B at various time points. All images were taken at a magnification of 3.2x. Exposure time for fluorescent images was fixed at 12 seconds with a gain of 8.

Figure 12A.

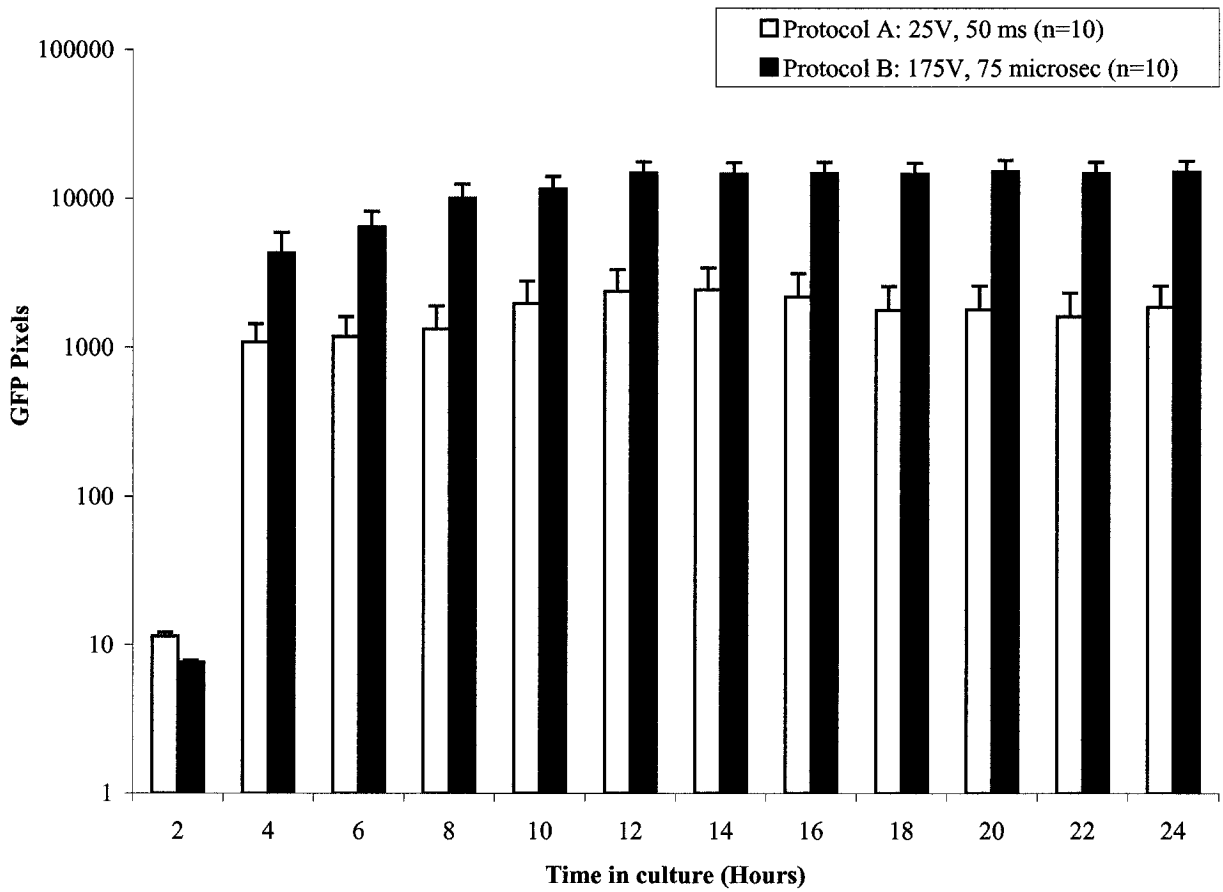
Protocol A: 25V, 50 ms (n=10)
Protocol B: 175V, 75 microsec (n=10)
GFP Pixels
100000
10000
1000
100
10
1
2
4
6
8
10
12
14
16
18
20
22
24
Time in culture (Hours)

6 Hours
12 Hours
18 Hours
24 Hours
175 volts; 75 us
25 volts; 50 ms

5. *Tissue targeting within the ureteric bud and the metanephric mesenchyme*

We examined whether the UB or the metanephric mesenchyme (MM) could be specifically targeted using this method (Figure 13). Kidneys were grown for 24 hours, fixed and stained for the ureteric bud marker cytokeratin. To target the MM, the needle was localized in the outer cortex of the developing kidney. Little to no eGFP expressing cells (asterisks) overlapped with the rhodamine stained ureteric buds (arrows). Most expression was located in the mesenchyme surrounding the stalk and the developing ureter. By microinjecting the renal pelvis, ureteric bud cells were targeted. By doing so, we noticed a clear overlap between eGFP-expressing cells, in green, along with cytokeratin-positive cells, in red. Ureteric bud cells within the stalk and at the tips expressed eGFP transgene. Furthermore, while needling the renal pelvis we also managed to target cells of the developing ureter. Therefore, this method can be used to target cells in both the UB and its derivatives or in the MM.

Figure 13. Microinjection and electroporation allows for spatial targeting within the developing kidney.

E13 kidneys were microinjected with the e-GFP vector either in the pelvic area to target the ureteric bud or in the outer cortex to target mesenchymal cells and then electroporated with protocol B. Following 24 hours of growth, the kidneys were fixed and the ureteric bud was labeled using an antibody to cytokeratin followed by a rhodamine-conjugated secondary antibody. Confocal microscopy images taken at 2μm thickness under 10x magnification allowed for visualization between the cytokeratin-labeled ureteric bud (arrows) cells and e-GFP targeted cells (asterisks). Mesenchyme targeted cells show little overlap between ureteric bud cells. Microinjecting the eGFP vector in the pelvis of the kidney allows the ureteric bud to be targeted at its tips and stalks; as well it is possible to target the developing ureter.

Figure 13.

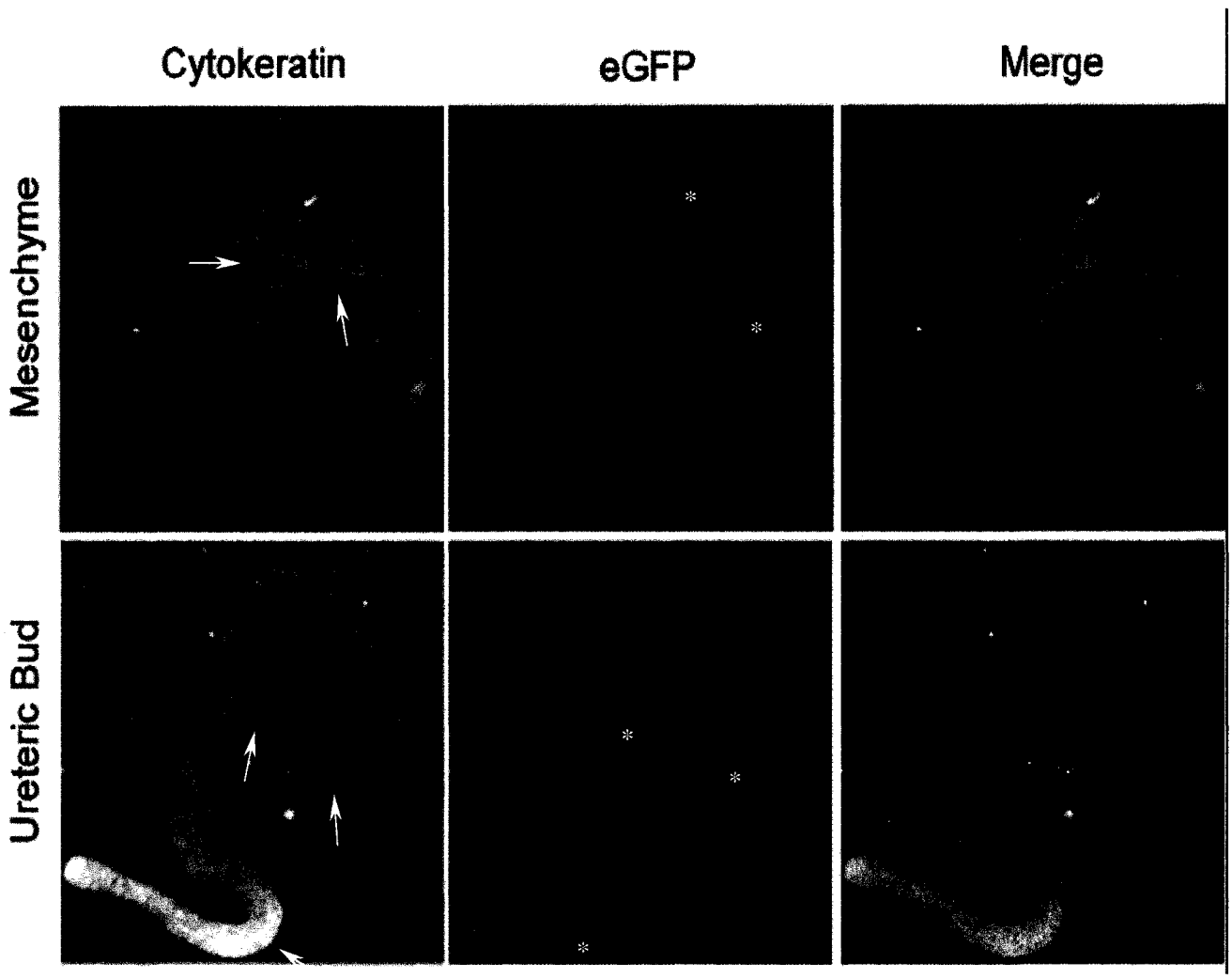

V. DISCUSSION

The goal of this study was to determine the optimal conditions for microinjecting and electroporating DNA-encoding vectors in mouse embryonic kidney explants. Several reports have shown high transgene incorporation using a high voltage/short pulse electric field [96-98]. Therefore, we compared a high voltage/short pulse protocol (HV/SP: 175V; 75 μs) to a low voltage/long pulse electroporation protocol (LV/LP: 25V; 50 ms) and assessed several outcomes including whole organ growth, ureteric bud branching, mesenchymal to epithelial transition, and the level of transgene incorporation. From this, we determined that an electric field consisting of 175 volts (~440 kV/cm) with a pulse duration of 75 μs allowed kidneys to grow well and show a higher and more sustained level of transgene expression compared to a LV/LP protocol.

1. HV/SP electrical fields lead to higher transgene incorporation than LV/LP electrical fields in the embryonic kidney

Kidneys treated with either a LV/LP protocol, protocol A, or a HV/SP protocol, protocol B, had similar growth within the first two days in culture (Figure 8A). However, we found that kidneys treated with a HV/SP electric field expressed ~100 fold more eGFP transgene when compared to those treated with LV/LP protocols. The number of pixels from the GFP protein in the HV/SP protocol was normalized to the number of pixels representing the total planar surface area and found to be 15% (Figure 8C). This in fact underestimates the efficiency of GFP incorporation since only a portion of the kidney is microinjected with the DNA and able to express GFP. However, it does provide a method to compare different electroporation protocols including that reported by Gao *et al.* (2005). In that work, where a LV/LP protocol was used to electroporate mouse kidneys at E11.5-12, we estimate that the level of GFP expression represents ~0.5% of the total kidney planar surface area. Interestingly, this is consistent with our data since we showed that electroporation with a LV/LP protocol led to GFP expression in ~0.2% of the total kidney planar surface area. It is important to note that in our experiments, we microinjected and electroporated kidneys that were at a later stage in development, embryonic day 13, compared to the other study [100]. On further examination of our

data, there was a tendency for younger kidneys to express more GFP than older ones, although this did not reach statistical significance (Fig. 11C). Therefore, the lower level of GFP expression in the work of Gao *et al.* appears to be a direct result of the LV/LP protocol since this developmental stage is well-suited for electroporation. In summary, both HV/SP and LV/LP protocols can be used to microinject and electroporate transgenes in the embryonic kidney. However, it appears that a HV/SP protocol is more effective: a higher electric field is generated, and this appears to be an important consideration when electroporating tissues like the embryonic kidney as opposed to cells [99].

2. HV/SP electrical fields are better suited for intracellular transport in multi-cellular environments

It has been proposed that the electroporation of multicellular tissues may have certain challenges because of the heterogeneity of the tissue and the physical barriers created by the extracellular matrix and basement membranes. Canatella *et al.* (2004) explored this further by creating and then electroporating multicellular spheroids of prostate cancer cells. Isolated cells or spheroids were incubated with a fluorescent, membrane-impermeable dye, calcein, and then electroporation was performed. From their work, they noted that individual cells had a much greater uptake of calcein than those that were part of a spheroid. Furthermore, within the spheroids, cells that were located more deeply showed less uptake than those that were more superficial. They concluded that cells within a tissue showed an unpredictable uptake of a transgene because of variations in cell state, the local electric field, and the local solute concentration [99]. They also examined different electroporation parameters and found that spheroids treated with a HV/SP protocol had a higher amount of calcein incorporation than those treated with a LV/LP protocol. From this, they concluded that LV/LP protocols are much more sensitive to voltage such that a small decrease in the applied transmembrane potential may be sufficient to impair intracellular transport of DNA, particularly in multicellular tissues where there are physical barriers created by the extracellular matrix and basement membranes. In contrast, by using a HV/SP protocol there may be more cellular toxicity, but there is a lower likelihood that the threshold for

intracellular transport will not be surpassed. Other advantages from a HV/SP protocol include a reduction in thermal heating of individual cells [104] and a larger cell surface area for DNA interaction and passage through the lipid bilayer [86].

Gehl (2003) reported that in order for an electrical field to be sufficient to create electropores, it needed to exceed the resting transmembrane potential of the cell at its lipid bilayer. The transmembrane potential induced by electroporation can be mathematically described where:

$$\Delta V_m = f E_{ext} r \cos(\phi)$$

"ΔV_m" is the transmembrane potential, "f" is a coefficient that describes how the cell impacts on the distribution of the electric field, "E_{ext}" is the applied electric field, "r" is the radius of the targeted cell and "ϕ" is the angle by which the cell is oriented with respect to the electric field [89]. Therefore, when an electric field is applied to a cell and is greater than the ΔV_m of a cell, electropores are formed. The developing kidney consists of multiple cell types, such as ureteric bud cells, metanephric mesenchymal cells, stromal cells and endothelial cells that vary in size, which impacts on the radius, r, and in location, which impacts on the angle of orientation with respect to the electric field, ϕ, within the organ [48, 105]. It has been shown that the induced transmembrane potential is higher when the longest axis of the cell is parallel to the electric field [86]. Here, it is evident that cell shape must also be considered since cellular orientation with respect to the electric field is of greater importance for elongated cells than spherical ones. Optimal parameters for electroporation of mouse embryonic kidneys must consider the variation in cell size within this tissue as well as the location of these different cell types.

Thus far, we have concentrated on the effects of electroporation, but the microinjection step in itself is important because it permits specific regions within the developing kidney to be targeted. We preferentially targeted either the ureteric bud or mesenchymal cells of the developing kidney (Figure 13). By needling the renal pelvis, ureteric bud cells could be targeted as shown by the fact that cells expressing the UB marker, cytokeratin, also demonstrated GFP signal. In addition, we could target mesenchymal cells by needling the peripheral cortex of the kidney. While both methods

do permit specific regions of the kidney to be targeted, the method is not yet refined enough to restrict expression exclusively to one tissue type. The ability to target both the mesenchyme and the ureteric bud was facilitated by using an HV/SP protocol since the electric field was strong enough to affect most cells within the region of microinjection, regardless of their position within the kidney.

3. The electroporation of embryonic kidneys affects embryonic kidney development

As the energy of the electric field is increased, there is a greater likelihood for cell and tissue toxicity [106]. In our work, we assessed toxicity by monitoring growth in culture, ureteric bud branching and mesenchymal to epithelial transition. We and others have shown that renal branching morphogenesis is affected by the presence of an electric field (Figure 10) [100]. Electroporated kidneys continue to undergo branching morphogenesis in culture, but at a lower rate than untreated kidneys (Figure 10A and B). The overall patterning of the ureteric bud is affected such that the stalks continue to elongate, but fewer lateral branch points and peripheral ureteric bud tips are formed. Watanabe and Costantini (2004) have described renal branching morphogenesis in depth using the HoxB7/GFP mouse where GFP is expressed in the UB and its derivatives. From their work, it is clear that there are three types of branching events: terminal trifid, terminal bifid and lateral branching events. In terminal bifid or trifid branching, an ampulla arises by expansion of a UB tip and then either bifurcates or trifurcates to form either two or three segments or stalks. In contrast, lateral branching arises from a UB segment as opposed to a terminal ampulla and accounts for approximately 6% of the total number of branches. They usually form from ureteric bud segments of at least 100 μm in length and arise during the 2^{nd} or 3^{rd} branching event of the ureteric bud tree [107]. Cells at the tips of the developing ureteric bud tree, also referred to as ampullae, have been postulated to have two fates [108] and can either 1) contribute to the segments/stalks of the ureteric bud tree or 2) expand by proliferation and form new tips under the influence of GDNF. In addition, cells that initially commit to the stalks of the ureteric bud tree, can extend from the stalk to give rise to new tips [108]. The defects in forming ureteric bud tips at either the extremities of the branching ureteric bud tree or at the stalks in electroporated kidneys suggests that the presence of an electric field affects the

developmental potential of ureteric bud cells. This hypothesis would account for the long ureteric bud stalks and the reduction in the number of both lateral branches and ureteric bud tips. Studies comparing differences at the level of gene expression between electroporated and untreated kidneys could facilitate the identification of genes responsible for ureteric bud branching and cell differentiation.

The differentiation of the metanephric mesenchyme appeared to be intact since electroporated kidneys showed the presence of mesenchymal cells undergoing MET. A closer examination of cellular events, such as proliferation or apoptosis would give further insight into the health of this cell population.

4. Considerations when manipulating electroporated embryonic kidneys

A. Experimental observations to improve kidney growth in culture

Exposing an embryonic kidney to electric fields that are too strong causes a range in phenotypes ranging from a slight retardation in growth to necrosis of the kidney. We have noticed that there are many factors pertaining to the care of the embryonic kidneys after electroporation that can improve their growth. First, the cultures need to be rapidly incubated once the electroporation treatment is completed. Cultures that were frequently removed from the incubator post- electroporation took twice as long to recover in terms of their growth (data not shown). In experiments with a large number of samples, only two wells containing 10 kidneys each were grouped on a single 6-well plate. This feature diminished the time in which the kidneys were exposed to room temperature during imaging, and led to growth similar to untreated kidneys. The temperature post-electroporation has been shown to impact on the time required for electropores to reseal and the lipid bilayer to recover. It is reported that if cells are maintained at 37°C, their membranes will recover within 5 minutes [89]. A rapid restoration of the cell membrane is paramount for the recovery of the cells and the translational machinery that promotes transgene expression [89]. Lastly, a daily change in media allowed for electroporated kidneys to achieve a growth rate similar to untreated kidneys. In addition, some of these kidneys were able to express the transgene for up to 10 days in culture.

B. Postulated factors to improve electroporated kidney cultures

As described previously the electroporation of DNA into cells occurs through the electrophoretic forces of the electric field. However in multi-cellular environments there is a reduction on the overall applied electric field [99]. Therefore, applying the current in a medium that increases conduction would optimize the incorporation of the transgene into cells. The use of a highly saline solution has been shown to increased the electroporation efficiency by 22% when compared to a less saline solution [99].

By electroporating multi-cellular tissues with a HV/SP electric field followed by a LV/LP electric field, transgene expression can be significantly increased [109-111]. Using the two types of electric fields allows the advantages of both: the HV/SP protocol allows for a greater cell surface area to be permeabilized, while the LV/LP protocol permits greater intracellular transport of DNA because of the longer pulse time [110].

5. Electroporation, gene therapy and the mature kidney

Elucidating the appropriate parameters for electroporation will allow us to better understand the use of this technique in research and in clinical settings. In the field of developmental nephrology, it is important to identify and characterize the key genes involved in formation of the kidney. Defects in kidney development predispose individuals to a range of health complications leading from hypertension to end-stage renal disease [39]. The rodent embryonic kidney remains one of the most common *in vitro* models for the study of kidney development. Therefore, techniques which allow genes to be manipulated in kidney explants will enable researchers to address multiple questions about development [80, 112].

In the clinical setting, an important goal in the treatment of kidney diseases would be the use of gene therapy to ameliorate fibrosis, for example [83, 89]. Progressive fibrosis is the end-product of a variety of different renal pathologies and is often due to an accumulation of extra-cellular matrix caused by the upregulation of TGF-β1 protein. Many studies have looked into targeting TGF-β1 to reduce the progression of fibrosis [113, 114]. Isaka *et al.* (1996) identified decorin as an inhibitor of TGF-β1 expression. To ensure that the decorin protein would be produced for an extended period of time they

targeted the skeletal muscles of rat, which then acted as a "bio-reactor" to produce a substantial amount of decorin [115, 116]. Other strategies to target TGF-β1 include microinjecting transgenes in the renal artery of the mature kidney followed by electroporation. This has been done and resulted in the presence of fluorescently-labeled nucleotides in the glomeruli of mature rat kidneys [117, 118].

In conclusion, the use of electroporation in the field of kidney development and gene therapy is promising. Future research needs to address how more sustained expression of transgenes can be achieved so that clinical disease can be effectively treated.

VI. FUTURE ENDEAVOURS

The preceding report has described more optimal parameters to electroporate embryonic kidneys. As stated previously, culturing embryonic kidneys remains the most suitable *in vitro* model to investigate the effect of candidate genes [80] in either their role in renal branching morphogenesis or in mesenchymal-to-epithelial transition. By understanding the multiple tools that one can use to manipulate candidate gene expression in the mouse embryonic kidney, researchers can address questions and get answers.

Establishing optimal parameters for microinjection and electroporation stems from several efforts in our laboratory to study gene function using the model of the cultured embryonic kidney. The first gene, ALK6, is a receptor involved in the transforming growth factor (TGF)-β/bone morphogenetic protein (BMP) pathway. As shown previously, BMPs play an important role in mesenchymal cell survival in addition to their crucial role in ureteric bud initiation, elongation and ureter maturation [30, 31]. The cellular response to growth factors of the TGF-β/BMP pathway is partly mediated through the type 1 activin-like-kinase (ALK) transmembrane receptors [119]. We have focused our efforts on the ALK6 receptor in order to better understand its significance during kidney development.

The second gene family that we have become interested in, stems from a collaboration with Dr. Pamela Hoodless's group at the British Columbia Cancer Research Center. They have performed serial analysis of gene expression (SAGE) on a variety of tissues including the embryonic kidney where they have compared gene expression in E12 metanephric mesenchyme and ureteric bud. Through this work, members of the tight junction Claudin gene family were identified to have strong expression in the ureteric bud. Reports already describe the expression pattern of claudins in the nephron and mature kidneys [120-122] along with their involvement in diseases, such as hypomagnesemia and hypercalciuria, a defect in paracellular transport of magnesium and calcium in the nephron [123]. Our goal is to understand the role of claudins during kidney development. Here, I present a quick review of our knowledge of the BMP pathway and the claudins with emphasis on their role in the developing kidney. I show

preliminary data that may lead to interesting research proposals that have not yet been addressed.

1. The TGF-β/BMP pathway and its function during kidney development

A. The TGF-β/BMP pathway

The TGF-β superfamily consists of 30 ligands, which are divided into three groups: Activins, Bone morphogenetic proteins (BMP) and Transforming growth factor (TGF)-β [119]. BMPs, along with other members of this family, bind to the type II transmembrane receptor which then leads to the phosphorylation of serine/threonine residues within the kinase domain of the type 1 receptor. There are 7 type 1 receptors, also known as Activin Like Kinase (ALK) receptors, which directly activate the transcription factors of the TGF-β pathway, the SMAD proteins. There are eight SMADs divided into three groups (Figure 14). The receptor-activated SMADs (R-SMADs 1-3, 5 and 8) are activated when ALKs are phosphorylated [124]. In their inactive state, the SMADs are tethered to the cell membrane through anchoring proteins known as SARA as well as to the microtubular network of the cell [124, 125]. Once phosphorylated, R-SMADs shuttle to the nucleus of the cell and participate in gene transcription. All of the R-SMADS are accompanied to the nucleus by a common partner SMAD, known as SMAD4. SMAD4 shuttles continuously between the cytoplasm and the nucleus and couples with a given R-SMAD in the cytoplasm. Finally. the third group of SMADs are the inhibitory SMADs (I-SMAD 6 and 7). These inhibitory SMADs interfere with the phosphorylation of R-SMADs by the ALK receptors and this antagonizes downstream signaling (Figure 14) [124].

Figure 14. TGFβ superfamily signaling pathway.

A) Overview of the proteins involved in the signaling pathway of the TGFβ superfamily. A ligand (Activin/TGF-β/BMP) binds first to a Type II receptor (serine/threonine kinase), which phosphorylates a Type I receptor (also known as the Activin Like Kinase Receptors (ALKs). The phosphorylation of the Type I receptor will cause phosphorylation and oligomerization of the receptor-regulated Smad proteins (R-Smads) with the common-partner Smad (Smad4). Inhibitory Smads (I-Smads) can hinder the oligomerization of the R-Smads.

B) Flow-chart describing which ligand activates which Smad pathway (*Adapted from [124]).*

C) Diagram describing the signaling components shown in A). Once the R-Smads and Smad4 have oligomerized, the protein complex is translocated to the nucleus where regulation of gene transcription occurs *(Taken from [126]).*

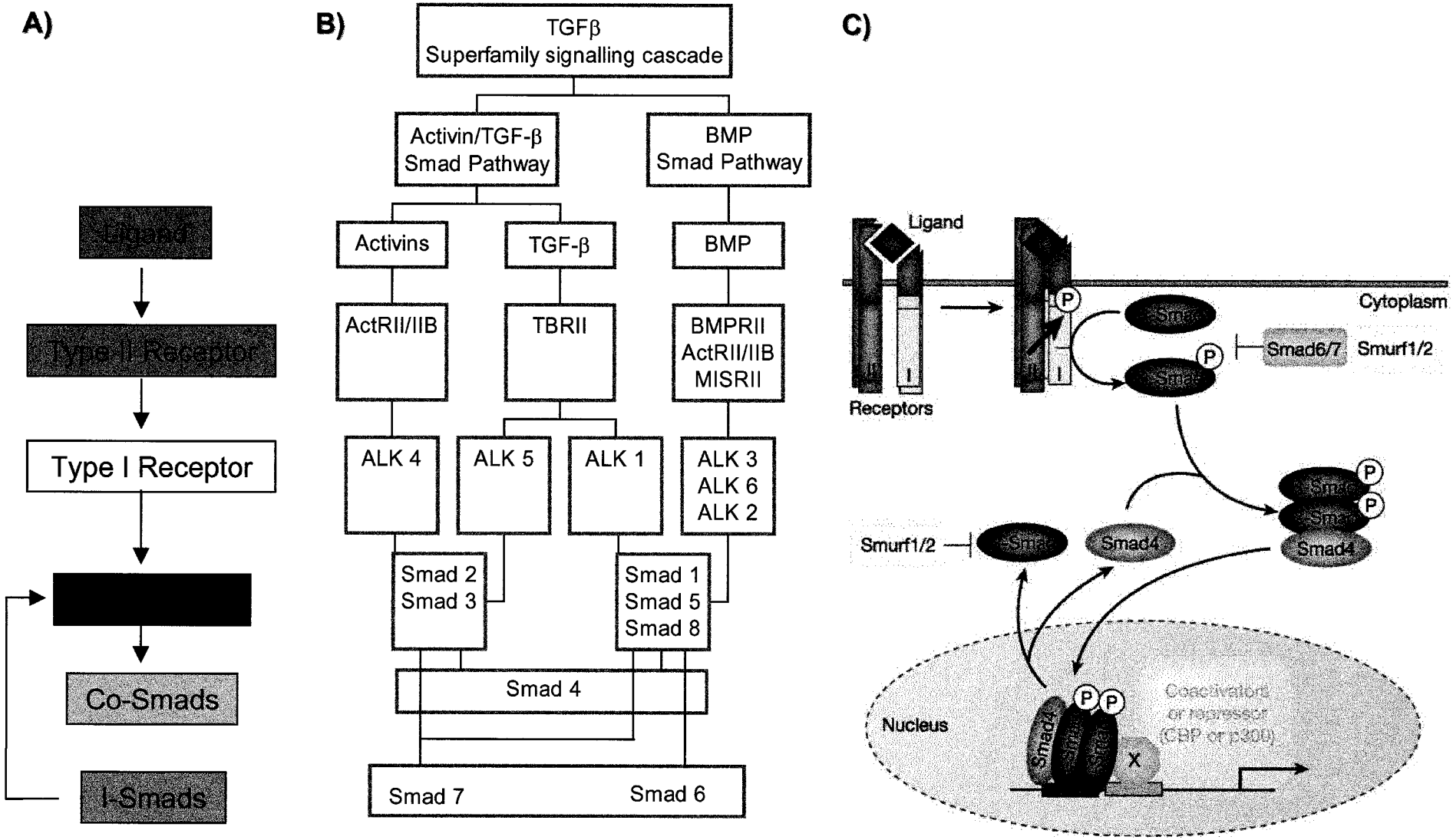
A)
Ligand
Type II Receptor
Type I Receptor
Co-Smads
I-Smads
B)
TGFβ
Superfamily signalling cascade
Activin/TGF-β
Smad Pathway
BMP
Smad Pathway
Activins
TGF-β
BMP
ActRII/IIB
TBRII
BMPRII
ActRII/IIB
MISRII
ALK 4
ALK 5
ALK 1
ALK 3
ALK 6
ALK 2
Smad 2
Smad 3
Smad 1
Smad 5
Smad 8
Smad 4
Smad 7
Smad 6
C)
Ligand
Cytoplasm
Receptors
Smad6/7
Smurf1/2
Smurf1/2
Smad4
Smad4
Nucleus
X

Although BMPs and other members of the TGF-β family signal to cells in a similar fashion, they utilize unique receptors and SMADs to transduce their signal. BMP proteins signal through ALKs 2, 3 and 6, which in turn activate R-SMADs 1, 5 and 8. TGF-β preferentially activates ALK 1 and 5 that turns on SMAD proteins 2 and 3 [124]. It has been reported that TGF-βs can signal through ALK 1 to activate SMADs 1, 5 and 8. Finally, activins transduce their signal through ALK 4, which then activates SMAD 2 and 3 [127].

B. ALK receptors are mediators of the cell's response to BMP signaling

In the developing kidney BMP2, 4 and 7 have been extensively investigated. BMP2 and 4 show a sequence homology close to 90%, whereas both cytokines share ~60% homology with BMP7 [128]. Both BMP2 and BMP4 are expressed in the metanephric mesenchyme that surrounds the ureteric bud tips and the ureter (Dudley and Robertson, 1997). Both cytokines affect ureteric bud branching: BMP2 is inhibitory, while BMP4 stimulates branching [30, 105]. The receptor for BMP2 and BMP4 is ALK3 which by northern analysis is strongly expressed in the heart, lung, and kidneys of the adult mouse [129]. The function of ALK3 has been elucidated by using an *in vitro* model of renal branching morphogenesis in which mIMCD-3 cells can be induced to form tubules when seeded in type I collagen gels [105, 130]. When mIMCD-3 cells were stably transfected with a constitutively active form of the ALK3 receptor, the cells failed to form tubules [130], suggesting that BMP2 signals through ALK3 to regulate collecting duct branching.

The *Bmp2*$^{-/-}$ and *Alk3*$^{-/-}$ mouse models have not been informative in establising the role of this signaling cascade in the developing kidney. Homozygous mutant embryos for both the ligand and the receptor die between E7.0 and E9.5 prior to formation of the kidneys due to defects in mesodermal development [131, 132]. Hu *et al.* (2003) created a transgenic mouse model whereby a constitutively active form ofALK3 was overexpressed in the ureteric bud. They observed that the kidneys of these mice had a decrease in ureteric bud branching and cyst formation in the medulla [133]. However, BMP2 also binds to other type I receptors including ALK6. Therefore, we have chosen to look at the role of this receptor during kidney development.

C. The role of BMP2/ALK6 in the two main cell types of the developing kidney

We treated mesenchymal cells (mK3) and epithelial ureteric bud cells (mIMCD-3) with BMP2 and then monitored the protein expression for the R-SMAD, SMAD1, a known downstream effector of BMP2 signaling [124]. Under basal conditions, R-SMADs are situated in the cytoplasm of cells where they are tethered to the cell membrane and microtubules [124, 125]. However, when exposed to ligand,the R-SMADs become phosphorylated by ALKs and shuttle to the nucleus. Upon treatment with BMP2, SMAD1 is expressed strongly in the nucleus of both a mesenchymal, mk3, and an epithelial ureteric bud cell line, mIMCD-3 (Figure 15). This data shows that *in vitro*, both metanephric mesenchymal and ureteric bud cells respond to BMP2 signalling. We then determined what type I receptors are expressed by these cell lines and the embryonic kidney.

We report RT-PCR data that shows the expression of ALKs during several time points during mouse metanephric kidney development (Figure 16A). ALK 1-6 are expressed during all time points, whereas ALK7 is only detected in the adult kidney. To better understand the role of these receptors we investigated the expression of all 7 ALKs in mK3 cells and in another epithelial ureteric bud cell line known as RUB1. mK3 cells expressed ALKs 2-5, whereas RUB1 cells expressed ALK 2-6 (Figure 16B). Therefore, mK3 cells express BMP2 type 1 receptors ALK 2 and 3; whereas RUB1 showed expression of ALKs 2, 3 and 6. The presence of ALK6 in the ureteric bud was confirmed by *in situ* hybridization. *ALK6* expression was located in the ureteric bud tips, along with the stalks of the branching ureteric bud: we did not detect any staining in the metanephric mesenchyme (Figure 16 C and D). This expression data is in agreement with a report from Martinez *et al.* [134].

Figure 15. BMP2 stimulation in mesenchyme and ureteric bud cells.

Mesenchyme immortalized cell line, mK3, and collecting duct immortalized cell line, mIMCD-3, were grown either with or without the presence of BMP2. Cells were labeled for SMAD1 (red) staining pattern using fluorescent immunocytochemistry. The nuclei of cells are stained with DAPI (blue). The DAPI images correspond to the above SMAD1 images. In basal condition, SMAD1 stays localized to the cytoplasm, with little overlap staining the DAPI stained nuclei. However, BMP2-stimulated cells show an accumulation of SMAD1 in the nuclei; indicating that BMP2 ligand caused SMAD1 phosphorylation and therefore accumulation in the nucleus (40X magnification).

mK3 Cell line
mIMCD Cell line
Non BMP2 Treated cells
BMP2 Treated cells

Figure 16. ALK6 expression in the developing kidney.

A) RT-PCR analysis performed at several time points during metanephric kidney development showed expression of *ALK 1-6* throughout development, whereas *ALK7* is detectable in adult tissues.

B) RT-PCR in mK3 and RUB-1 cell line detected expression of ALK 2-5 and ALK 2-6.

C) Whole mount *in situ* hybridization in a E14 kidney, demonstrates that *ALK6* is expressed by the ureteric bud of the developing kidney (5X magnification).

D) Cryosection of E14 kidney labeled by whole mount *in situ* hybridization with a probe for Alk6. *ALK6* is expressed in the UB tips (20x magnification).

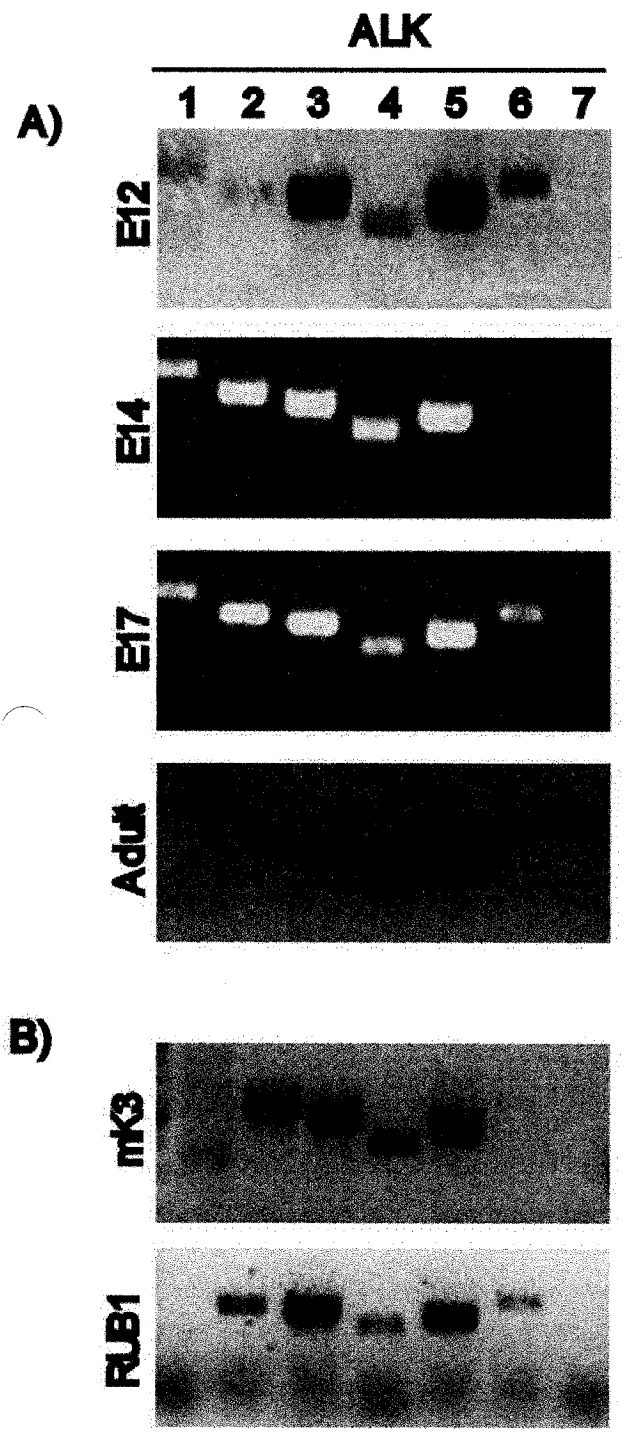
ALK
1 2 3 4 5 6 7
A)
E12
E14
E17
Adult
B)
mK3
RUB1

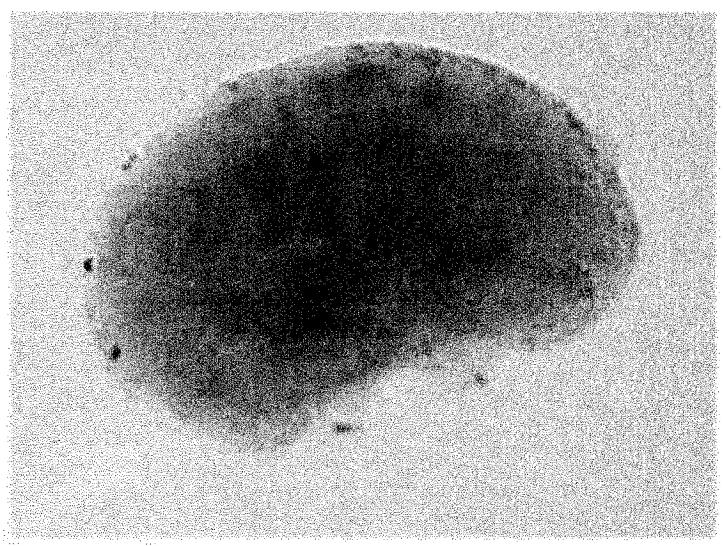
C)

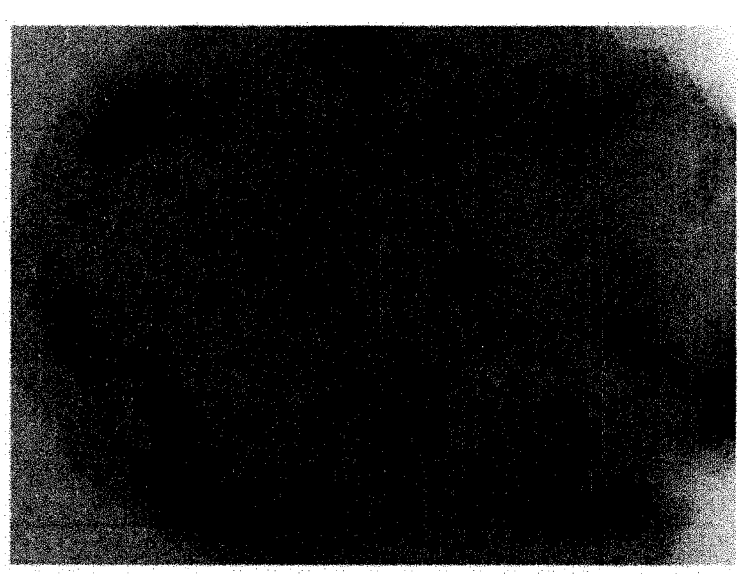
D)

It has been shown that BMP2 can bind to ALK6, which in fact shares great homology with ALK3 [135]. Mesenchymal and ureteric bud cells show a distinct response to BMP2 signaling and this could be a result of the ligand acting through different ALK receptors in each of these cell types. Based on their expression patterns, one might speculate that ALK3 mediates the response of mesenchymal cells to BMP2 while ALK6 transduces the signal for ureteric bud cells. *Alk6*$^{-/-}$ mice are viable and have defects in skeletal development. However, no gross kidney phenotype has been reported, suggesting that ALK6 is not essential for kidney development [136]. Alternatively, it is possible that ALK6 is important for kidney development, but the effect is more subtle and manifest as a decrease in nephron number that could be missed without a careful analysis. There could also be functional redundancy between ALK 3 and ALK6 such that in the absence of ALK6, ALK3 transduces BMP2 signals.

2. *The role of Claudins in the developing kidney*

A. Paracellular transport in the nephron

The nephron recycles water, ions (Na^+; Cl^-; Mg^{2+}) and other substances (glucose and amino acids) in order to maintain proper homeostasis in the body. The recycling of these molecules occurs, in part, by paracellular transport, which is the diffusion of molecules between epithelial cells[137]. Since paracellular transport is a passive process, epithelia must regulate the molecules that pass through the paracellular space according to size and ionic charge [137]. Paracellular transport relies on the formation of junctions between epithelia, known as tight junctions.

B. The claudin gene family: Regulators of tight junction paracellular transport

Tight junctions are comprised of three types of proteins, occludins, claudins and junction adhesion molecules (JAMs), which regulate the space between epithelial cells, known as the paracellular space, through which water and solutes can pass through an epithelial cell layer [137, 138]. The claudin gene family comprises of 23 members. The proteins range in size from 22-27 kD protein and consist of 211 to 230 amino acid

residues. All claudins are transmembrane proteins with four hybrophobic transmembrane domains that form two extracellular loops.

A large body of evidence suggests that claudins are necessary for the formation of tight junctions and the regulation of paracellular transport. Transfections of either claudin-1 or claudin-2 in L-fibroblastic cells resulted in the formation of tight junctions [139]. Further studies with Mardine-Darby-Canine-Kidney cells (MDCK cells) have shown the involvement of claudins in modulating paracellular transport of solutes. MDCK cells are known to exist in either the type I or type II forms, which are distinct from each other due to their striking difference in paracellular transport. Type I MDCK cells permit little paracellular transport to occur, due to the close proximity between epithelial cells, whereas the type II cells show a 20 fold increase in paracellular transport, due to the presence of more leaky tight junctions [140]. When type I cells were stably transfected with claudin-2, they were shown to become much more leaky like type II cells. In contrast, when type I cells were transfected with claudin-3, there was no change in the tight junction function of the cells. Alexandre *et al.* (2005), showed that overexpressing claudin-7 favored the passive diffusion of Na^+ while the paracellular transport of Cl^- was decreased. These studies have shown that individual claudins have different affects on paracellular transport across tight junctions [141].

It appears that claudin expression correlates with the function within particular nephron segments. Claudins that are known to allow paracellular transport between cells, including claudin-2, 7 and 8, are expressed in the proximal tubule and Henle's loop, where the bulk of solutes and water are reabsorbed through leaky tight junctions [120, 121]. In contrast, claudin-1, -3 and –4 show expression in the distal and collecting duct cells where most reabsorption of solutes and water occurs through active transport [121]. Interestingly *Claudin-1*$^{-/-}$ mice die within one day of birth due to dehydration, caused by defects of the epidermal layer: it is unknown whether they also have a renal defect in salt and water reabsorption [142].

Many hormonal responses regulate claudin expression and function, and therefore affect tight junction permeability. Le Moeillic *et al.* studied the effect of aldosterone, a hormone secreted by the adrenal cortex which stimulates Na^+ uptake, in a rat collecting duct cell-line with low paracellular activity (RCCD2) [143]. Aldosterone treatment

increased passive diffusion of molecules, such as iodine and sodium, along with the phosphorylation of claudin-4's threonine residue [143]. This work suggests that claudin-4 may play a role in aldosterone-mediated salt reabsorption in the distal nephron.

C. The expression of claudins in the developing kidney

We identified claudins as candidate genes important for kidney development by comparing the expression levels of genes in the E12 metanephric mesenchyme vs. the ureteric bud (Figure 17). Dr. Pamela Hoodless and her lab, at the British Columbia Cancer Research Center, performed Serial Analysis of Gene Expression (SAGE), for which they sequenced small 9-10 nucleotide sequences (known as "tags") that represent unique transcripts [144]. Following the sequencing, one can quantify the number of similar tags, which represent a given gene, and determine if there are differentially expressed transcripts when comparing the ureteric bud to the mesenchyme [145]. Through this analysis we noticed that claudin-3 was greatly expressed in the ureteric bud, as reported by Meyer *et al.* [146].

We looked at the expression of selected claudins at different time points in development. *Claudins-1, 3, 7* and *11* were all expressed in the developing and adult kidney; except for *Claudin-11* that we failed to detect in the adult tissue. We noted expression of *Claudin-1* in the mK3, mesenchymal cell line, whereas *Claudin-3* and *7* were only detected in the ureteric bud cell line RUB1. Although we found that *Claudin-11* was expressed in the developing kidney, we were unable to detect its expression in either mK3 or RUB1 cells. It is possible that *Claudin-11* may only be expressed in the stromal cell population. However, Claudin-11 has been reported to be found in the proximal and thick ascending limb of the nephron that originates from mesenchymal cells, so at the current time, the significance of our *Claudin-11* expression data is unclear [147]. Using *in situ* hybridization, we examined the expression pattern of *Claudin-3* and *-7*. Whole mount images of kidneys showed that claudin-3 is expressed throughout the ureteric bud and its derivatives and in the medulla. Upon examination of cryosections, it was evident that the medullary signal corresponded to labeling in mesenchymal cells adjacent to ureteric bud tips. From whole mount images and cryosections, *Claudin-7* expression was restricted to the ureteric bud tips, branches, stalks and ureter. In

collaboration with Dr. Aimee Ryan (McGill University), her laboratory has performed immunohistochemistry using antibodies directed to Claudin-3 and 7 in E12 and E15 kidneys, and their results are consistent with our *in situ* observations.

The possibility of using short interfering RNAs (siRNA) to knockdown gene expression has been a useful tool in development and a potential therapy for kidney disease [112, 118]. Now that we have optimized the electroporation technique in the developing kidney, we can combine the spatial targeting of transgenes with the gene silencing approach to address the role of claudins in the developing kidney, and the particular role that UB specific claudins may have in branching. Further, the possibility to conditionally knock-out genes from the ureteric bud can be efficiently achieved by expressing the *Cre* recombinase under the control of the *HoxB7* promoter [67, 70, 75]. The obtained phenotype from targeting a claudin gene member in a particular structure of a developing organ would be important because it is conceivable that knocking out claudins ubiquitously could be embryonic lethal [142, 147]. Simon *et al.* (1999), showed that defects in the sequence for claudin-16, also referred as paracellin-1, caused defects in tight junction organization leading to impaired paracellular transport of Mg^{2+} and Ca^{2+} in the thick ascending limb of Henle [123]. Therefore, it is possible that a defect in both development and in salt and water transport may arise when claudins are excised from ureteric bud cells.

Figure 17. Dissection of mesenchyme and ureteric bud from E12 embryonic kidneys.

E12 embryonic kidneys were dissected from timed embryos and trypsinized. The mesenchyme (A) and the ureteric bud (B) can then be dissected away from one another.

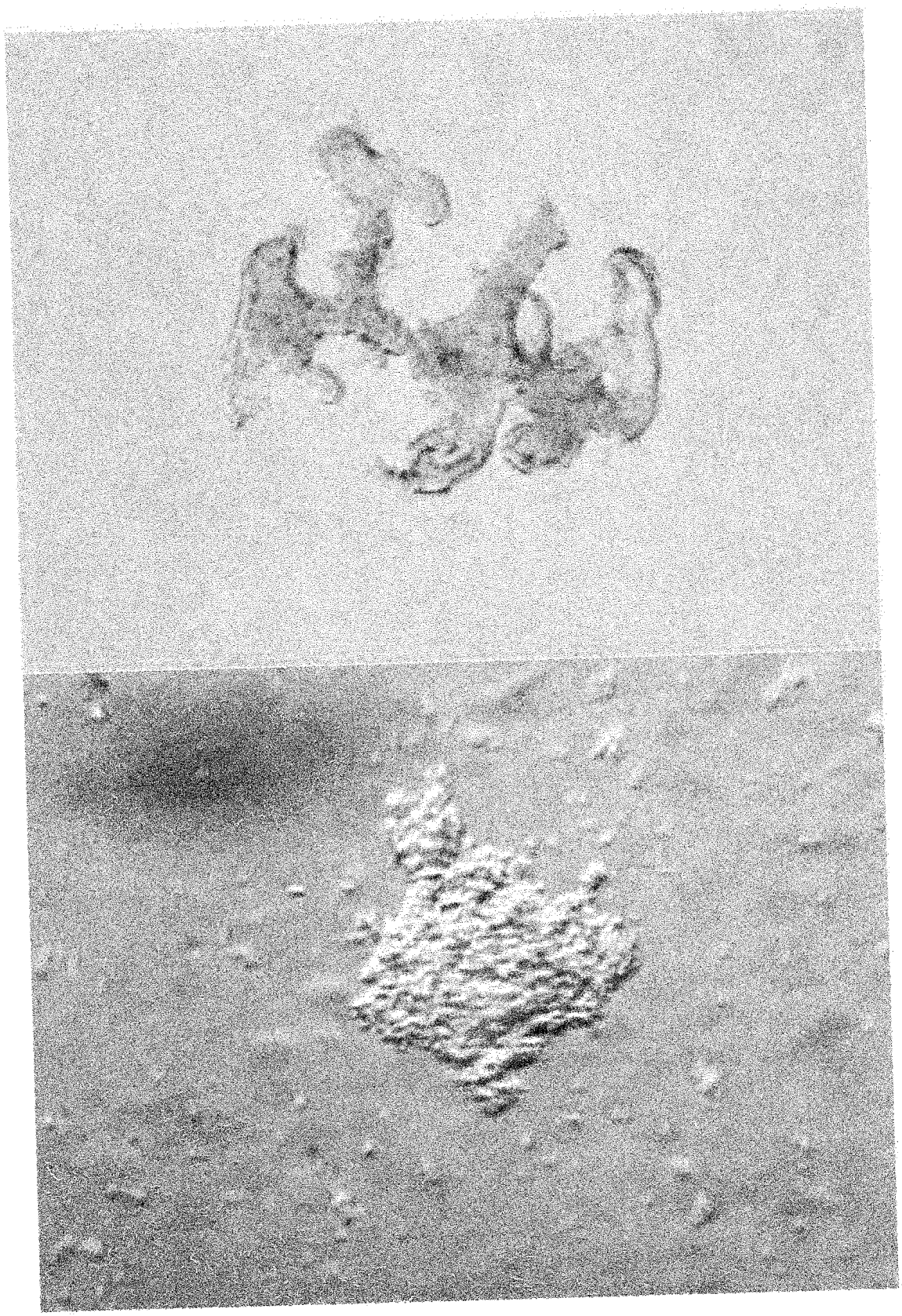

Figure 18. Expression of Claudin 1, 3, 7 and 11 in the developing kidney.

A) RT-PCR analysis detected expression of *Claudin 1*, *3*, *7* and *11* in the embryonic kidney. In adult kidney tissues we show expression of *Claudin 1*, *3* and *7*.

B) mK3 cells show expression of *Claudin-1*; whereas RUB1 cells express *Claudin-3* and *–7*. We did not detect *Claudin-11* in either cell line.

C) Whole mount *in situ* hybridization demonstrating *Claudin-3* and *–7* expression in E13.5 embryonic kidneys. *Claudin-3* is detectable in the ureteric bud tips and stalks. In the many samples that we tested we noticed the presence of *Claudin-3* expression in the medulla. The ureteric bud tips, stalks and ureters express *Claudin-7*. After *in situ* hybridization, the kidneys were cryosectioned and confirm the expression pattern observed in whole mount images.

A)
Claudin
1
3
7
11
E13
E15
E16
Adult
B)
mK3
RUB1
C)
Claudin-3
Claudin-7
5x magnification
20x magnification
40x magnification

VII. REFERENCES

1. Saxen L: *Organogenesis of the Kidney*, Cambridge University Press, 1987
2. Horster MF, Braun GS, Huber SM: Embryonic renal epithelia: induction, nephrogenesis, and cell differentiation. *Physiol Rev* 79:1157-1191, 1999
3. Bouchard M: Transcriptional control of kidney development. *Differentiation* 72:295-306, 2004
4. Vize PD, Woolf, A. S., Bard, J. B. L.: *The Kidney: From Normal Development to Congenital Disease*, Academic Press, 2003
5. Sainio K, Suvanto P, Davies J, *et al.*: Glial-cell-line-derived neurotrophic factor is required for bud initiation from ureteric epithelium. *Development* 124:4077-4087, 1997
6. Gilbert SF: *Developmental Biology*, 6th ed, Sinauer Associates, 2000
7. Vainio S, Lin Y: Coordinating early kidney development: lessons from gene targeting. *Nat Rev Genet* 3:533-543, 2002
8. Murawski IJ, Gupta IR: Vesicoureteric reflux and renal malformations: a developmental problem. *Clin Genet* 69:105-117, 2006
9. Sampogna RV, Nigam SK: Implications of gene networks for understanding resilience and vulnerability in the kidney branching program. *Physiology (Bethesda)* 19:339-347, 2004
10. Lechner MS, Dressler GR: The molecular basis of embryonic kidney development. *Mech Dev* 62:105-120, 1997
11. Schuchardt A, D'Agati V, Larsson-Blomberg L, *et al.*: Defects in the kidney and enteric nervous system of mice lacking the tyrosine kinase receptor Ret. *Nature* 367:380-383, 1994
12. Schuchardt A, D'Agati V, Pachnis V, *et al.*: Renal agenesis and hypodysplasia in ret-k- mutant mice result from defects in ureteric bud development. *Development* 122:1919-1929, 1996
13. Enomoto H, Araki T, Jackman A, *et al.*: GFR-alpha1- Deficient Mice have deficits in the Enteric Nervous System and Kidneys. *Neuron* 21:317-324, 1998
14. Durbec P, Marcos-Gutierrez CV, Kilkenny C, *et al.*: GDNF signalling through the Ret receptor tyrosine kinase. *Nature* 381:789-793, 1996
15. Pichel JG, Shen L, Sheng HZ, *et al.*: Defects in enteric innervation and kidney development in mice lacking GDNF. *Nature* 382:73-76, 1996
16. Qiao J, Sakurai H, Nigam SK: Branching morphogenesis independent of mesenchymal-epithelial contact in the developing kidney. *Proc Natl Acad Sci U S A* 96:7330-7335, 1999
17. Yu J, McMahon AP, Valerius MT: Recent genetic studies of mouse kidney development. *Curr Opin Genet Dev* 14:550-557, 2004
18. Dressler GR, Deutsch U, Chowdhury K, *et al.*: Pax2, a new murine paired-box-containing gene and its expression in the developing excretory system. *Development* 109:787-795, 1990
19. Rothenpieler UW, Dressler GR: Pax-2 is required for mesenchyme-to-epithelium conversion during kidney development. *Development* 119:711-720, 1993
20. Brophy PD, Ostrom L, Lang KM, *et al.*: Regulation of ureteric bud outgrowth by Pax2-dependent activation of the glial derived neurotrophic factor gene. *Development* 128:4747-4756, 2001

21. Nishinakamura R, Matsumoto Y, Nakao K, *et al.*: Murine homolog of SALL1 is essential for ureteric bud invasion in kidney development. *Development* 128:3105-3115, 2001
22. Wellik DM, Hawkes PJ, Capecchi MR: Hox11 paralogous genes are essential for metanephric kidney induction. *Genes Dev* 16:1423-1432, 2002
23. Brodbeck S, Englert C: Genetic determination of nephrogenesis: the Pax/Eya/Six gene network. *Pediatr Nephrol* 19:249-255, 2004
24. Kume T, Deng K, Hogan BL: Murine forkhead/winged helix genes Foxc1 (Mf1) and Foxc2 (Mfh1) are required for the early organogenesis of the kidney and urinary tract. *Development* 127:1387-1395, 2000
25. Grieshammer U, Le M, Plump AS, *et al.*: SLIT2-mediated ROBO2 signaling restricts kidney induction to a single site. *Dev Cell* 6:709-717, 2004
26. Basson MA, Akbulut S, Watson-Johnson J, *et al.*: Sprouty1 is a critical regulator of GDNF/RET-mediated kidney induction. *Dev Cell* 8:229-239, 2005
27. Pepicelli CV, Kispert A, Rowitch DH, *et al.*: GDNF induces branching and increased cell proliferation in the ureter of the mouse. *Dev Biol* 192:193-198, 1997
28. Ehrenfels CW, Carmillo PJ, Orozco O, *et al.*: Perturbation of RET signaling in the embryonic kidney. *Dev Genet* 24:263-272, 1999
29. Klein DJ, Brown DM, Moran A, *et al.*: Chondroitin sulfate proteoglycan synthesis and reutilization of beta-D-xyloside-initiated chondroitin/dermatan sulfate glycosaminoglycans in fetal kidney branching morphogenesis. *Dev Biol* 133:515-528, 1989
30. Miyazaki Y, Oshima K, Fogo A, *et al.*: Bone morphogenetic protein 4 regulates the budding site and elongation of the mouse ureter. *J Clin Invest* 105:863-873, 2000
31. Miyazaki Y, Oshima K, Fogo A, *et al.*: Evidence that bone morphogenetic protein 4 has multiple biological functions during kidney and urinary tract development. *Kidney Int* 63:835-844, 2003
32. Clark AT, Young RJ, Bertram JF: In vitro studies on the roles of transforming growth factor-beta 1 in rat metanephric development. *Kidney Int* 59:1641-1653, 2001
33. Bush KT, Sakurai H, Steer DL, *et al.*: TGF-beta superfamily members modulate growth, branching, shaping, and patterning of the ureteric bud. *Dev Biol* 266:285-298, 2004
34. Hu MC, Rosenblum ND: Genetic regulation of branching morphogenesis: lessons learned from loss-of-function phenotypes. *Pediatr Res* 54:433-438, 2003
35. Dressler GR, Woolf AS: Pax2 in development and renal disease. *Int J Dev Biol* 43:463-468, 1999
36. Torres M, Gomez-Pardo E, Dressler GR, *et al.*: Pax-2 controls multiple steps of urogenital development. *Development* 121:4057-4065, 1995
37. Tsang TE, Shawlot W, Kinder SJ, *et al.*: Lim1 activity is required for intermediate mesoderm differentiation in the mouse embryo. *Dev Biol* 223:77-90, 2000
38. Kobayashi A, Kwan KM, Carroll TJ, *et al.*: Distinct and sequential tissue-specific activities of the LIM-class homeobox gene Lim1 for tubular morphogenesis during kidney development. *Development* 132:2809-2823, 2005

39. Zandi-Nejad K, Luyckx VA, Brenner BM: Adult Hypertension and Kidney Disease. The Role of Fetal Programming. *Hypertension*, 2006
40. Merlet-Benichou C: Influence of fetal environment on kidney development. *Int J Dev Biol* 43:453-456, 1999
41. Lelievre-Pegorier M, Vilar J, Ferrier ML, *et al.*: Mild vitamin A deficiency leads to inborn nephron deficit in the rat. *Kidney Int* 54:1455-1462, 1998
42. Mendelsohn C, Lohnes D, Decimo D, *et al.*: Function of the retinoic acid receptors (RARs) during development (II). Multiple abnormalities at various stages of organogenesis in RAR double mutants. *Development* 120:2749-2771, 1994
43. Mendelsohn C, Batourina E, Fung S, *et al.*: Stromal cells mediate retinoid-dependent functions essential for renal development. *Development* 126:1139-1148, 1999
44. Batourina E, Gim S, Bello N, *et al.*: Vitamin A controls epithelial/mesenchymal interactions through Ret expression. *Nat Genet* 27:74-78, 2001
45. Batourina E, Choi C, Paragas N, *et al.*: Distal ureter morphogenesis depends on epithelial cell remodeling mediated by vitamin A and Ret. *Nat Genet* 32:109-115, 2002
46. Batourina E, Tsai S, Lambert S, *et al.*: Apoptosis induced by vitamin A signaling is crucial for connecting the ureters to the bladder. *Nat Genet* 37:1082-1089, 2005
47. Herzlinger D, Abramson R, Cohen D: Phenotypic conversions in renal development. *J Cell Sci Suppl* 17:61-64, 1993
48. Al-Awqati Q, Oliver JA: Stem cells in the kidney. *Kidney Int* 61:387-395, 2002
49. Herzlinger D, Koseki C, Mikawa T, *et al.*: Metanephric mesenchyme contains multipotent stem cells whose fate is restricted after induction. *Development* 114:565-572, 1992
50. Oliver JA, Barasch J, Yang J, *et al.*: Metanephric mesenchyme contains embryonic renal stem cells. *Am J Physiol Renal Physiol* 283:F799-809, 2002
51. Kuure S, Vuolteenaho R, Vainio S: Kidney morphogenesis: cellular and molecular regulation. *Mech Dev* 92:31-45, 2000
52. Dressler GR, Wilkinson JE, Rothenpieler UW, *et al.*: Deregulation of Pax-2 expression in transgenic mice generates severe kidney abnormalities. *Nature* 362:65-67, 1993
53. Armstrong JF, Pritchard-Jones K, Bickmore WA, *et al.*: The expression of the Wilms' tumour gene, WT1, in the developing mammalian embryo. *Mech Dev* 40:85-97, 1993
54. Kreidberg JA, Sariola H, Loring JM, *et al.*: WT-1 is required for early kidney development. *Cell* 74:679-691, 1993
55. Discenza MT, He S, Lee TH, *et al.*: WT1 is a modifier of the Pax2 mutant phenotype: cooperation and interaction between WT1 and Pax2. *Oncogene* 22:8145-8155, 2003
56. Stark K, Vainio S, Vassileva G, *et al.*: Epithelial transformation of metanephric mesenchyme in the developing kidney regulated by Wnt-4. *Nature* 372:679-683, 1994

57. Kispert A, Vainio S, McMahon AP: Wnt-4 is a mesenchymal signal for epithelial transformation of metanephric mesenchyme in the developing kidney. *Development* 125:4225-4234, 1998
58. Carroll TJ, Park JS, Hayashi S, *et al.*: Wnt9b plays a central role in the regulation of mesenchymal to epithelial transitions underlying organogenesis of the mammalian urogenital system. *Dev Cell* 9:283-292, 2005
59. Perantoni A, Kan FW, Dove LF, *et al.*: Selective growth in culture of fetal rat renal collecting duct anlagen. Morphologic and biochemical characterization. *Lab Invest* 53:589-596, 1985
60. Karavanova ID, Dove LF, Resau JH, *et al.*: Conditioned medium from a rat ureteric bud cell line in combination with bFGF induces complete differentiation of isolated metanephric mesenchyme. *Development* 122:4159-4167, 1996
61. Barasch J, Yang J, Ware CB, *et al.*: Mesenchymal to epithelial conversion in rat metanephros is induced by LIF. *Cell* 99:377-386, 1999
62. Plisov SY, Yoshino K, Dove LF, *et al.*: TGF beta 2, LIF and FGF2 cooperate to induce nephrogenesis. *Development* 128:1045-1057, 2001
63. Dudley AT, Godin RE, Robertson EJ: Interaction between FGF and BMP signaling pathways regulates development of metanephric mesenchyme. *Genes Dev* 13:1601-1613, 1999
64. Smithies O, Gregg RG, Boggs SS, *et al.*: Insertion of DNA sequences into the human chromosomal beta-globin locus by homologous recombination. *Nature* 317:230-234, 1985
65. Sorrell DA, Kolb AF: Targeted modification of mammalian genomes. *Biotechnol Adv* 23:431-469, 2005
66. Vasquez KM, Marburger K, Intody Z, *et al.*: Manipulating the mammalian genome by homologous recombination. *Proc Natl Acad Sci U S A* 98:8403-8410, 2001
67. Gawlik A, Quaggin SE: Conditional gene targeting in the kidney. *Curr Mol Med* 5:527-536, 2005
68. Tremblay KD, Dunn NR, Robertson EJ: Mouse embryos lacking Smad1 signals display defects in extra-embryonic tissues and germ cell formation. *Development* 128:3609-3621, 2001
69. Oxburgh L, Robertson EJ: Dynamic regulation of Smad expression during mesenchyme to epithelium transition in the metanephric kidney. *Mech Dev* 112:207-211, 2002
70. Oxburgh L, Chu GC, Michael SK, *et al.*: TGFbeta superfamily signals are required for morphogenesis of the kidney mesenchyme progenitor population. *Development* 131:4593-4605, 2004
71. Lechleider RJ, Ryan JL, Garrett L, *et al.*: Targeted mutagenesis of Smad1 reveals an essential role in chorioallantoic fusion. *Dev Biol* 240:157-167, 2001
72. Branda CS, Dymecki SM: Talking about a revolution: The impact of site-specific recombinases on genetic analyses in mice. *Dev Cell* 6:7-28, 2004
73. Gu H, Marth JD, Orban PC, *et al.*: Deletion of a DNA polymerase beta gene segment in T cells using cell type-specific gene targeting. *Science* 265:103-106, 1994

74. Tronche F, Casanova E, Turiault M, *et al.*: When reverse genetics meets physiology: the use of site-specific recombinases in mice. *FEBS Lett* 529:116-121, 2002
75. Srinivas S, Goldberg MR, Watanabe T, *et al.*: Expression of green fluorescent protein in the ureteric bud of transgenic mice: a new tool for the analysis of ureteric bud morphogenesis. *Dev Genet* 24:241-251, 1999
76. Yu J, Carroll TJ, McMahon AP: Sonic hedgehog regulates proliferation and differentiation of mesenchymal cells in the mouse metanephric kidney. *Development* 129:5301-5312, 2002
77. Grieshammer U, Cebrian C, Ilagan R, *et al.*: FGF8 is required for cell survival at distinct stages of nephrogenesis and for regulation of gene expression in nascent nephrons. *Development* 132:3847-3857, 2005
78. Perantoni AO, Timofeeva O, Naillat F, *et al.*: Inactivation of FGF8 in early mesoderm reveals an essential role in kidney development. *Development* 132:3859-3871, 2005
79. Engleka KA, Gitler AD, Zhang M, *et al.*: Insertion of Cre into the Pax3 locus creates a new allele of Splotch and identifies unexpected Pax3 derivatives. *Dev Biol* 280:396-406, 2005
80. Gupta IR, Lapointe M, Yu OH: Morphogenesis during mouse embryonic kidney explant culture. *Kidney Int* 63:365-376, 2003
81. Hendrie PC, Russell DW: Gene targeting with viral vectors. *Mol Ther* 12:9-17, 2005
82. Ogura T: In vivo electroporation: a new frontier for gene delivery and embryology. *Differentiation* 70:163-171, 2002
83. Chou T-HW, Biswas S, Lu S: *Nonviral Gene Transfer Techniques: Volume 1*, Humana Press, 2003
84. Potter H: Electroporation in biology: methods, applications, and instrumentation. *Anal Biochem* 174:361-373, 1988
85. Imai E, Isaka Y: Gene electrotransfer: Potential for gene therapy of renal diseases. *Kidney Int* 61:37-41, 2002
86. Phez E, Faurie C, Golzio M, *et al.*: New insights in the visualization of membrane permeabilization and DNA/membrane interaction of cells submitted to electric pulses. *Biochim Biophys Acta* 1724:248-254, 2005
87. Tieleman DP: The molecular basis of electroporation. *BMC Biochem* 5:10, 2004
88. Rols MP, Teissie J: Electropermeabilization of mammalian cells to macromolecules: control by pulse duration. *Biophys J* 75:1415-1423, 1998
89. Gehl J: Electroporation: theory and methods, perspectives for drug delivery, gene therapy and research. *Acta Physiol Scand* 177:437-447, 2003
90. Lodish HF, Berk A, Zipursky LS, *et al.*: *Molecular Cell Biology*, 4th ed, W. H. Freeman, 2000
91. Akinlaja J, Sachs F: The breakdown of cell membranes by electrical and mechanical stress. *Biophys J* 75:247-254, 1998
92. Muramatsu T, Mizutani Y, Ohmori Y, *et al.*: Comparison of three nonviral transfection methods for foreign gene expression in early chicken embryos in ovo. *Biochem Biophys Res Commun* 230:376-380, 1997

93. Itasaki N, Bel-Vialar S, Krumlauf R: 'Shocking' developments in chick embryology: electroporation and in ovo gene expression. *Nat Cell Biol* 1:E203-207, 1999
94. Nakamura H, Funahashi J: Introduction of DNA into chick embryos by in ovo electroporation. *Methods* 24:43-48, 2001
95. Pierreux CE, Poll AV, Jacquemin P, *et al.*: Gene transfer into mouse prepancreatic endoderm by whole embryo electroporation. *Jop* 6:128-135, 2005
96. Heller R, Jaroszeski M, Atkin A, *et al.*: In vivo gene electroinjection and expression in rat liver. *FEBS Lett* 389:225-228, 1996
97. Vicat JM, Boisseau S, Jourdes P, *et al.*: Muscle transfection by electroporation with high-voltage and short-pulse currents provides high-level and long-lasting gene expression. *Hum Gene Ther* 11:909-916, 2000
98. Heller R, Schultz J, Lucas ML, *et al.*: Intradermal delivery of interleukin-12 plasmid DNA by in vivo electroporation. *DNA Cell Biol* 20:21-26, 2001
99. Canatella PJ, Black MM, Bonnichsen DM, *et al.*: Tissue electroporation: quantification and analysis of heterogeneous transport in multicellular environments. *Biophys J* 86:3260-3268, 2004
100. Gao X, Chen X, Taglienti M, *et al.*: Angioblast-mesenchyme induction of early kidney development is mediated by Wt1 and Vegfa. *Development* 132:5437-5449, 2005
101. Valerius MT, Patterson LT, Witte DP, *et al.*: Microarray analysis of novel cell lines representing two stages of metanephric mesenchyme differentiation. *Mech Dev* 112:219-232, 2002
102. Vrljicak P, Myburgh D, Ryan AK, *et al.*: Smad expression during kidney development. *Am J Physiol Renal Physiol* 286:F625-633, 2004
103. Mathiesen I: Electropermeabilization of skeletal muscle enhances gene transfer in vivo. *Gene Ther* 6:508-514, 1999
104. Joshi RP, Schoenbach KH: Mechanism for membrane electroporation irreversibility under high-intensity, ultrashort electrical pulse conditions. *Phys Rev E Stat Nonlin Soft Matter Phys* 66:052901, 2002
105. Piscione TD, Yager TD, Gupta IR, *et al.*: BMP-2 and OP-1 exert direct and opposite effects on renal branching morphogenesis. *Am J Physiol* 273:F961-975, 1997
106. Golzio M, Rols MP, Teissie J: In vitro and in vivo electric field-mediated permeabilization, gene transfer, and expression. *Methods* 33:126-135, 2004
107. Watanabe T, Costantini F: Real-time analysis of ureteric bud branching morphogenesis in vitro. *Dev Biol* 271:98-108, 2004
108. Shakya R, Watanabe T, Costantini F: The role of GDNF/Ret signaling in ureteric bud cell fate and branching morphogenesis. *Dev Cell* 8:65-74, 2005
109. Bureau MF, Gehl J, Deleuze V, *et al.*: Importance of association between permeabilization and electrophoretic forces for intramuscular DNA electrotransfer. *Biochim Biophys Acta* 1474:353-359, 2000
110. Satkauskas S, Bureau MF, Puc M, *et al.*: Mechanisms of in vivo DNA electrotransfer: respective contributions of cell electropermeabilization and DNA electrophoresis. *Mol Ther* 5:133-140, 2002

111. Satkauskas S, Andre F, Bureau MF, *et al.*: Electrophoretic Component of Electric Pulses Determines the Efficacy of In Vivo DNA Electrotransfer. *Hum Gene Ther*, 2005
112. Polgar K, Burrow CR, Hyink DP, *et al.*: Disruption of polycystin-1 function interferes with branching morphogenesis of the ureteric bud in developing mouse kidneys. *Dev Biol* 286:16-30, 2005
113. Fukasawa H, Yamamoto T, Suzuki H, *et al.*: Treatment with anti-TGF-beta antibody ameliorates chronic progressive nephritis by inhibiting Smad/TGF-beta signaling. *Kidney Int* 65:63-74, 2004
114. Wang W, Koka V, Lan HY: Transforming growth factor-beta and Smad signalling in kidney diseases. *Nephrology (Carlton)* 10:48-56, 2005
115. Isaka Y, Brees DK, Ikegaya K, *et al.*: Gene therapy by skeletal muscle expression of decorin prevents fibrotic disease in rat kidney. *Nat Med* 2:418-423, 1996
116. Kessler PD, Podsakoff GM, Chen X, *et al.*: Gene delivery to skeletal muscle results in sustained expression and systemic delivery of a therapeutic protein. *Proc Natl Acad Sci U S A* 93:14082-14087, 1996
117. Tsujie M, Isaka Y, Nakamura H, *et al.*: Electroporation-mediated gene transfer that targets glomeruli. *J Am Soc Nephrol* 12:949-954, 2001
118. Takabatake Y, Isaka Y, Mizui M, *et al.*: Exploring RNA interference as a therapeutic strategy for renal disease. *Gene Ther* 12:965-973, 2005
119. Derynck R, Zhang YE: Smad-dependent and Smad-independent pathways in TGF-beta family signalling. *Nature* 425:577-584, 2003
120. Enck AH, Berger UV, Yu AS: Claudin-2 is selectively expressed in proximal nephron in mouse kidney. *Am J Physiol Renal Physiol* 281:F966-974, 2001
121. Reyes JL, Lamas M, Martin D, *et al.*: The renal segmental distribution of claudins changes with development. *Kidney Int* 62:476-487, 2002
122. Li WY, Huey CL, Yu AS: Expression of claudin-7 and -8 along the mouse nephron. *Am J Physiol Renal Physiol* 286:F1063-1071, 2004
123. Simon DB, Lu Y, Choate KA, *et al.*: Paracellin-1, a renal tight junction protein required for paracellular Mg2+ resorption. *Science* 285:103-106, 1999
124. Moustakas A, Souchelnytskyi S, Heldin CH: Smad regulation in TGF-beta signal transduction. *J Cell Sci* 114:4359-4369, 2001
125. Dong C, Li Z, Alvarez R, Jr., *et al.*: Microtubule binding to Smads may regulate TGF beta activity. *Mol Cell* 5:27-34, 2000
126. Derynck R, Zhang Y, Feng XH: Smads: transcriptional activators of TGF-beta responses. *Cell* 95:737-740, 1998
127. Moustakas A, Stournaras C: Regulation of actin organisation by TGF-beta in H-ras-transformed fibroblasts. *J Cell Sci* 112 (Pt 8):1169-1179, 1999
128. Zhao GQ: Consequences of knocking out BMP signaling in the mouse. *Genesis* 35:43-56, 2003
129. Dewulf N, Verschueren K, Lonnoy O, *et al.*: Distinct spatial and temporal expression patterns of two type I receptors for bone morphogenetic proteins during mouse embryogenesis. *Endocrinology* 136:2652-2663, 1995
130. Gupta IR, Macias-Silva M, Kim S, *et al.*: BMP-2/ALK3 and HGF signal in parallel to regulate renal collecting duct morphogenesis. *J Cell Sci* 113 Pt 2:269-278, 2000

131. Mishina Y, Suzuki A, Ueno N, *et al.*: Bmpr encodes a type I bone morphogenetic protein receptor that is essential for gastrulation during mouse embryogenesis. *Genes Dev* 9:3027-3037, 1995
132. Zhang H, Bradley A: Mice deficient for BMP2 are nonviable and have defects in amnion/chorion and cardiac development. *Development* 122:2977-2986, 1996
133. Hu MC, Piscione TD, Rosenblum ND: Elevated SMAD1/beta-catenin molecular complexes and renal medullary cystic dysplasia in ALK3 transgenic mice. *Development* 130:2753-2766, 2003
134. Martinez G, Loveland KL, Clark AT, *et al.*: Expression of bone morphogenetic protein receptors in the developing mouse metanephros. *Exp Nephrol* 9:372-379, 2001
135. ten Dijke P, Yamashita H, Sampath TK, *et al.*: Identification of type I receptors for osteogenic protein-1 and bone morphogenetic protein-4. *J Biol Chem* 269:16985-16988, 1994
136. Yi SE, Daluiski A, Pederson R, *et al.*: The type I BMP receptor BMPRIB is required for chondrogenesis in the mouse limb. *Development* 127:621-630, 2000
137. Fanning AS, Mitic LL, Anderson JM: Transmembrane proteins in the tight junction barrier. *J Am Soc Nephrol* 10:1337-1345, 1999
138. Mitic LL, Anderson JM: Molecular architecture of tight junctions. *Annu Rev Physiol* 60:121-142, 1998
139. Furuse M, Sasaki H, Fujimoto K, *et al.*: A single gene product, claudin-1 or -2, reconstitutes tight junction strands and recruits occludin in fibroblasts. *J Cell Biol* 143:391-401, 1998
140. Furuse M, Furuse K, Sasaki H, *et al.*: Conversion of zonulae occludentes from tight to leaky strand type by introducing claudin-2 into Madin-Darby canine kidney I cells. *J Cell Biol* 153:263-272, 2001
141. Alexandre MD, Lu Q, Chen YH: Overexpression of claudin-7 decreases the paracellular Cl- conductance and increases the paracellular Na+ conductance in LLC-PK1 cells. *J Cell Sci* 118:2683-2693, 2005
142. Furuse M, Hata M, Furuse K, *et al.*: Claudin-based tight junctions are crucial for the mammalian epidermal barrier: a lesson from claudin-1-deficient mice. *J Cell Biol* 156:1099-1111, 2002
143. Le Moellic C, Boulkroun S, Gonzalez-Nunez D, *et al.*: Aldosterone and tight junctions: modulation of claudin-4 phosphorylation in renal collecting duct cells. *Am J Physiol Cell Physiol* 289:C1513-1521, 2005
144. Tuteja R, Tuteja N: Serial analysis of gene expression (SAGE): unraveling the bioinformatics tools. *Bioessays* 26:916-922, 2004
145. Knox DP, Skuce PJ: SAGE and the quantitative analysis of gene expression in parasites. *Trends Parasitol* 21:322-326, 2005
146. Meyer TN, Schwesinger C, Bush KT, *et al.*: Spatiotemporal regulation of morphogenetic molecules during in vitro branching of the isolated ureteric bud: toward a model of branching through budding in the developing kidney. *Dev Biol* 275:44-67, 2004
147. Balkovetz DF: Claudins at the gate: determinants of renal epithelial tight junction paracellular permeability. *Am J Physiol Renal Physiol* 290:F572-579, 2006

APPENDIX A – RESEARCH COMPLIANCE APPROVAL LETTER (ANIMAL PROTOCOL)

APPENDIX B – REPRODUCTION OF FIGURE PERMISSION FROM EDITORS